Deep Learning in CT Optimization

Marc Kachelrieß

German Cancer Research Center (DKFZ)
Heidelberg, Germany
www.dkfz.de/ct

DEUTSCHES
KREBSFORSCHUNGSZENTRUM
IN DER HELMHOLTZ-GEMEINSCHAFT

Fully Connected Neural Network

- Each layer fully connects to previous layer
- Difficult to train (many parameters in *W* and *b*)
- Spatial relations not necessarily preserved

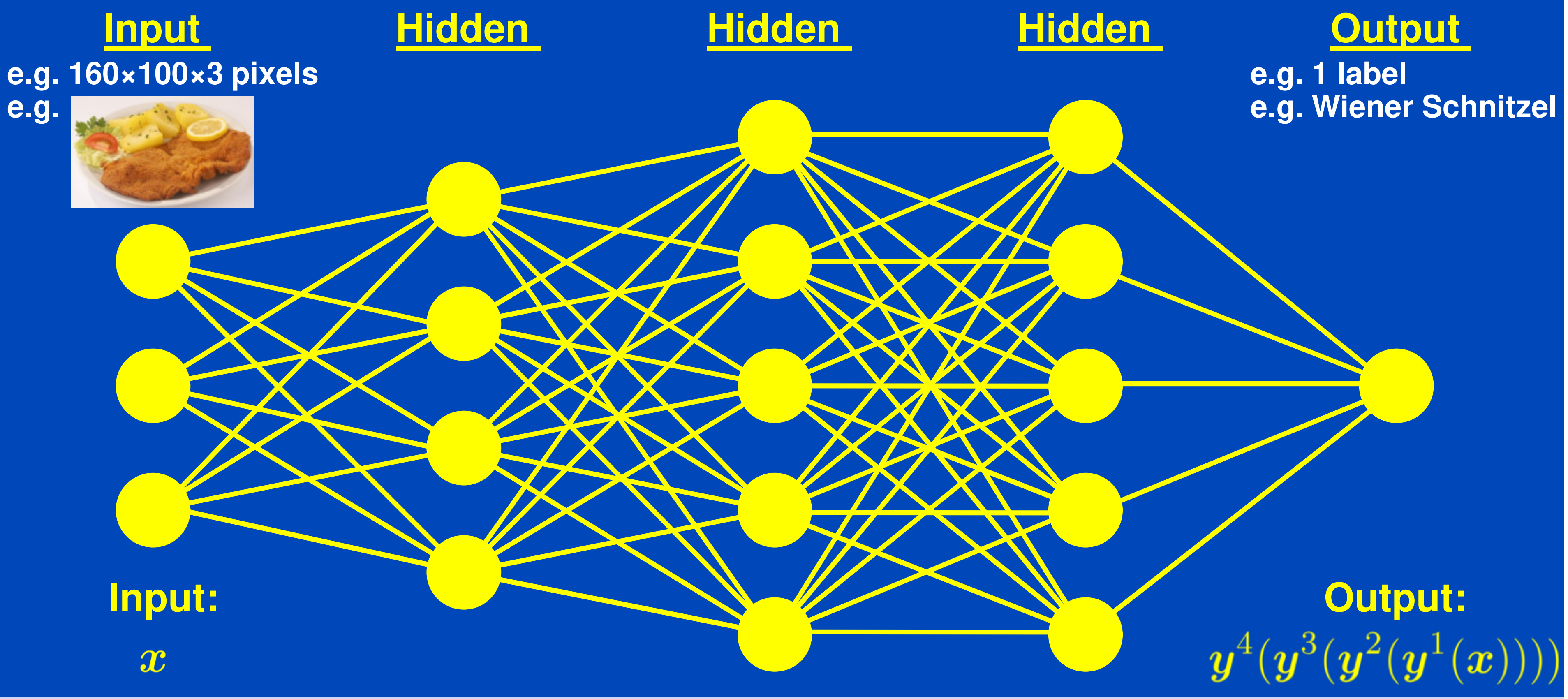

$\boldsymbol{y}(\boldsymbol{x}) = \boldsymbol{f}(\boldsymbol{W} \cdot \boldsymbol{x} + \boldsymbol{b})$ with $\boldsymbol{f}(\boldsymbol{x}) = \big(f(x_1), f(x_2), \ldots\big)$ point-wise scalar, e.g. $f(x) = x \vee 0 = \text{ReLU}$

Convolutional Neural Network (CNN)

- Replace dense *W* in $y(x) = f(W \cdot x + b)$ by a sparse matrix *W* with sparsity being of convolutional type.
- CNNs consist (mainly) of convolutional layers.
- Convolutional layers are not fully connected.
- Convolutional layers are connected by small, say 3×3, convolution kernels whose entries need to be found by training.
- CNNs preserve spatial relations to some extent.

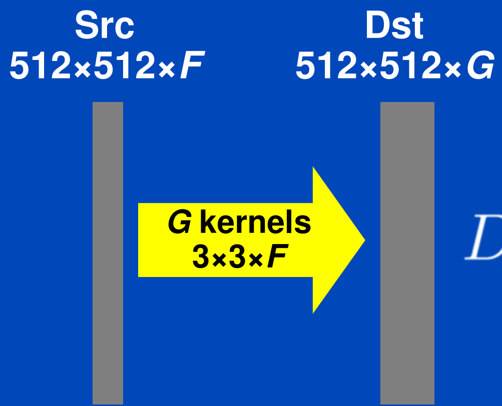

$$D_{i,j,g} = \sum_f S_{i,j,f} * K^g_{i,j,f} = \sum_{a,b,f} S_{i-a,j-b,f} K^g_{a,b,f}$$

Attention: No convolution in depth direction!

U-Net[1]

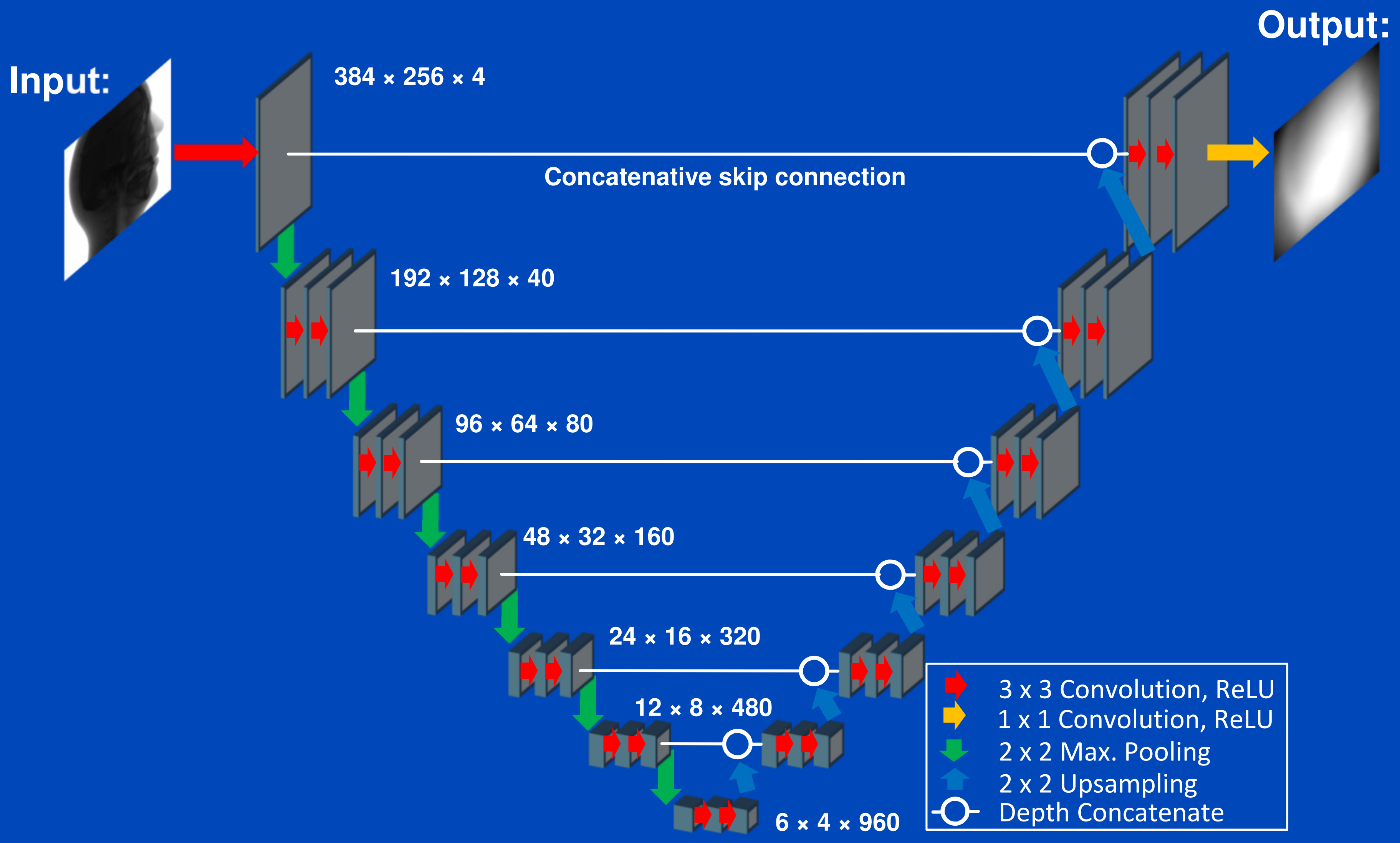

[1]O. Ronneberger, P. Fischer, and T. Brox. U-net: Convolutional networks for biomedical image segmentation. Proc. MICCAI:234-241, 2015.

dkfz.

Generative Adversarial Network[1] (GAN)

- **Useful, if no direct ground truth (GT) is available, the training data are unpaired, unsupervised learning**

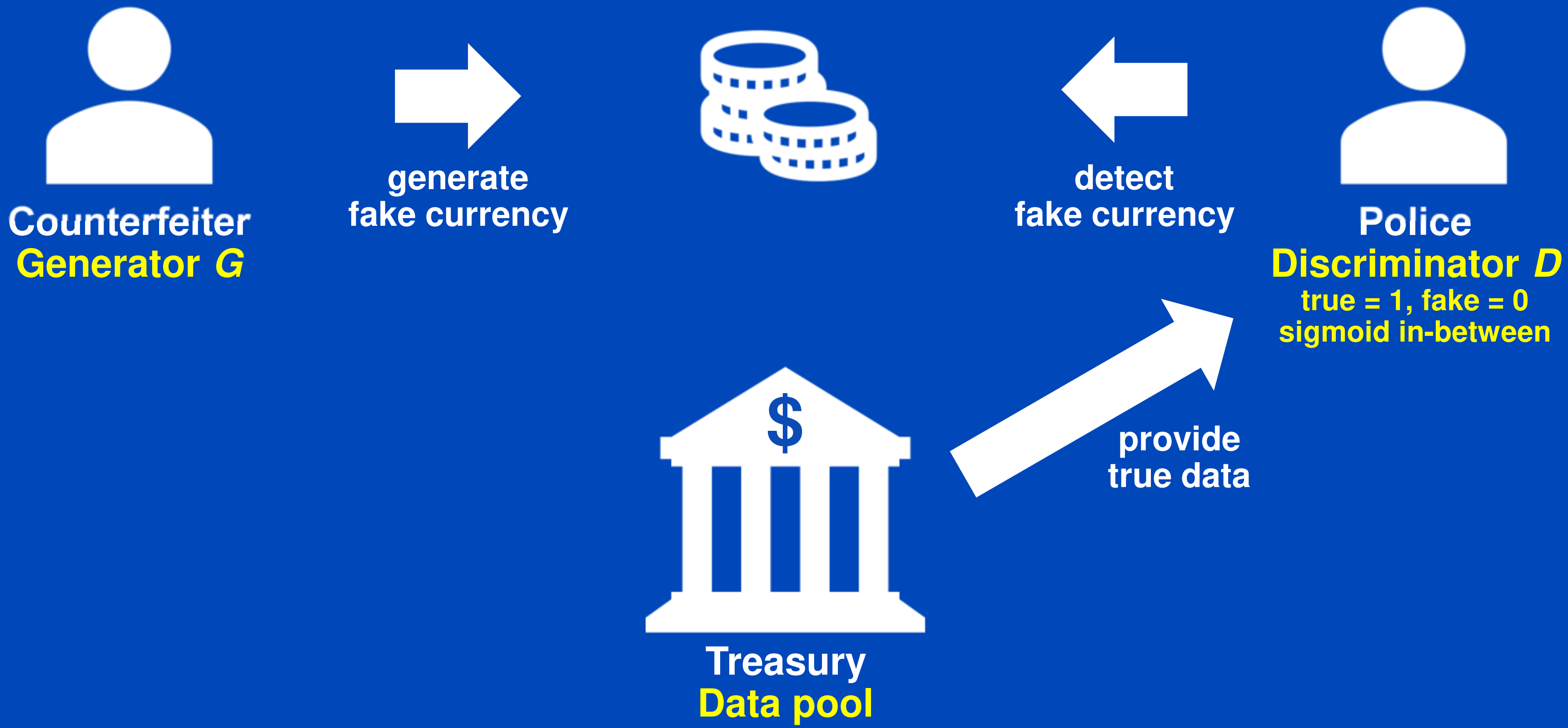

[1]Goodfellow et al. 2014

Generative Adversarial Network (GAN)

- **Typical loss function and minimax game:**

$$\min_{G} \max_{D} L(D, G) := \mathrm{E}_x \ln\big(1 - D(G(x))\big) + \mathrm{E}_y \ln D(y)$$

- **Conditional GAN**[1]
  - Conditinal GANs sample the generator input *x* not from a uniform distribution but from a conditional distribution, e.g. noisy CT images.
  - Need some measure to ensure similarity to input distribution (e.g. pixelwise loss added to the minimax loss function)
- **Cycle GAN**[2]
  - Two GANs (X $\rightarrow$ Y and Y $\rightarrow$ X)
  - Demand cyclic consistency, i.e. $x = G_X(G_Y(x))$ and $y = G_Y(G_X(x))$

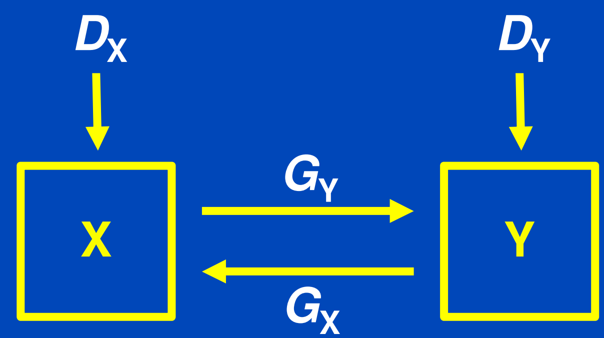

[1]Isola et al. 2017
[2]Zhu et al., 2017

Outline

1. Making up data
2. Noise removal
3. Replacement of lenghty computations
4. Image reconstruction

Part 1:

Making up Data

Limited Angle Example

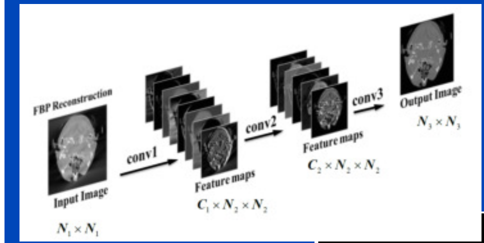

GT FBP (150°) CNN

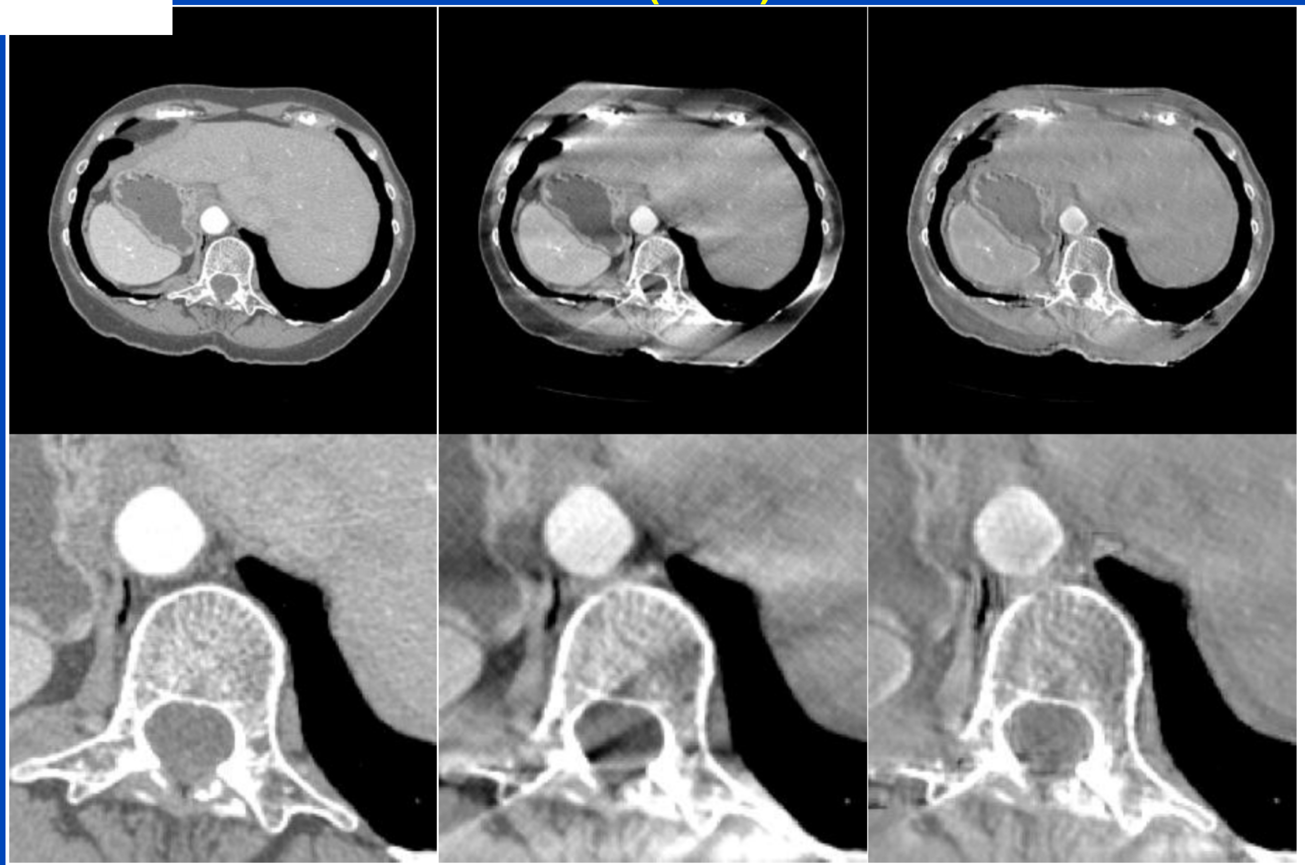

Image Prediction for Limited-Angle Tomography via Deep Learning with Convolutional Neural Network.
Hanming Zhang, Liang Li, Kai Qiao, Linyuan Wang, Bin Yan, Lei Li, Guoen Hu. arXiv 2016.

MAR Example

- Deep CNN-driven patch-based combination of the advantages of several MAR methods trained on simulated artifacts

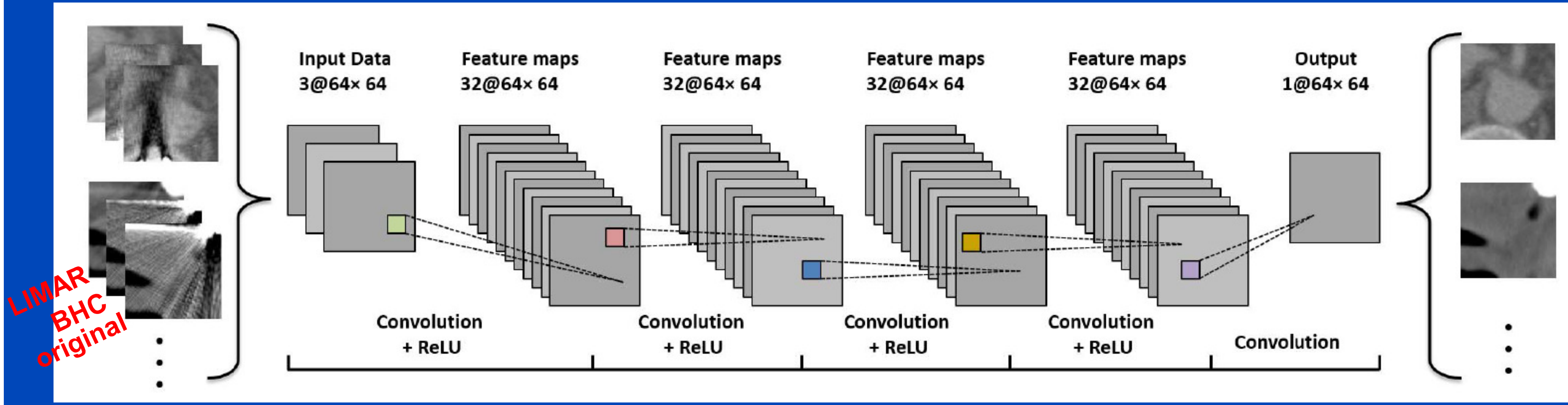

- followed by segmentation into tissue classes
- followed by forward projection of the CNN prior and replacement of metal areas of the original sinogram
- followed by reconstruction

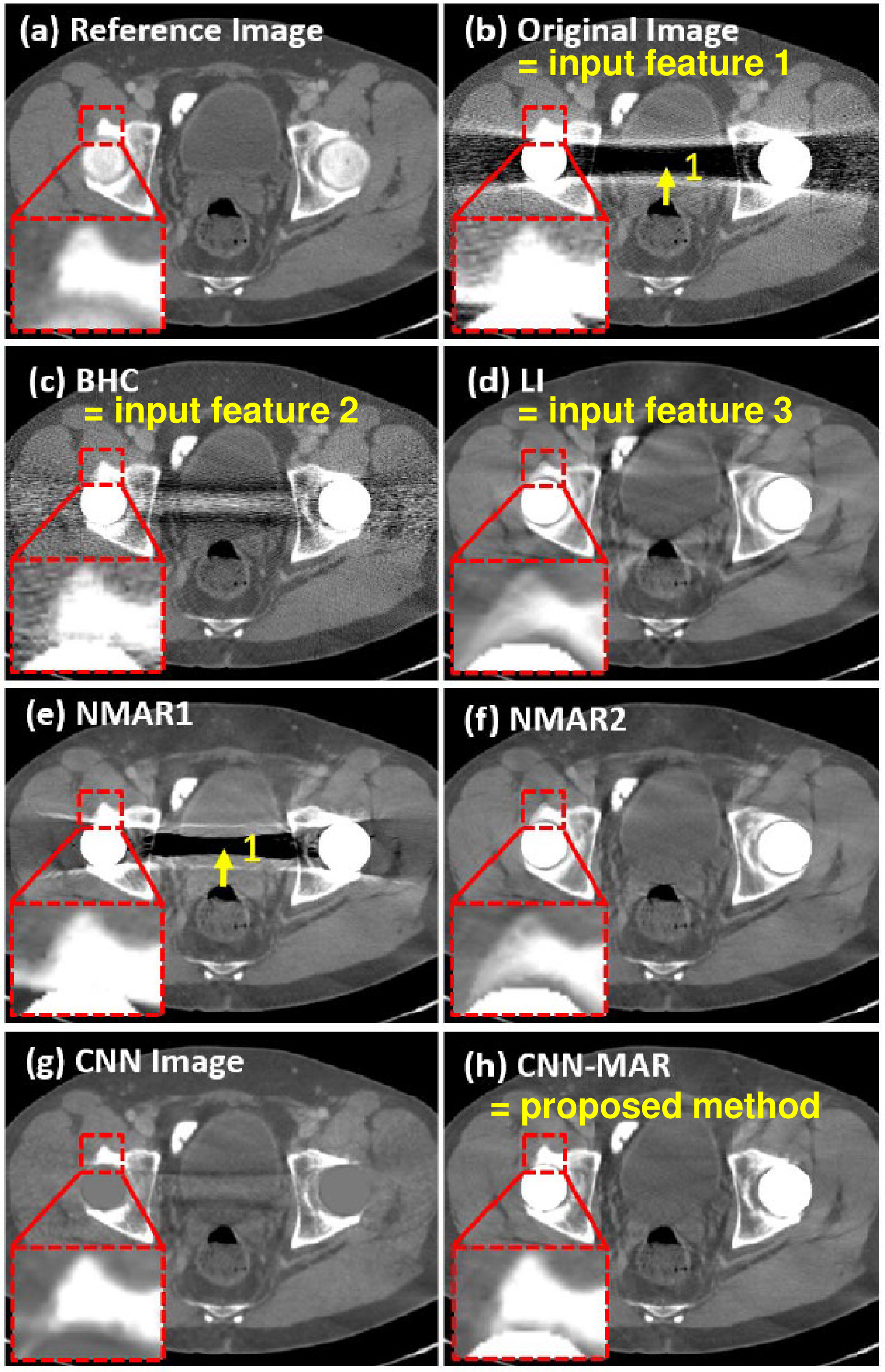
(a) Reference Image
(b) Original Image
= input feature 1
1
(c) BHC
= input feature 2
(d) LI
= input feature 3
(e) NMAR1
1
(f) NMAR2
(g) CNN Image
(h) CNN-MAR
= proposed method

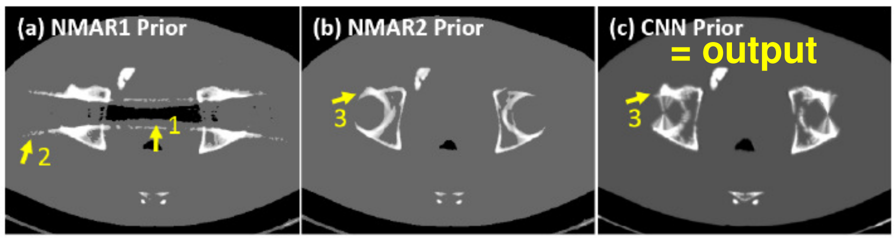
(a) NMAR1 Prior
1
2
(b) NMAR2 Prior
3
(c) CNN Prior
= output
3

MAR without Machine Learning is a Good Alternative: Frequency Split Normalized MAR[1,2]

Uncorrected FSLIMAR FSNMAR

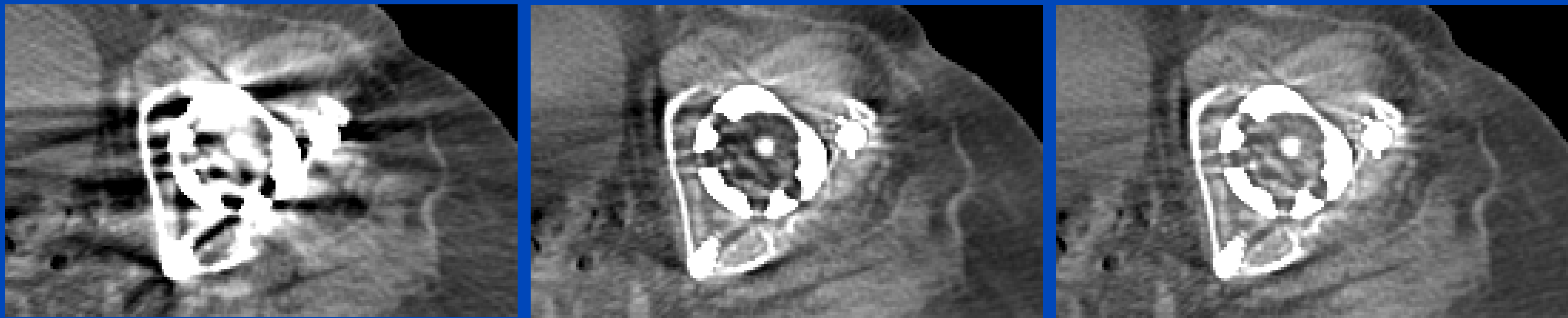

Patient with bilateral hip prosthesis, Somatom Definition Flash, (C=40/W=500).

[1]E. Meyer, M. Kachelrieß. Normalized metal artifact reduction (NMAR) in computed tomography. Med. Phys. 37(10):5482-5493, Oct. 2010.

[2]E. Meyer, M. Kachelrieß. Frequency split metal artifact reduction (FSMAR) in CT. Med. Phys. 39(4):1904-1916, April 2012.

Resolution Improvement Example

- 2D U-net to converts 5 mm thick images into 1 mm ones.
- E.g. to “replace a scanning protocol for a 1 mm slice with a 5 mm protocol”

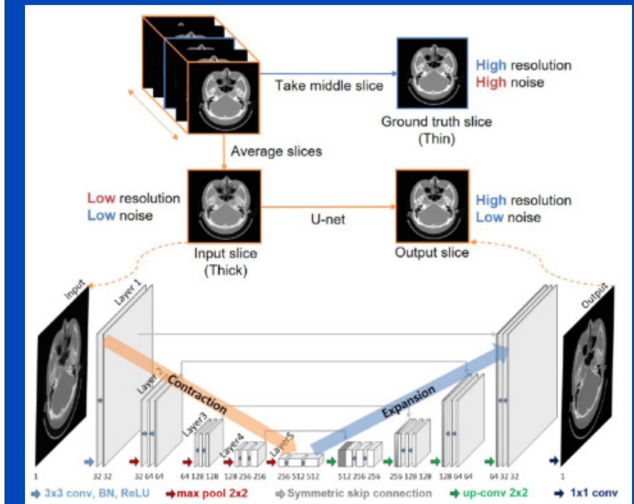

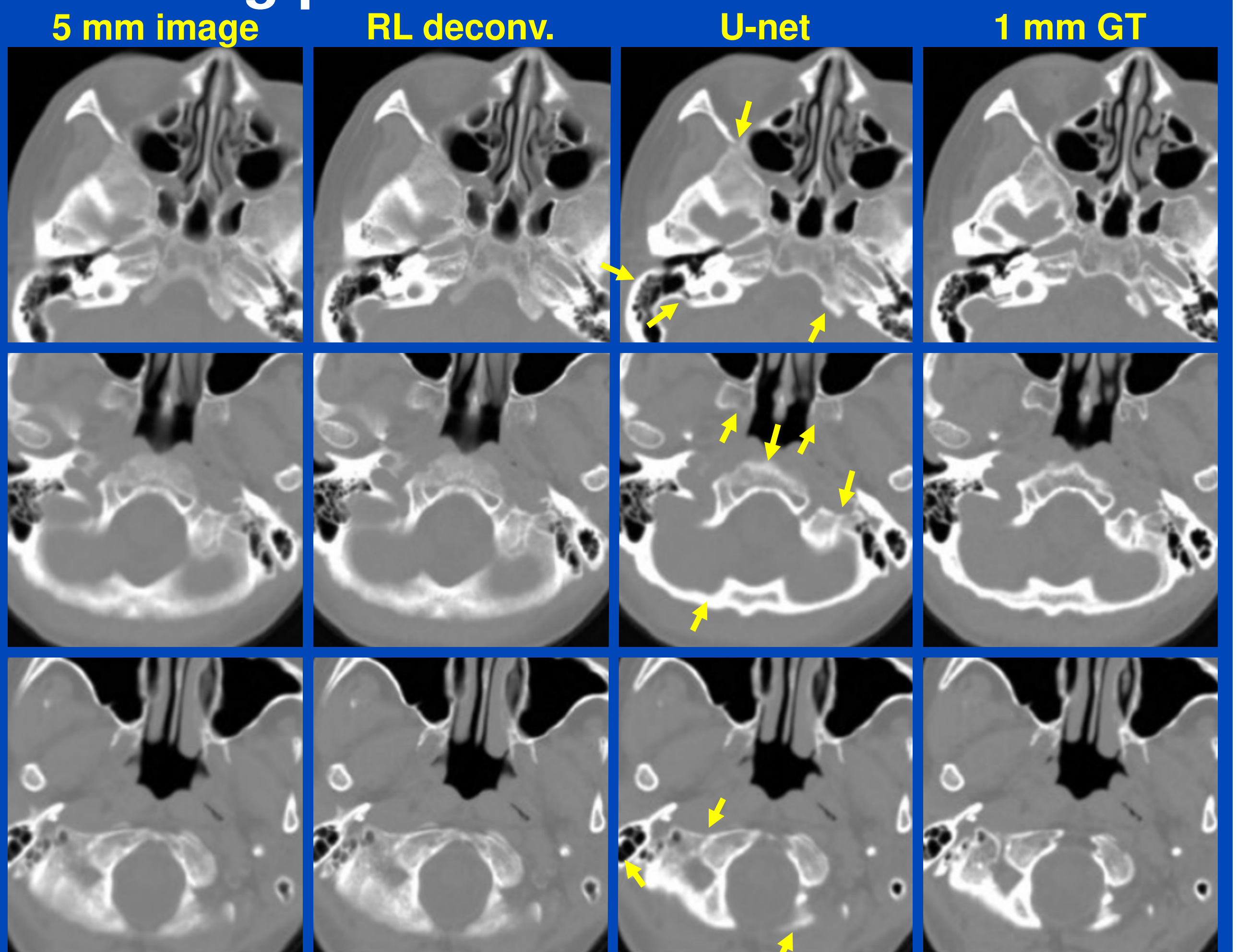

Junyoung Park, Donghwi Hwang, Kyeong Yun Kim, Seung Kwan Kang, Yu Kyeong Kim and Jae Sung Lee. Computed tomography super-resolution using deep convolutional neural network. Phys. Med. Biol. 63: 145011, 2018

dkfz.

Sparse View Restoration Example

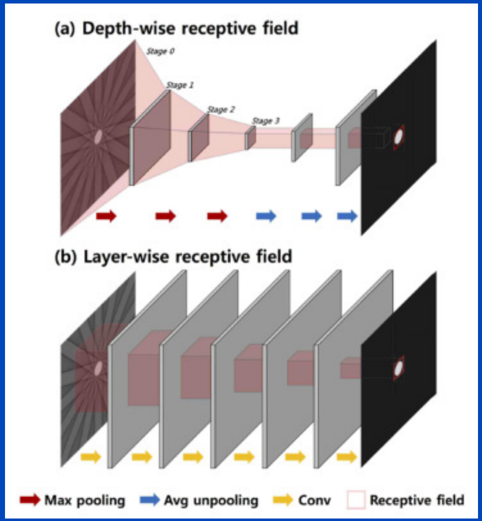

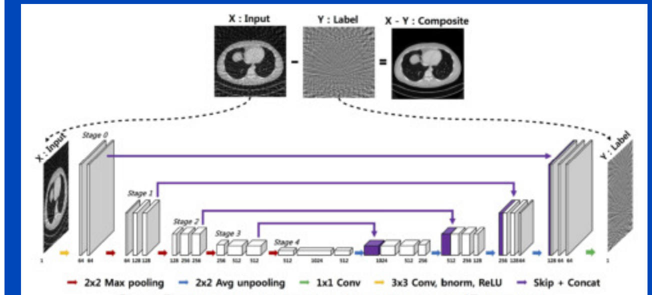

Figure 1. The proposed deep residual learning architecture for sparse view CT reconstruction.

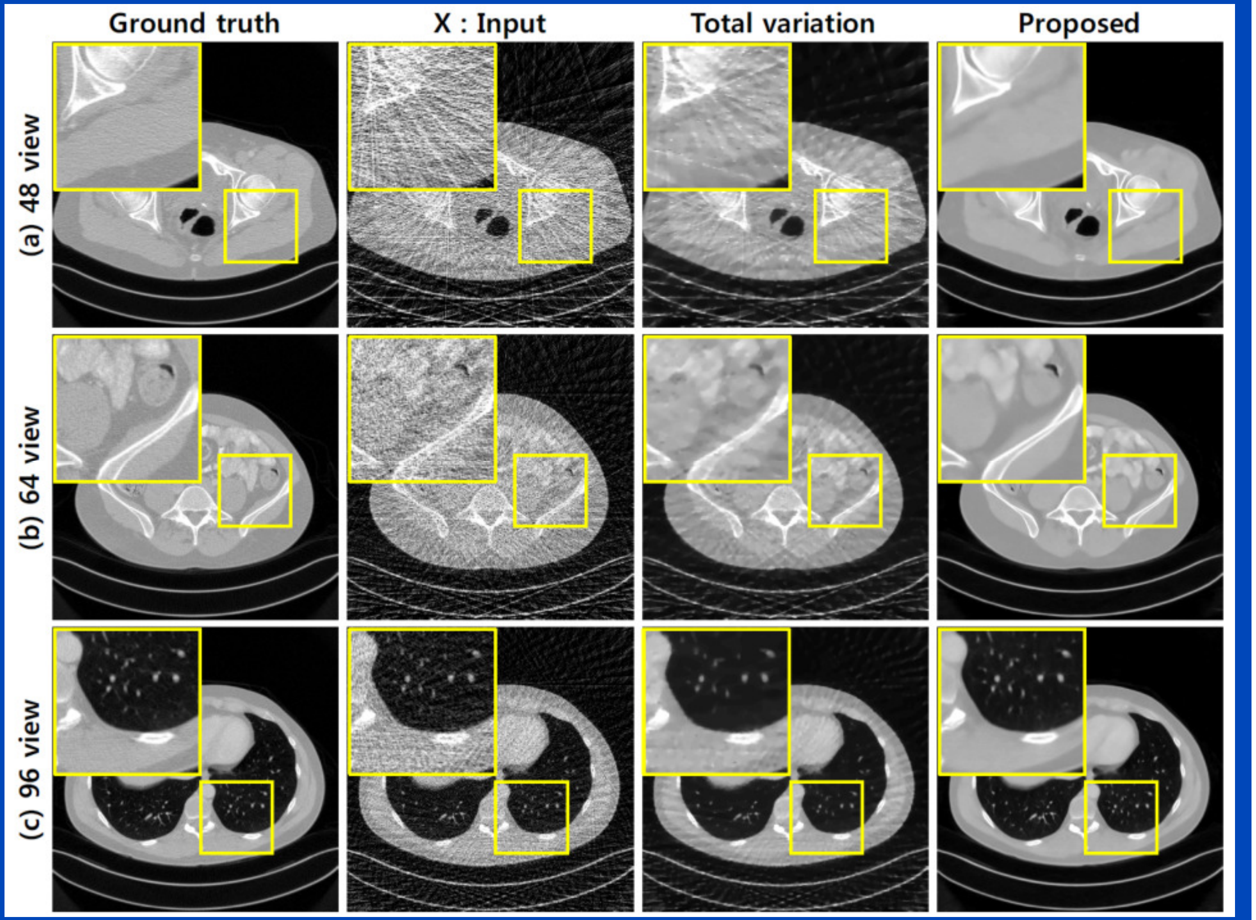

Yo Seob Han, Jaejun Yoo and Jong Chul Ye. Deep Residual Learning for Compressed Sensing CT Reconstruction via Persistent Homology Analysis. ArXiv 2016.

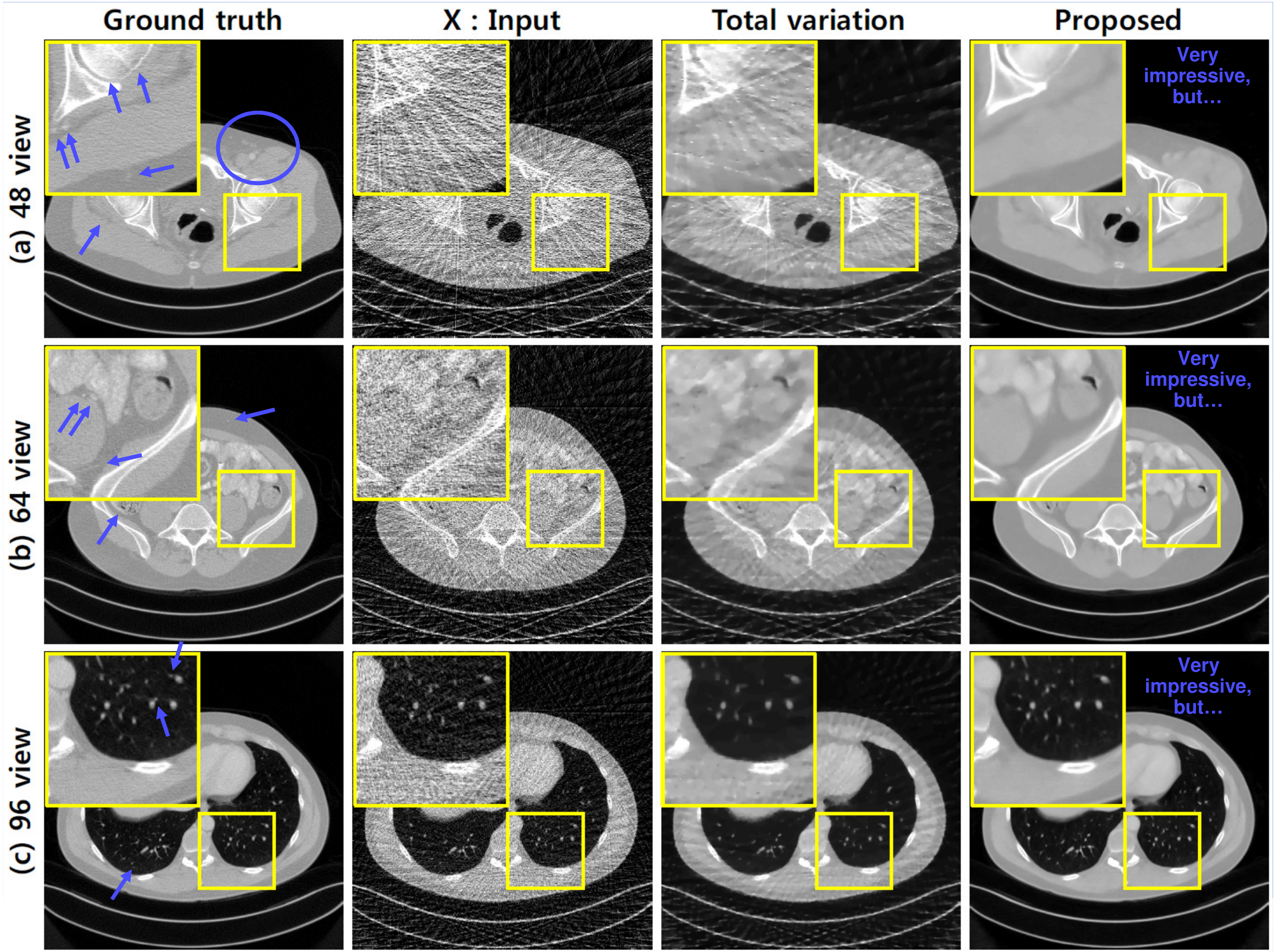
Ground truth
X : Input
Total variation
Proposed
(a) 48 view
(b) 64 view
(c) 96 view
Very impressive, but…
Very impressive, but…
Very impressive, but…

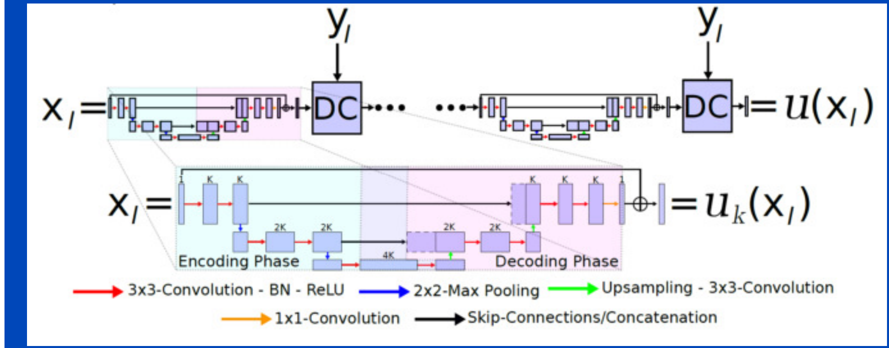

Sparse CT Recon with Data Consistency Layers (DCLs)

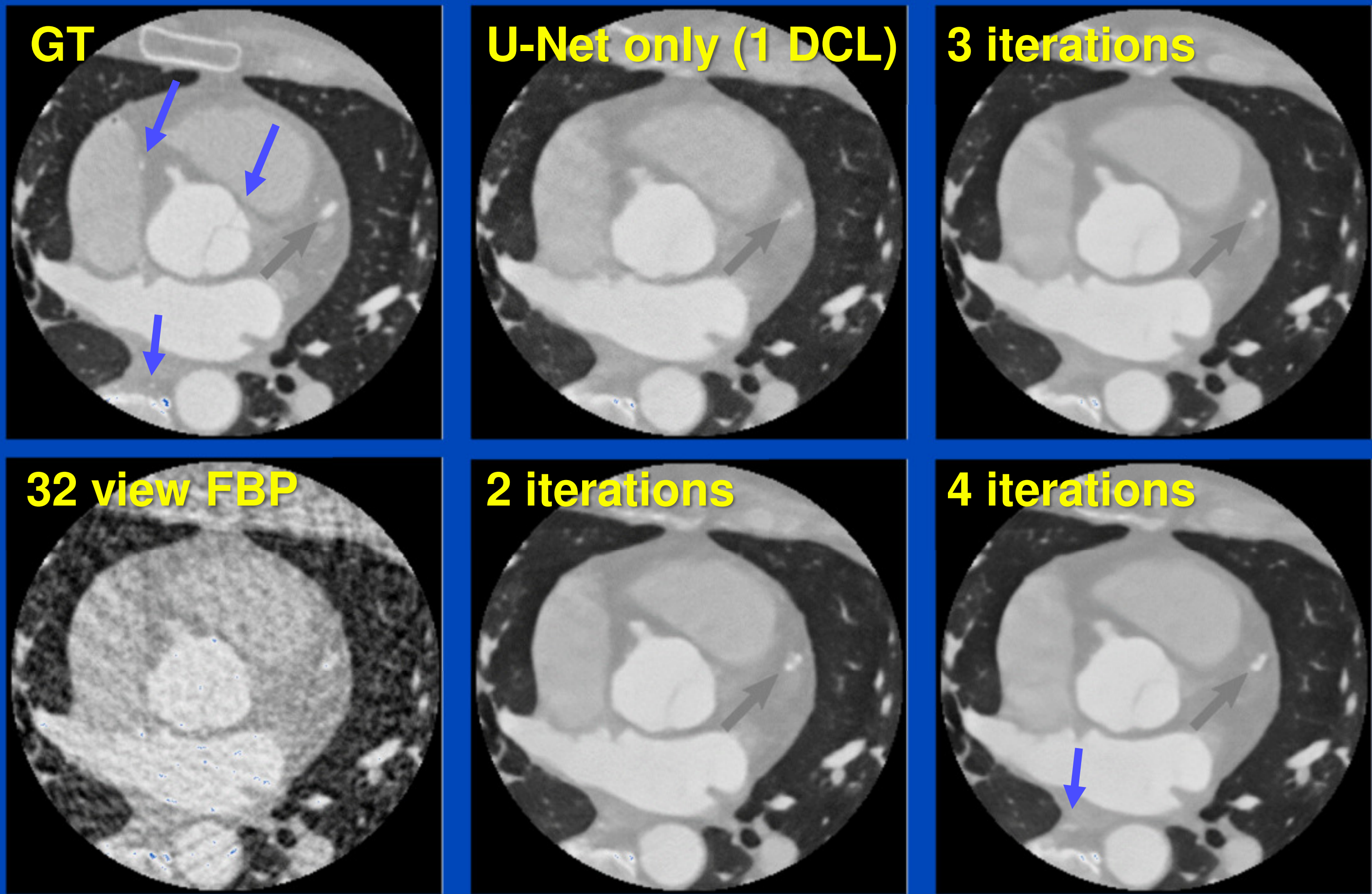

A. Kofler, M. Haltmeier, C. Kolbitsch, M. Kachelrieß, and M. Dewey. A U-Nets Cascade for Sparse View Computed Tomography, MICCAI 2018

Part 2:

Noise Removal

Noise Removal Example 1

- 3-layer CNN uses low dose and corresponding normal dose image patches for training

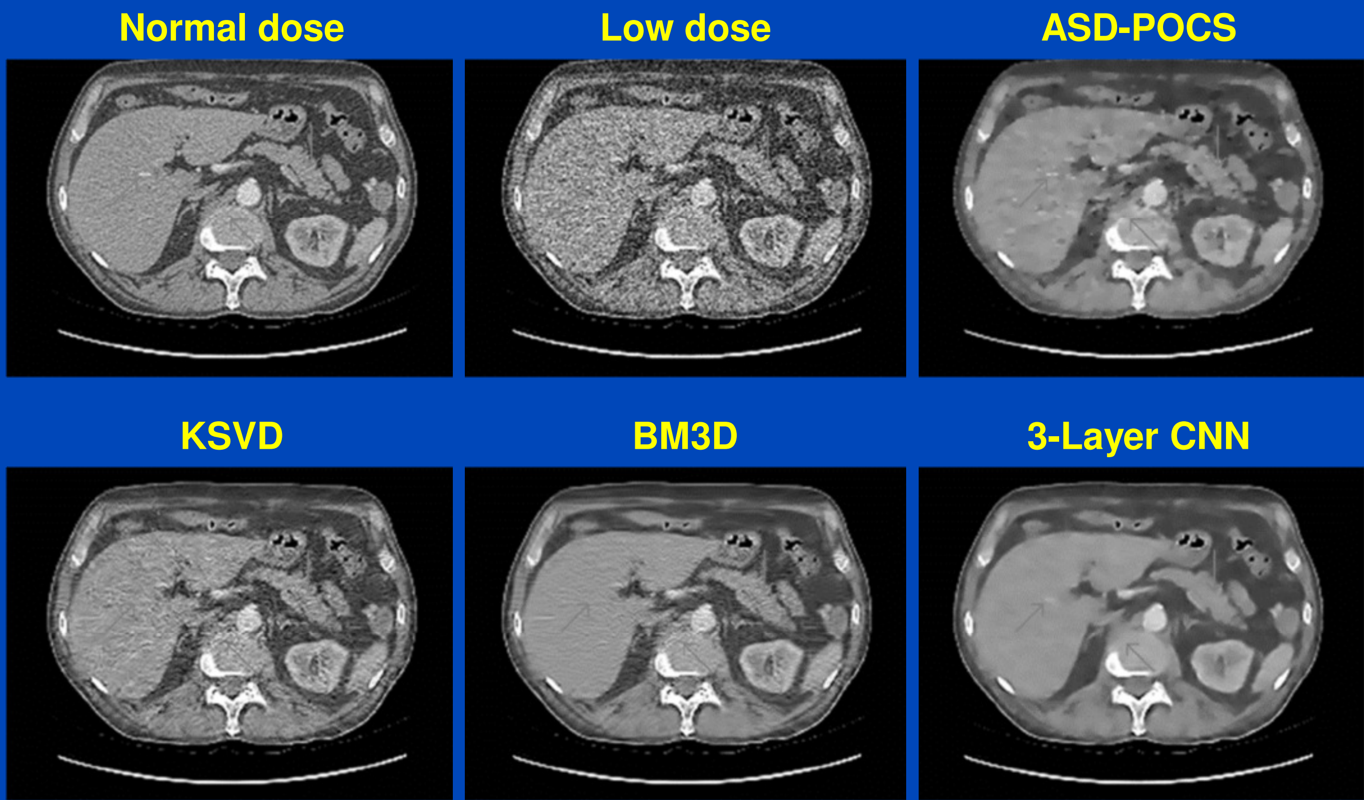

Hu Chen, Yi Zhan, Weihua Zhang, Peixi Liao, Ke Li, Jiliu Zhou, and Ge Wang. Low-dose CT via convolutional neural network. Biomedical Optics Express 8(2):278381, February 2017.

Noise Removal Example 2

- Task: Reduce noise from low dose CT images.
- A conditional generative adversarial networks (GAN) is used
- Generator *G*:
  - 3D CNN that operates on small cardiac CT sub volumes
  - Seven 3×3×3 convolutional layers yielding a receptive field of 15×15×15 voxels for each destination voxel
  - Depths (features) from 32 to 128
  - Batch norm only in the hidden layers
  - Subtracting skip connection
- Discriminator *D*:
  - Sees either routine dose image or a generator-denoised low dose image
  - Two 3×3×3 layers followed by several 3×3 layers with varying strides
  - Feedback from *D* prevents smoothing.
- Training:
  - Unenhanced (why?) patient data acquired with Philips Briliance iCT 256 at 120 kV.
  - Two scans (why?) per patient, one with 0.2 mSv and one with 0.9 mSv effective dose.

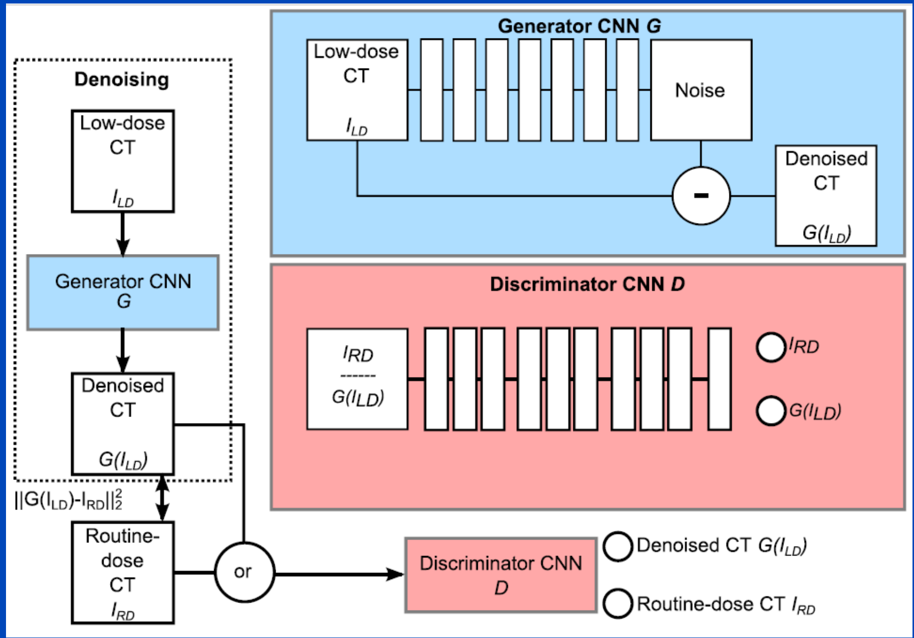

J. Wolterink, T. Leiner, M. Viergever, and I. Išgum. Generative Adversarial Networks for Noise Reduction in Low-Dose CT. IEEE TMI 36(12):2536-2544, Dec. 2017.

Noise Removal Example 2

- G_1 and G_2 include supervised learning and thus perform only with phantom measurements.
- G_3 is unsupervised.
- G_3 is said to generate images with a more similar appearance to the routine-dose CT. Feedback from the discriminator D prevents smoothing the image.

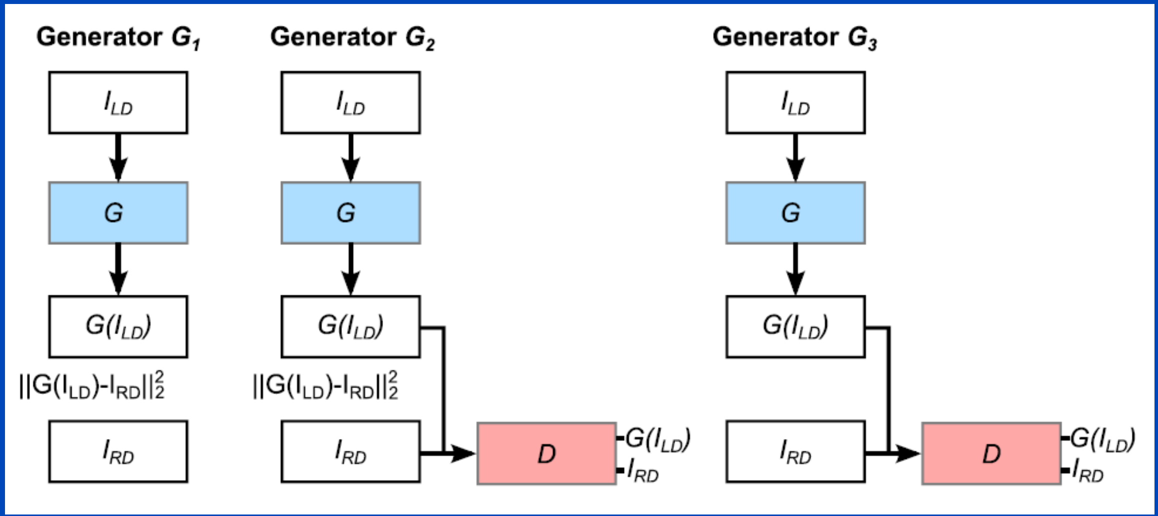

J. Wolterink, T. Leiner, M. Viergever, and I. Išgum. Generative Adversarial Networks for Noise Reduction in Low-Dose CT. IEEE TMI 36(12):2536-2544, Dec. 2017.

Noise Removal Example 2

Low dose image (0.2 mSv)

Noise Removal Example 2

iDose level 3 reconstruction (0.2 mSv)

J. Wolterink, T. Leiner, M. Viergever, and I. Išgum. Generative Adversarial Networks for Noise Reduction in Low-Dose CT. IEEE TMI 36(12):2536-2544, Dec. 2017.

Noise Removal Example 2

Denoised low dose image (0.2 mSv)

J. Wolterink, T. Leiner, M. Viergever, and I. Išgum. Generative Adversarial Networks for Noise Reduction in Low-Dose CT. IEEE TMI 36(12):2536-2544, Dec. 2017.

Noise Removal Example 2

Normal dose image (0.9 mSv)

J. Wolterink, T. Leiner, M. Viergever, and I. Išgum. Generative Adversarial Networks for Noise Reduction in Low-Dose CT. IEEE TMI 36(12):2536-2544, Dec. 2017.

dkfz.

Noise Removal Example 3

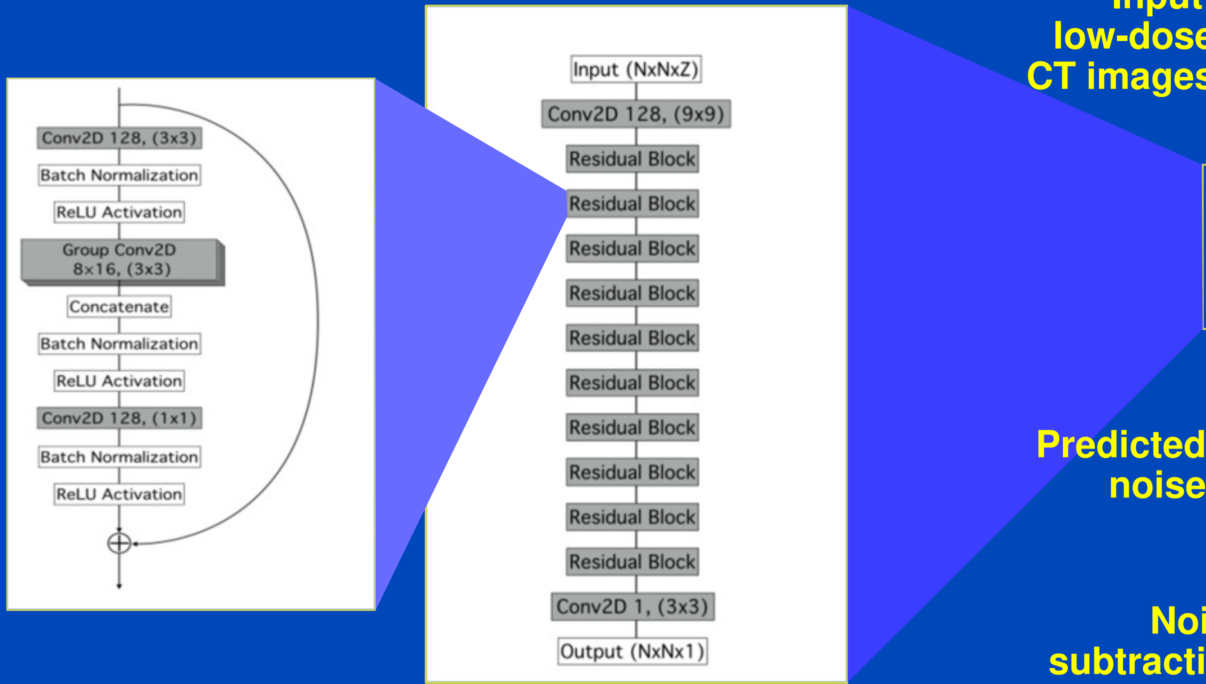

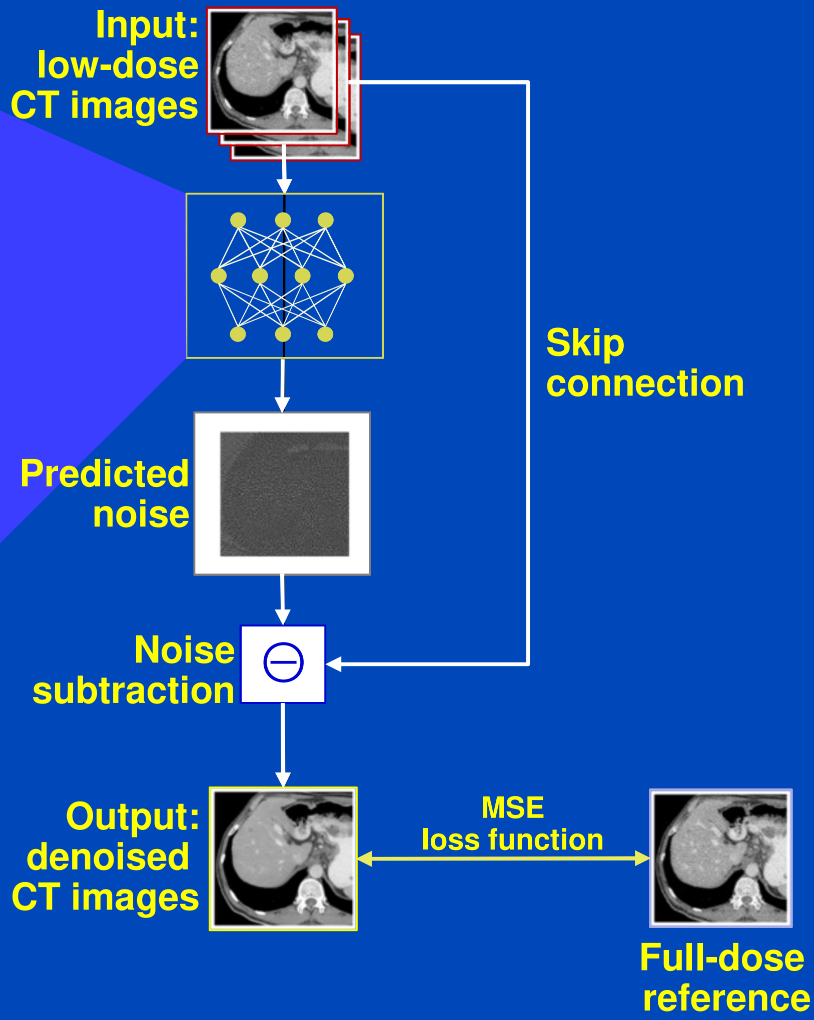

- Architecture based on state-of-the art networks for image classification (ResNet).
- 32 conv layers with skip connections
- About 2 million tunable parameters in total
- Input is arbitrarily-size stack of images, with a fixed number of adjacent slices in the channel/feature dimension.

Andrew D. Missert, Shuai Leng, Lifeng Yu, and Cynthia H. McCollough. Noise Subtraction for Low-Dose CT Images Using a Deep Convolutional Neural Network. Proceedings of the 5th CT-Meeting: 399-402, 2018.

Noise Removal Example 3

Low dose images (1/4 of full dose)

Noise Removal Example 3

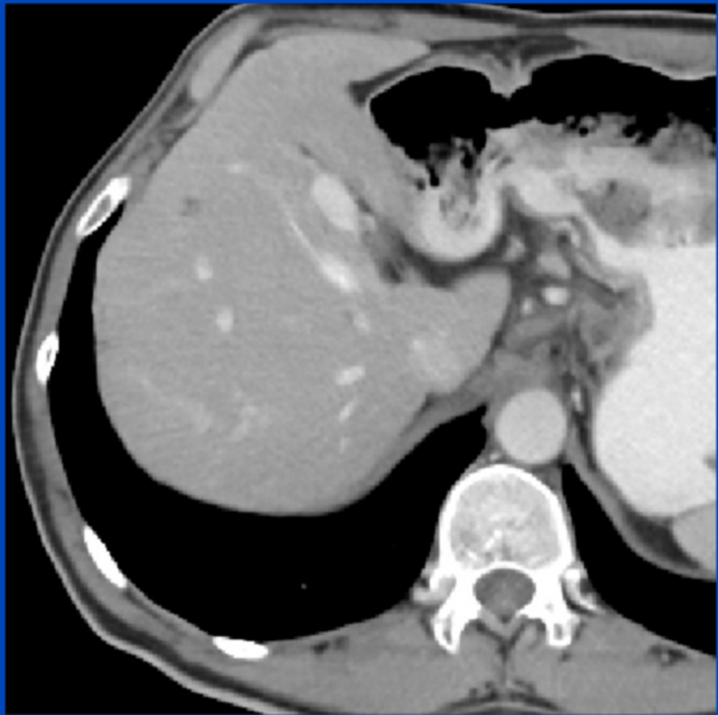

Denoised low dose

Andrew D. Missert, Shuai Leng, Lifeng Yu, and Cynthia H. McCollough. Noise Subtraction for Low-Dose CT Images Using a Deep Convolutional Neural Network. Proceedings of the 5th CT-Meeting: 399-402, 2018.

Noise Removal Example 3

Full dose

Andrew D. Missert, Shuai Leng, Lifeng Yu, and Cynthia H. McCollough. Noise Subtraction for Low-Dose CT Images Using a Deep Convolutional Neural Network. Proceedings of the 5th CT-Meeting: 399-402, 2018.

Noise Removal Example 3

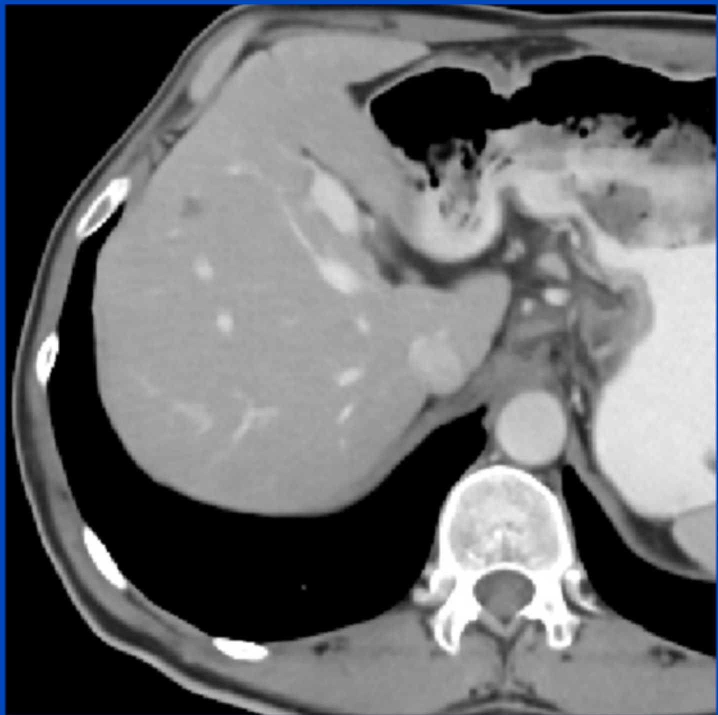

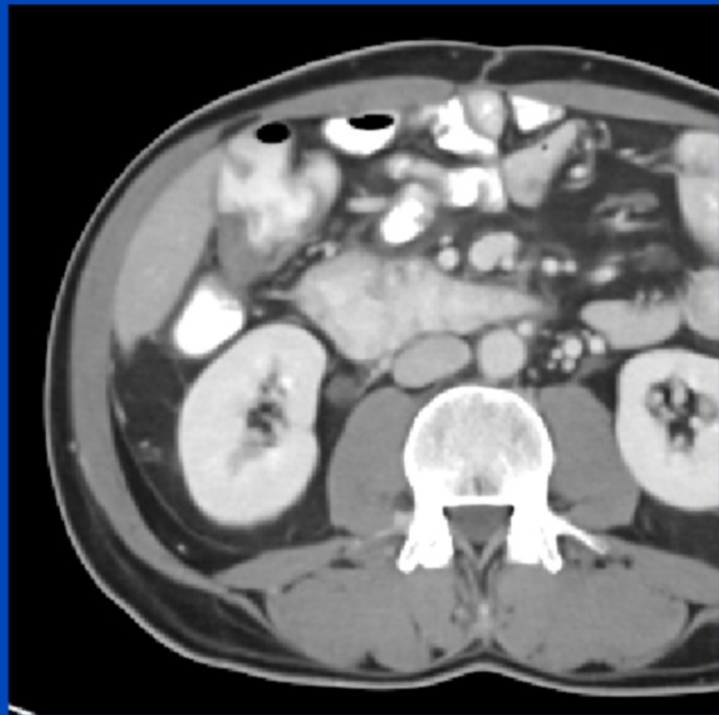

Denoised full dose

Noise Removal Example 4

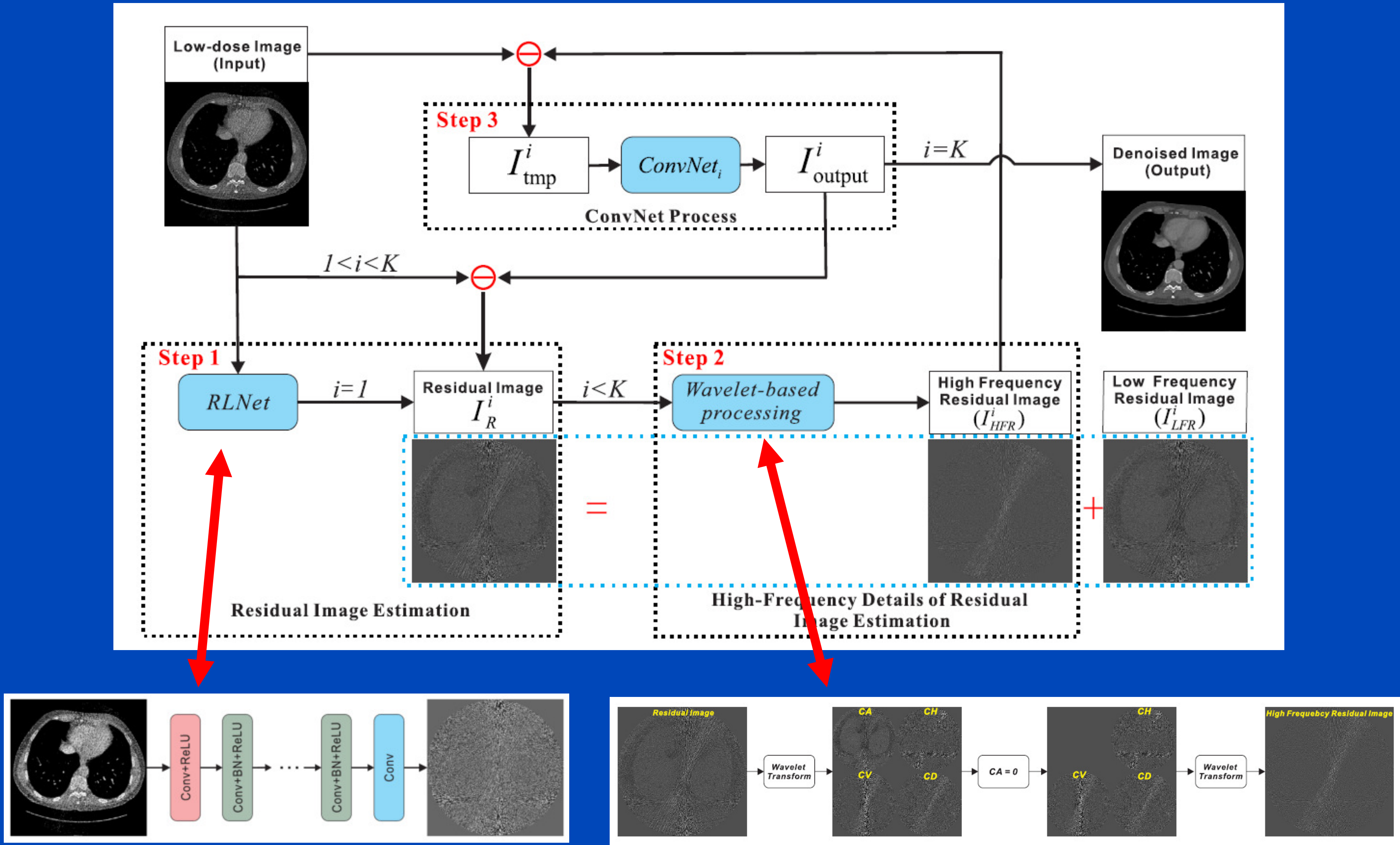

Y. Wang et al. Iterative quality enhancement via residual-artifact learning networks for low-dose CT.
Phys. Med. Biol. 63:215004, 2018.

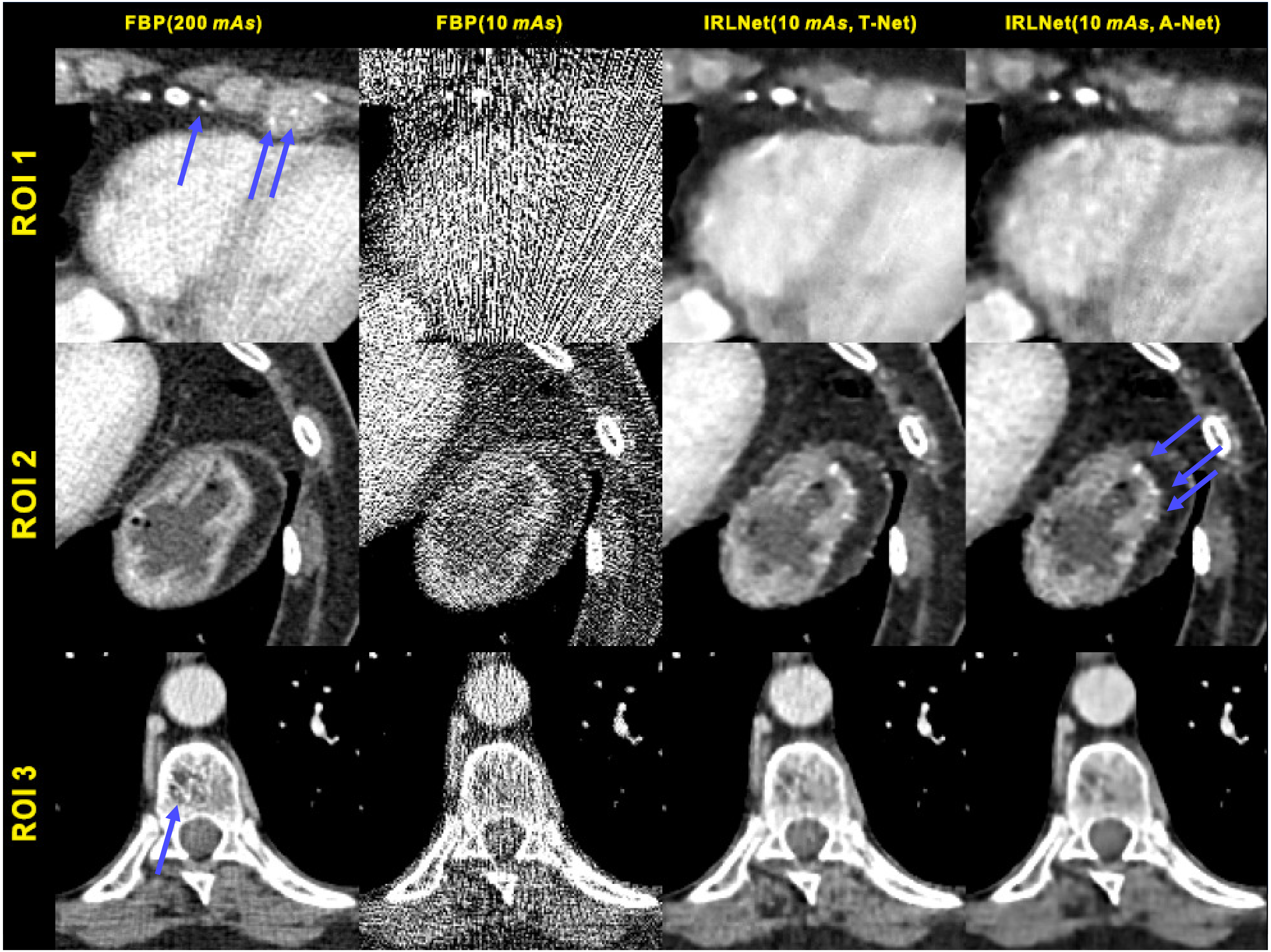

FBP(200 *mAs*)
FBP(10 *mAs*)
IRLNet(10 *mAs*, T-Net)
IRLNet(10 *mAs*, A-Net)
ROI 1
ROI 2
ROI 3

Noise Removal Example 5

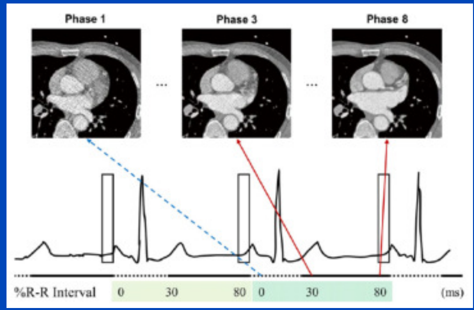

- ECG-based TCM yields cardiac phases with high noise.
- Train a cycle GAN that learns from the low noise phases to remove noise in the high noise phases.
- 50 patient cases used for training.
- Nice results!

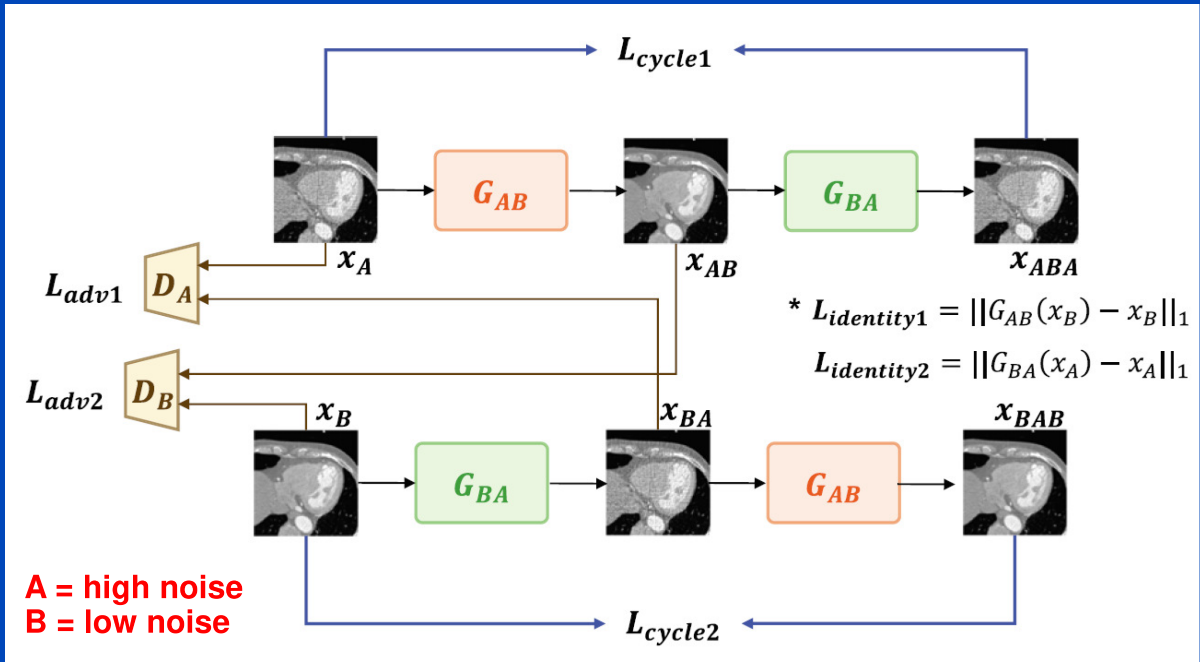

E. Kang, J.C. Ye et al. Cycle-consistent adversarial denoising network for multiphase coronary CT angiography. Med. Phys. 46(2), February 2019.

dkfz.

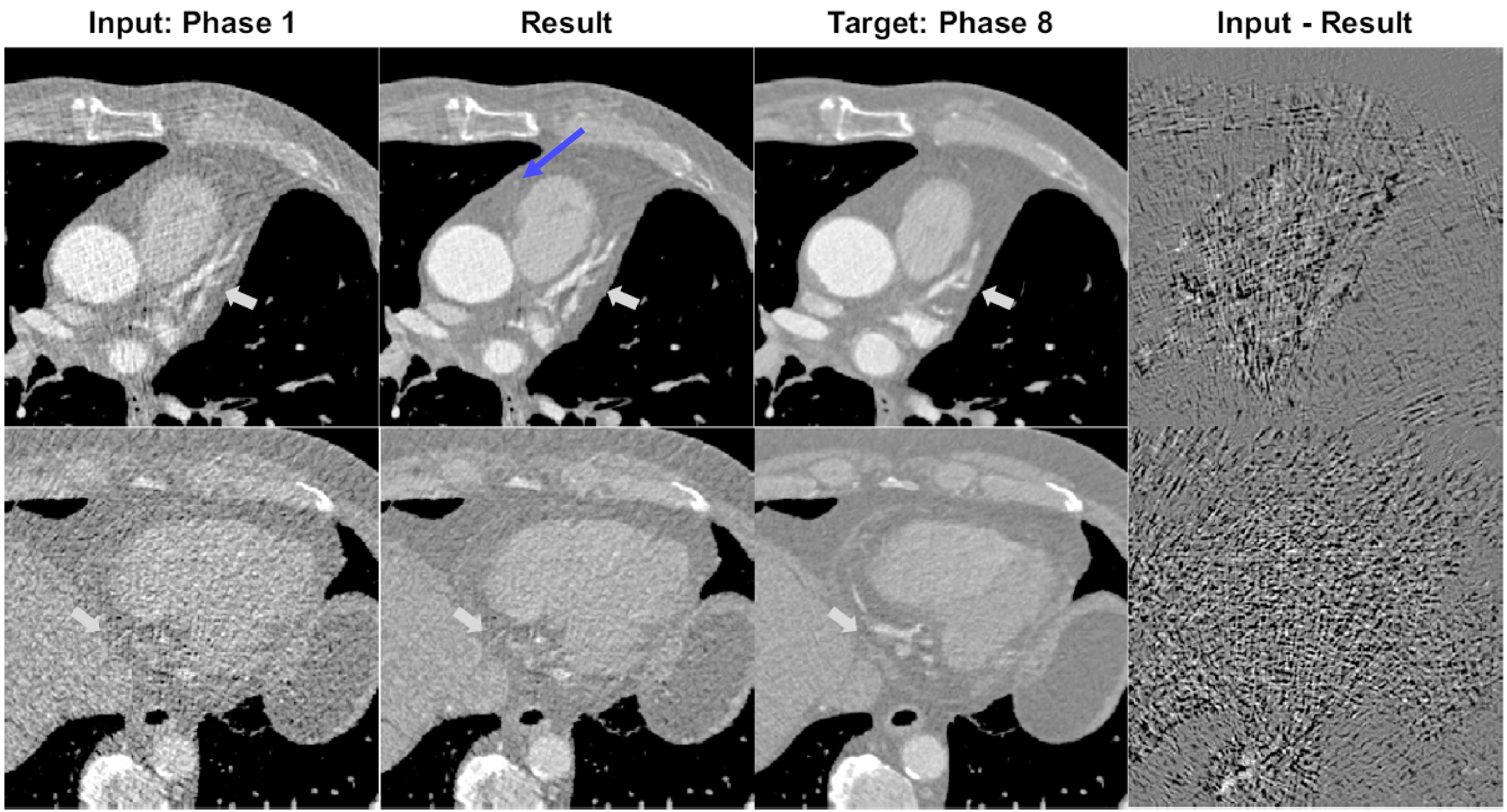

Input: Phase 1
Result
Target: Phase 8
Input - Result

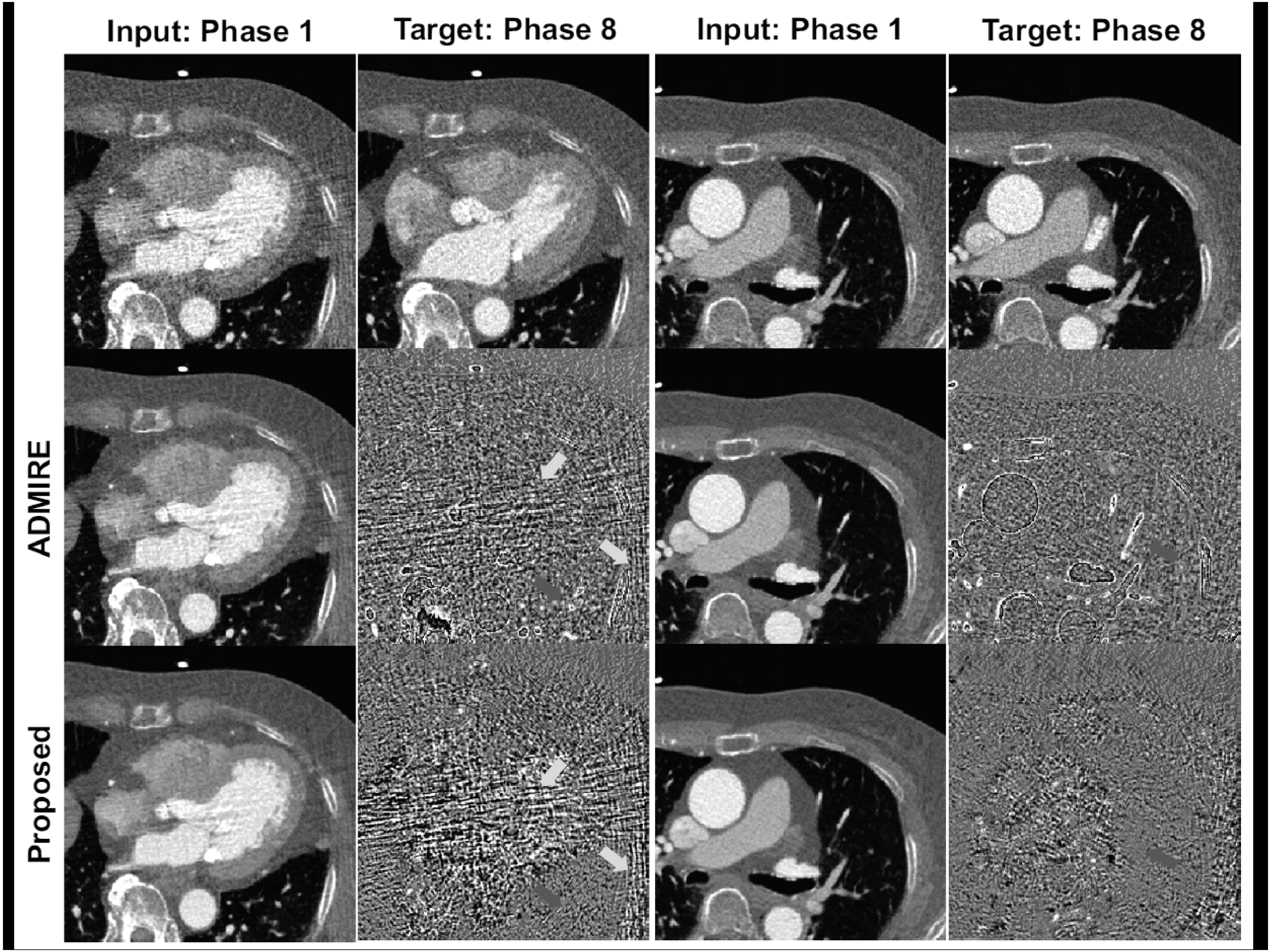

Input: Phase 1
Target: Phase 8
Input: Phase 1
Target: Phase 8
ADMIRE
Proposed

Noise Removal Example 6
Canon‘s AiCE

- Ba
- Tr
  pr
- FI
  hi

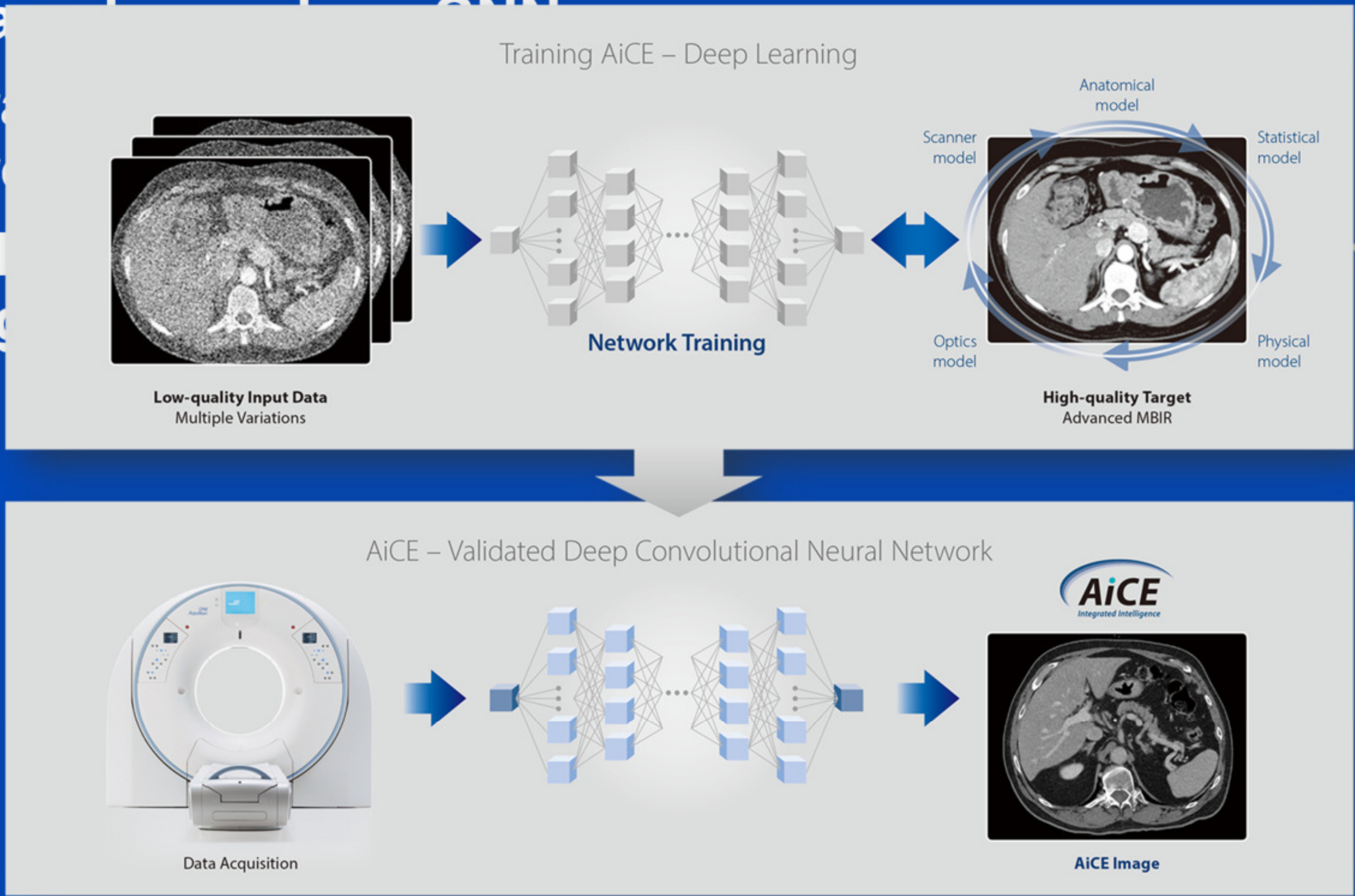

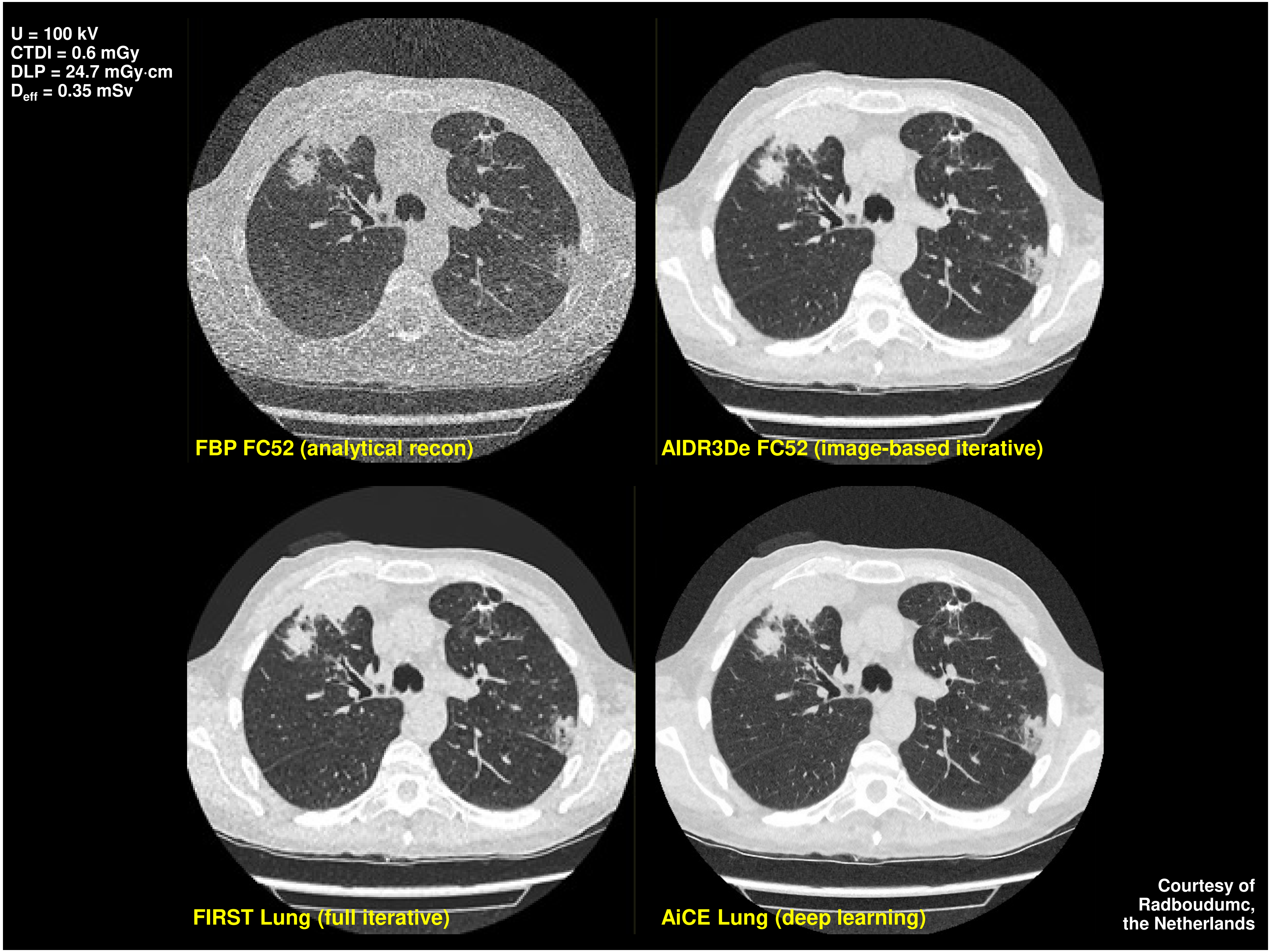
U = 100 kV
CTDI = 0.6 mGy
DLP = 24.7 mGy·cm
D_{eff} = 0.35 mSv
FBP FC52 (analytical recon)
AIDR3De FC52 (image-based iterative)
FIRST Lung (full iterative)
AiCE Lung (deep learning)
Courtesy of
Radboudumc,
the Netherlands

Part 3:

Replacement of Lengthy Computations

Empirical Shading Correction: ScatterNet

- Net to convert CBCT log (why?) rawdata into artifact-free data.
- Net architecture:
  - Small receptive field spectrum converter block adapts the attenuation values.
  - Residual U-Net then follows to account for scatter.
- Pixel-wise loss function comparing the corrected CBCT projections with those of the reference shading correction method.
- Reference shading correction method:
  - Use data from a clinical CT scan as an artifact-free prior.
  - Intensity domain frequency split between planning CT and CBCT:
    - » Deformably register planning CT onto CBCT and forward project and exponentiate to obtain “ideal” intensity data
    - » Scale CBCT intensities to match the prior CT intensities
    - » Corrected intensities = LP(forward proj. CT)+HP(scaled uncorr. CBCT)
- ScatterNet replaces the previous correction method and thus speeds up computation and does not make use of the planning CT.

ScatterNet

Spectrum converter block

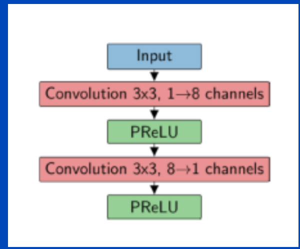

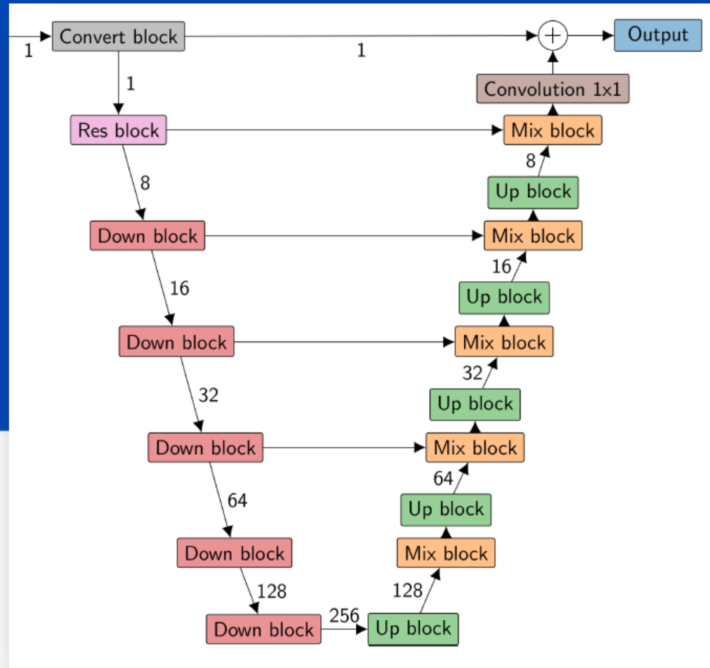

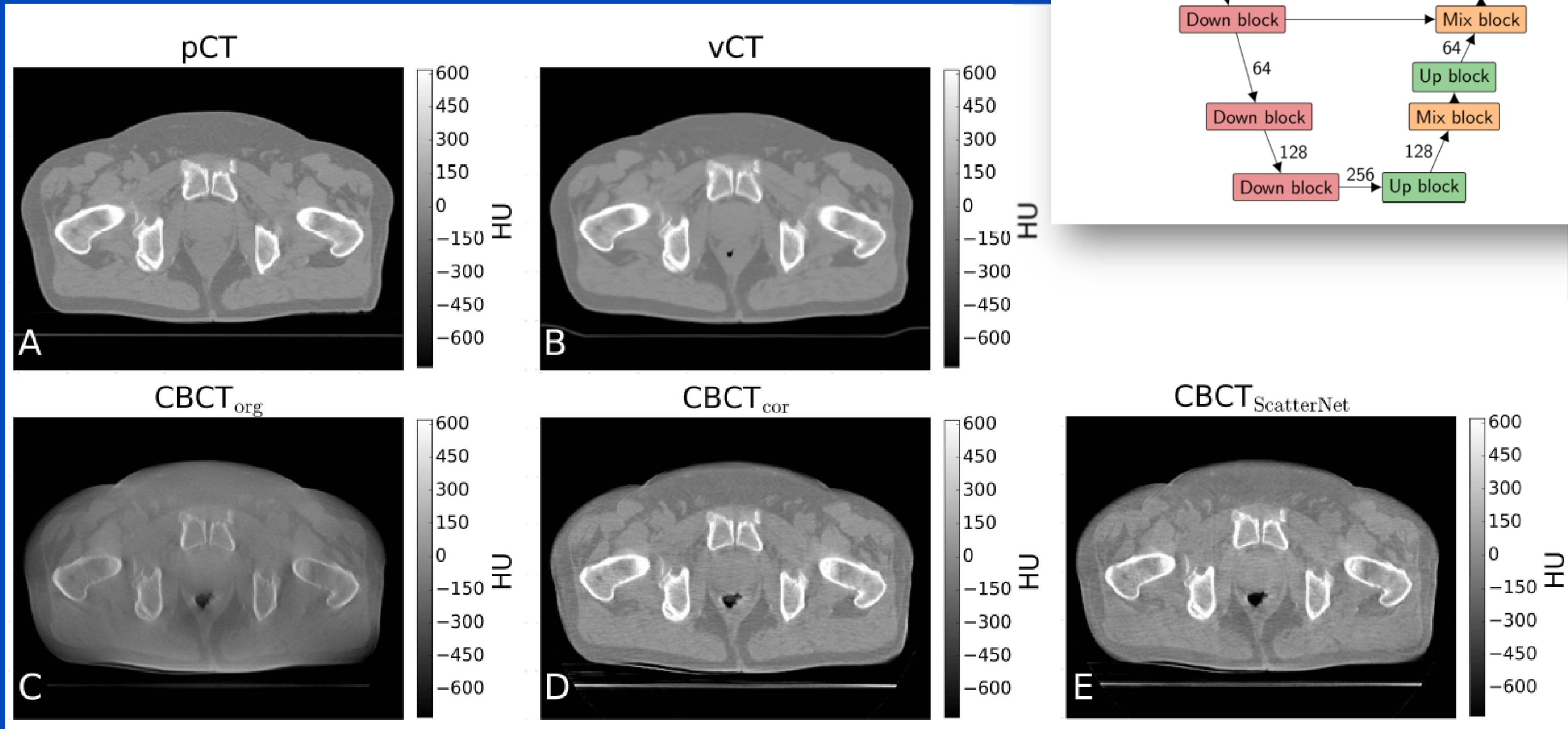

D. Hansen, K. Parodi et al. ScatterNet: A convolutional neural network for cone-beam CT intensity correction, MedPhys, Sep. 2018.

Scatter (or Shading) Correction by Frequency Split (FS)

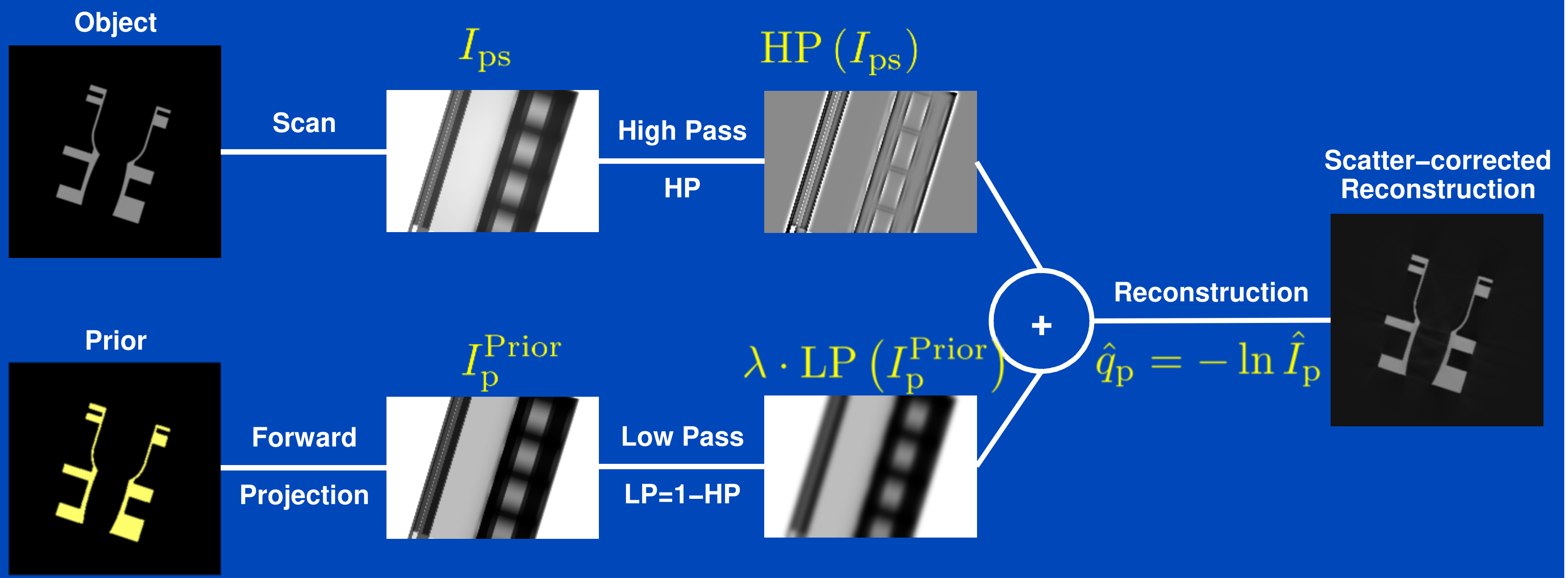

Similar method has been proposed by Niu et al. Med.Phys 37(10), pp. 5395 ff.

Scatter is Non-Smooth in Log and in Image Domain

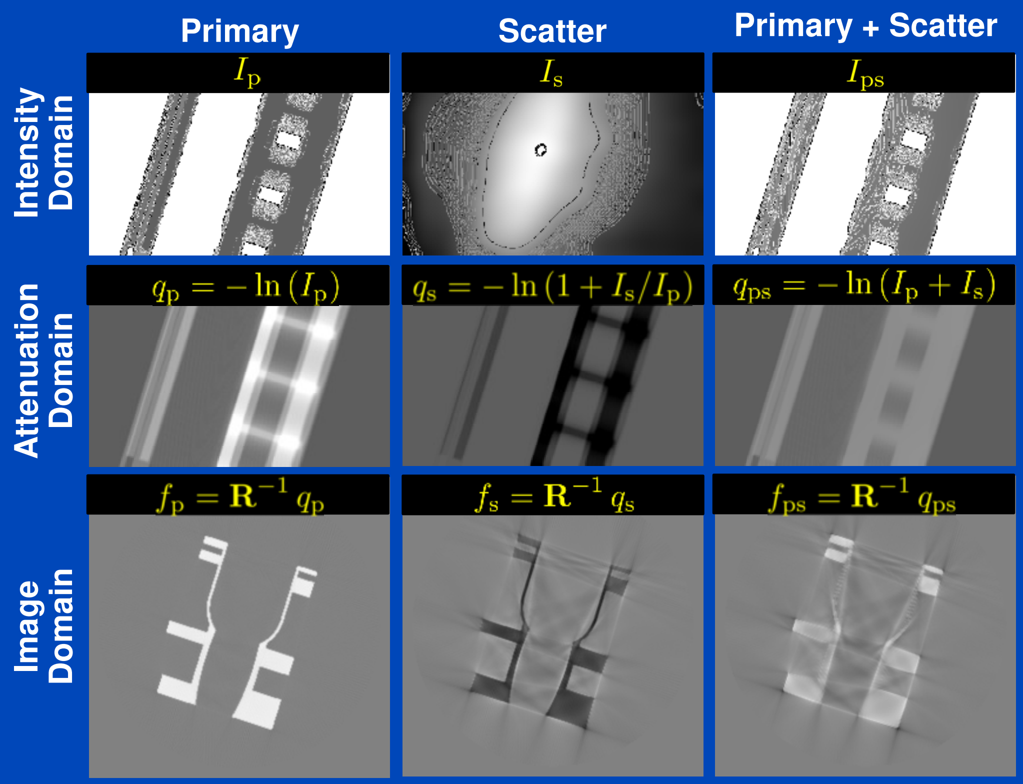

Scatter is Smooth only in Intensity Domain!

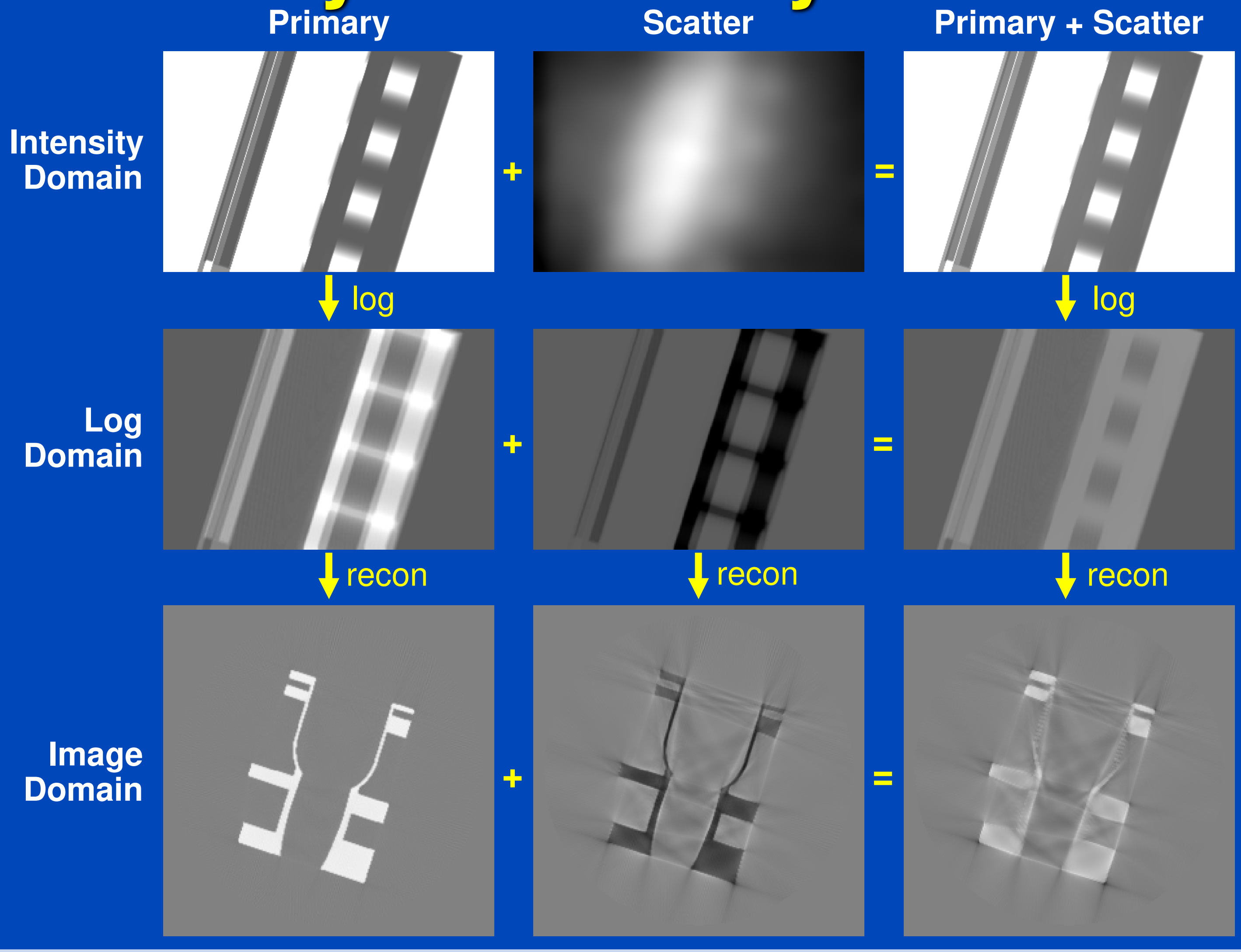

Scatter is Smooth only in Intensity Domain!

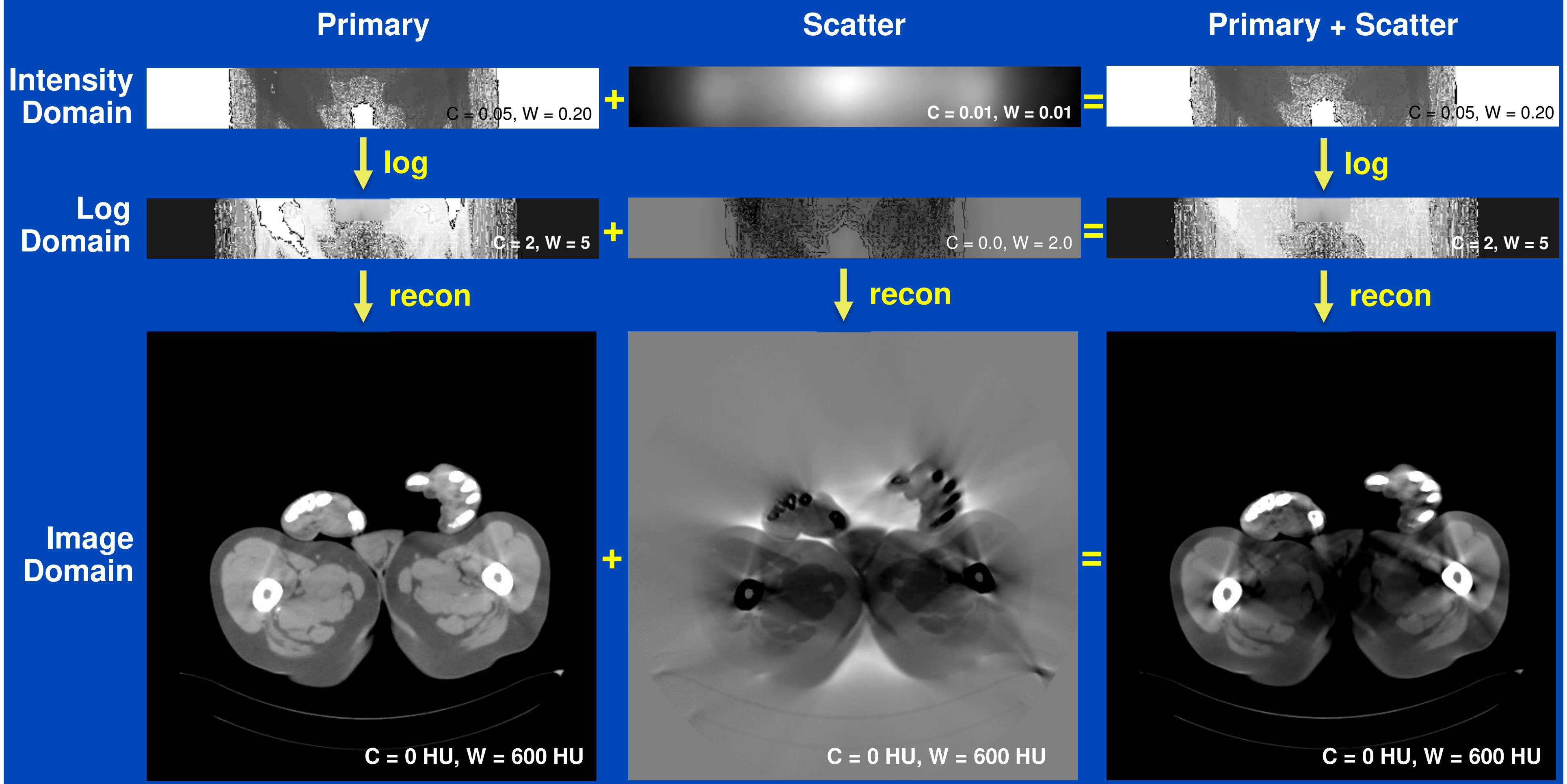

Scatter is Smooth only in Intensity Domain!

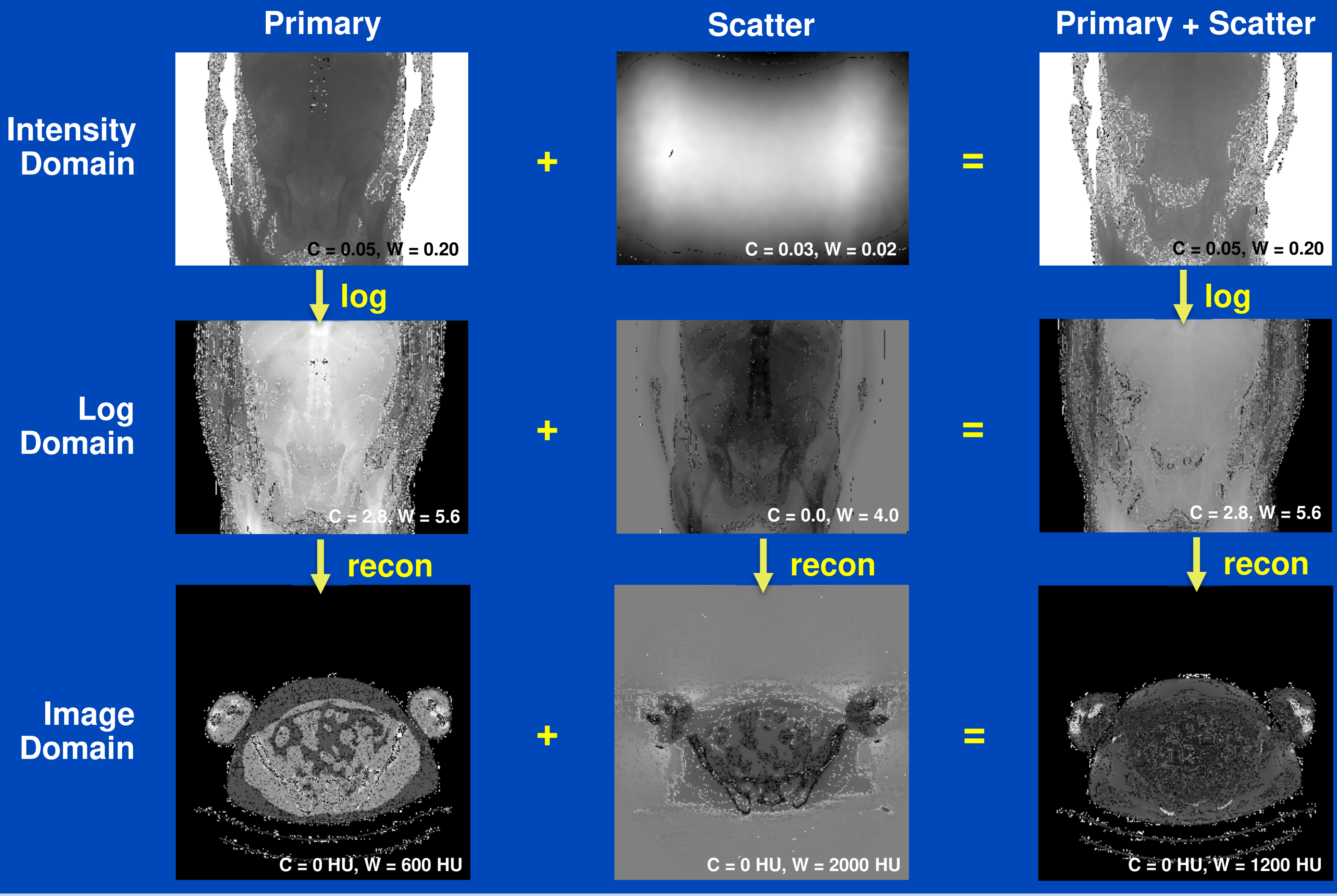

Deep Scatter Estimation

Motivation

- X-ray scatter is a major cause of image quality degradation in CT and CBCT.
- Appropriate scatter correction is crucial to maintain the diagnostic value of the CT examination.

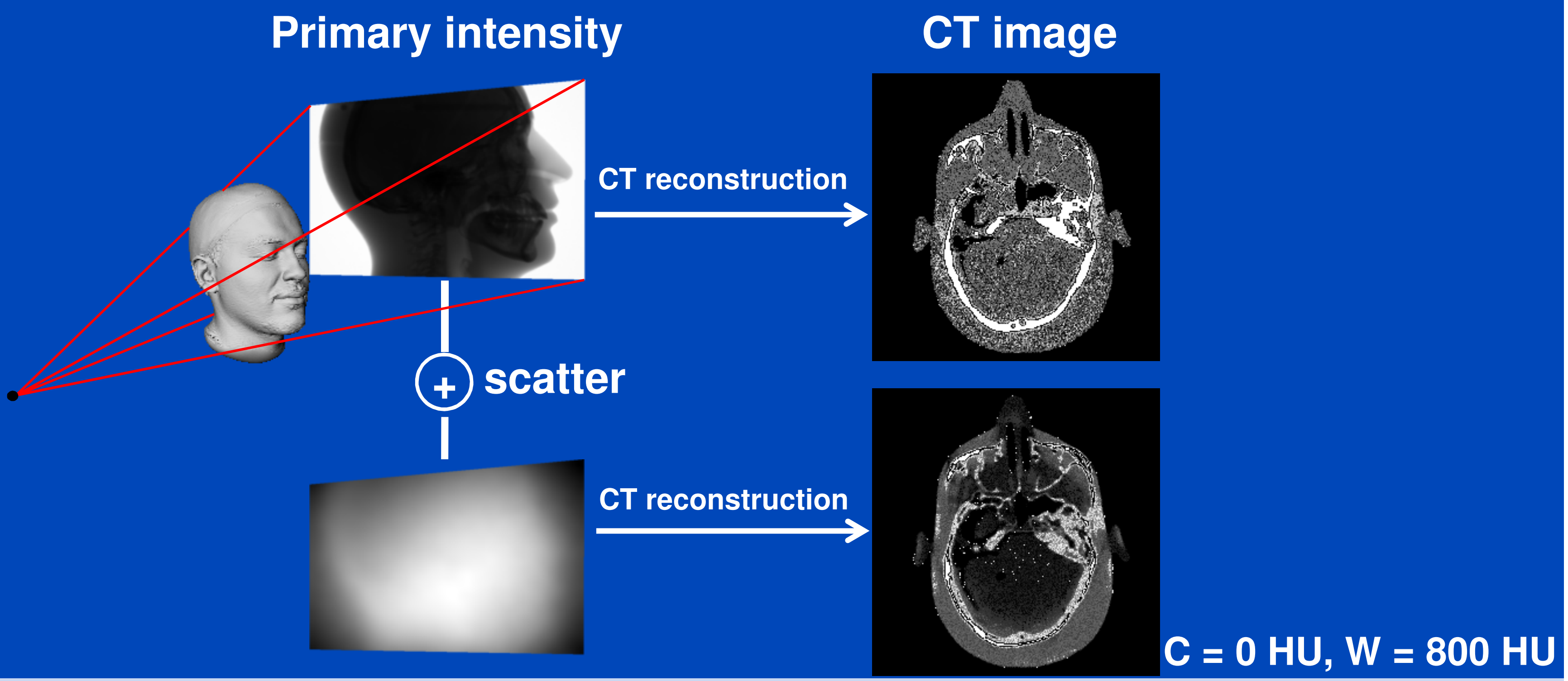

Scatter Correction

Scatter suppression

- Anti-scatter grids
- Collimators
- …

Scatter estimation

- Monte Carlo simulation
- Kernel-based approaches
- Boltzmann transport
- Primary modulation
- Beam blockers
- …

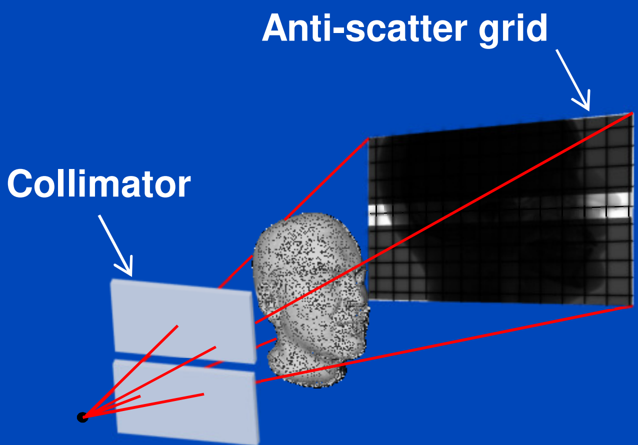

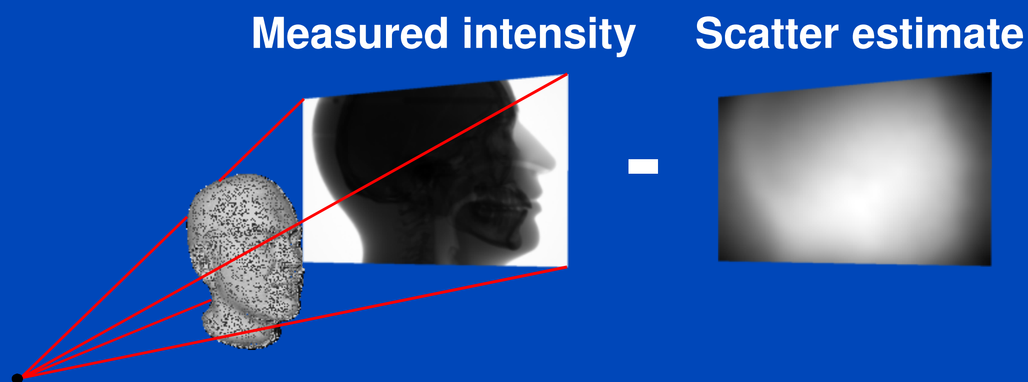

Kernel-Based Scatter Estimation

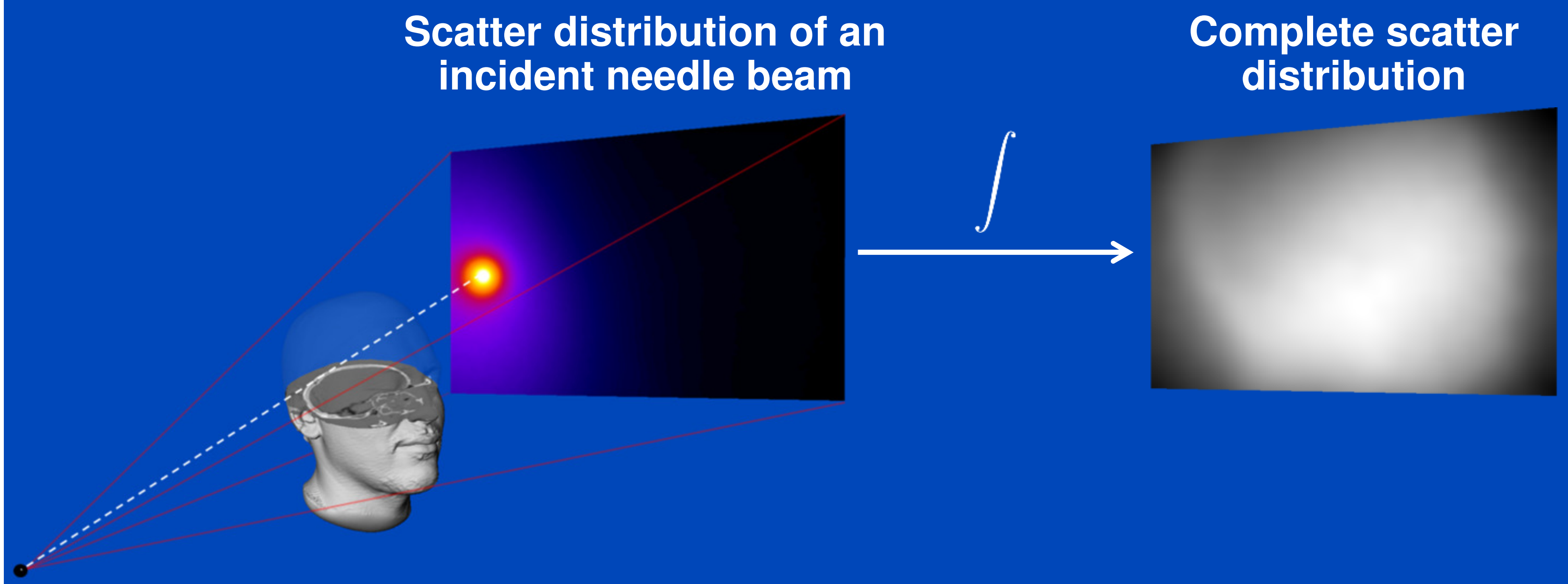

Kernel-Based Scatter Estimation

$T(p)$

Estimate needle beam scatter kernels as a function of the projection data p

$$I_{\text{s, est}}(\boldsymbol{u}) = \int T(p)(\boldsymbol{u}')G(\boldsymbol{u},\boldsymbol{u}',\boldsymbol{c})d\boldsymbol{u}'$$

Estimate mean scatter kernel that maps a function of the projection data p to scatter distribution

$$I_{\text{s, est}}(\boldsymbol{u}) = T(p)(\boldsymbol{u}) * G(\boldsymbol{u},\boldsymbol{c})$$

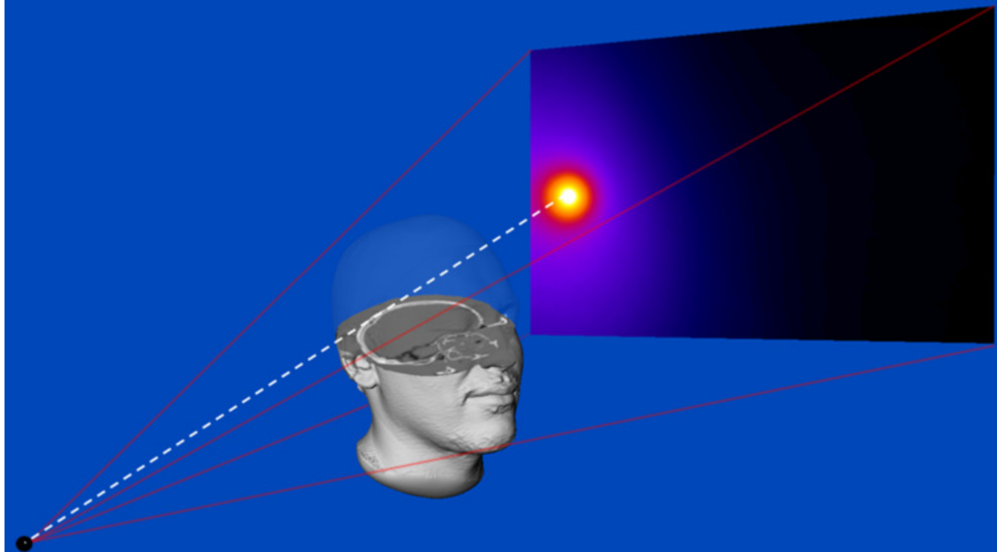

Monte Carlo Scatter Estimation

- Simulation of photon trajectories according to physical interaction probabilities.
- Simulating a large numb… …ries well approximat…

1 to 10 hours per tomographic data set

…omplete scatter distribution

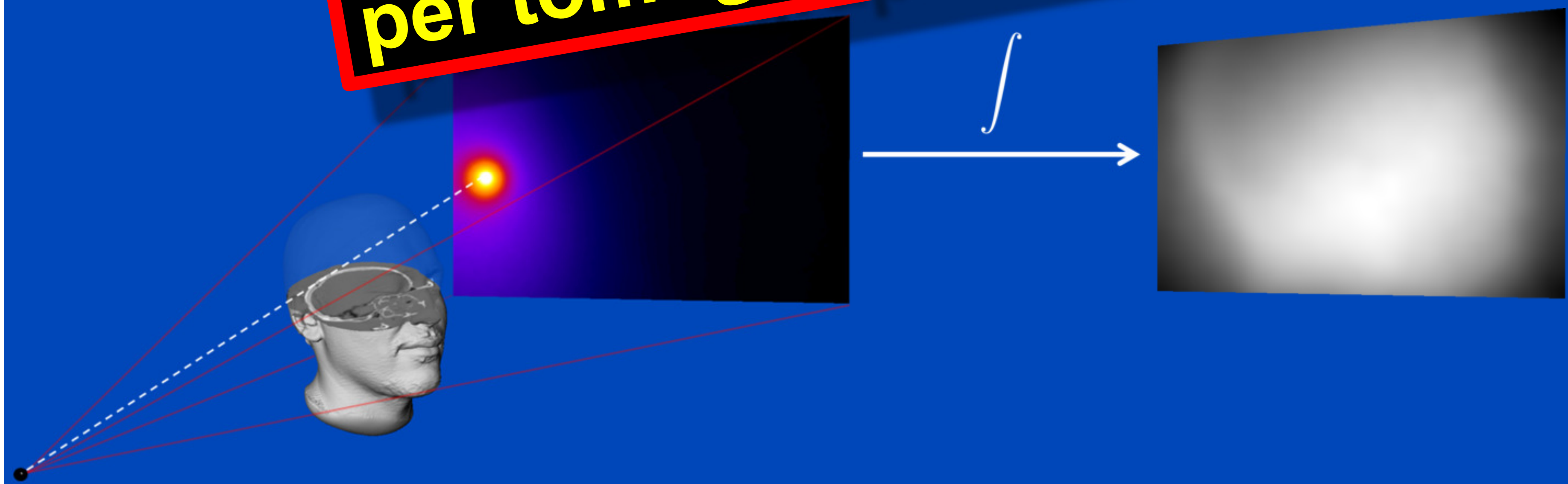

Deep Scatter Estimation (DSE)

Train a deep convolutional neural network (CNN) to estimate scatter using a function of d projection data as in

0.1 to 1 minute per tomographic data set

Input: $T(p)$

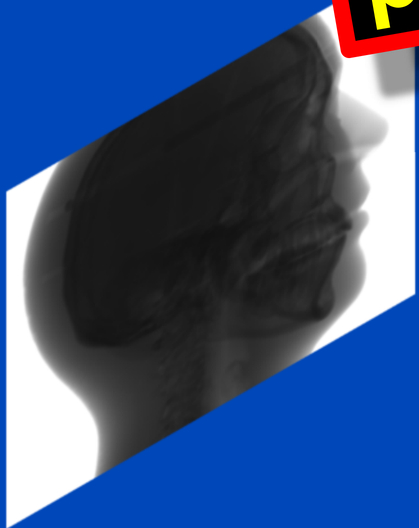

~~Monte Carlo~~

Convolutional neural network

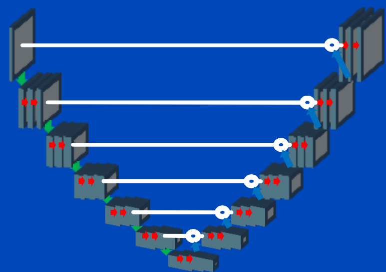

Scatter estimate

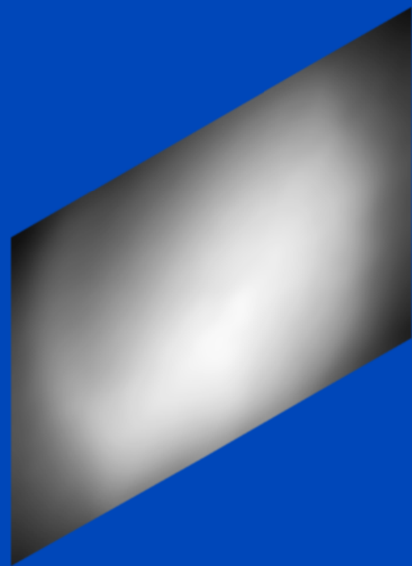

J. Maier, M. Kachelrieß et al. Deep scatter estimation (DSE). Journal of Nondestructive Evaluation 37:57, July 2018.
J. Maier, M. Kachelrieß et al. Robustness of DSE. Med. Phys. 46(1):238-249, January 2019.

Deep Scatter Estimation

Network architecture & scatter estimation framework

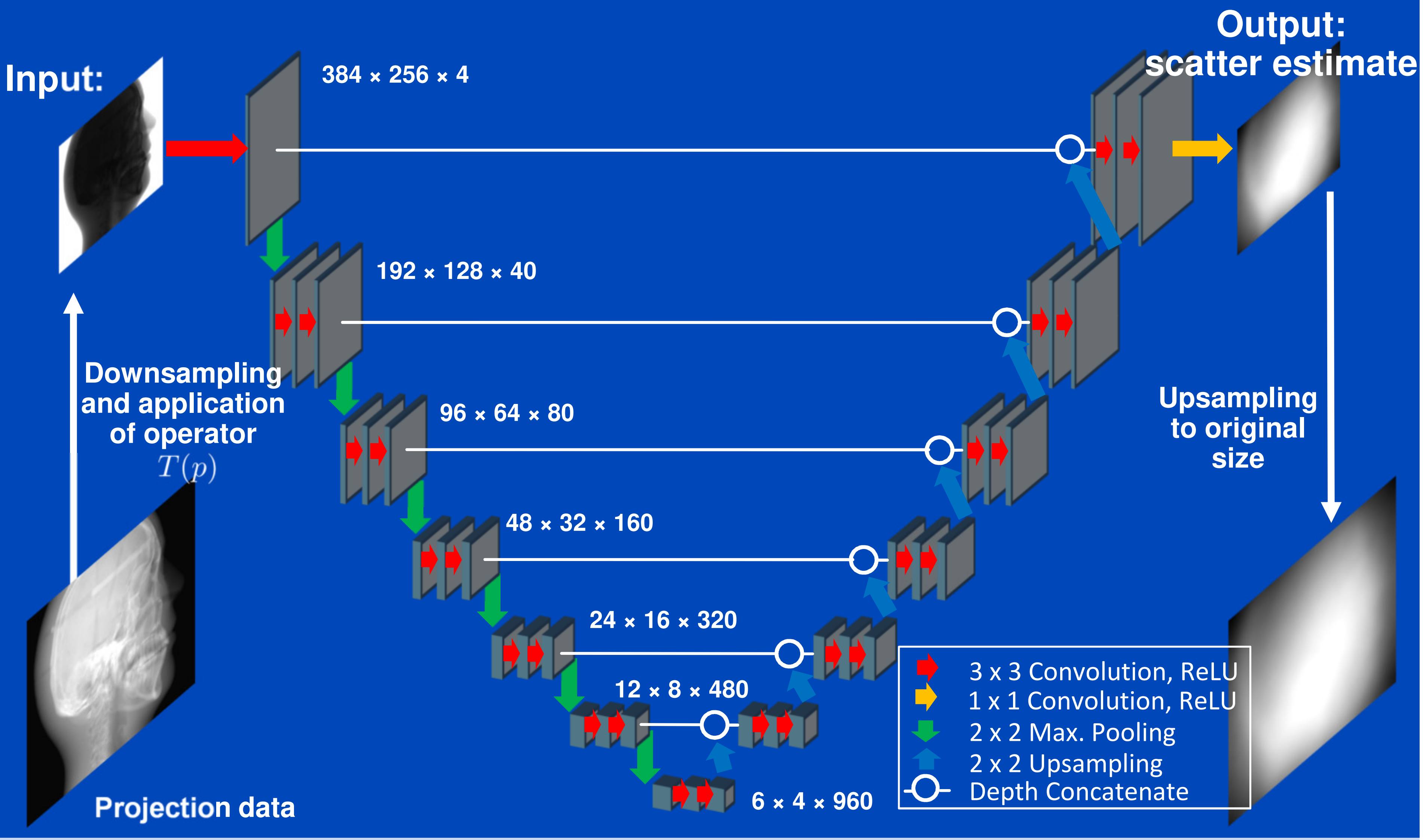

J. Maier, M. Kachelrieß et al. Deep scatter estimation (DSE). Journal of Nondestructive Evaluation 37:57, July 2018.
J. Maier, M. Kachelrieß et al. Robustness of DSE. Med. Phys. 46(1):238-249, January 2019.

Training the DSE Network

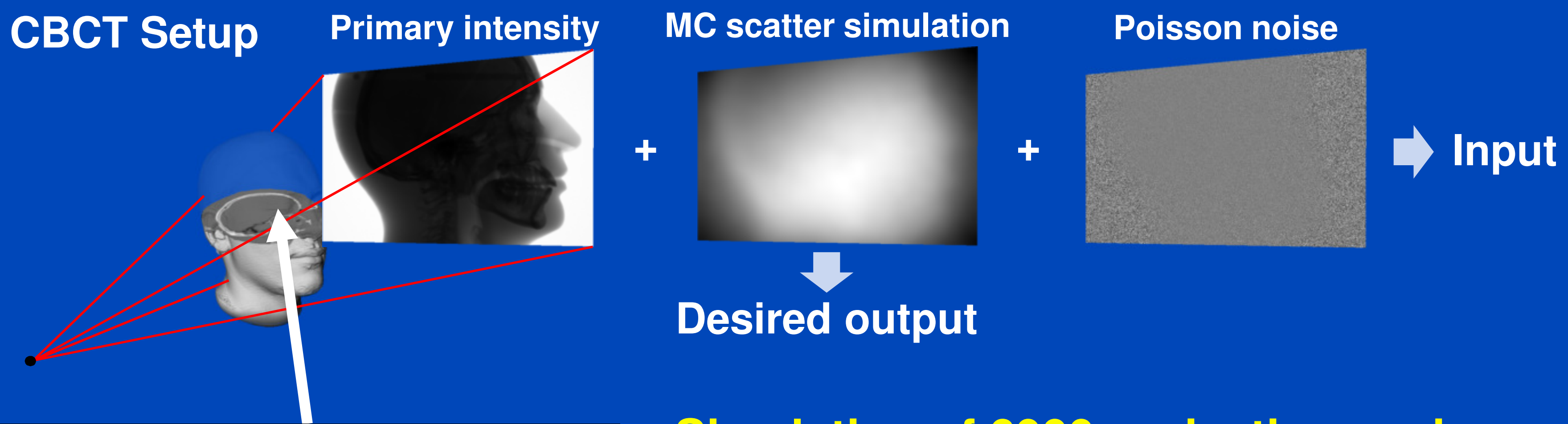

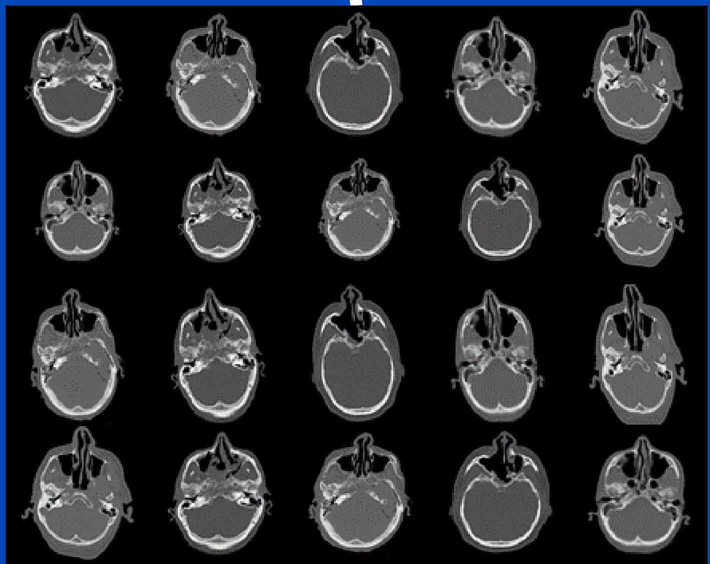

- Simulation of 6000 projections using different heads and acquisition parameters (80 kV, …, 140 kV in steps of 20 kV).
- Splitting into 80% training and 20% validation data.
- Mean $S/P = 0.9$
- 90^{th} percentile $S/P = 1.32$
- Training minimizes MSE pixel-wise loss on a GeForce GTX 1080 for 80 epochs.

J. Maier, M. Kachelrieß et al. Deep scatter estimation (DSE). Journal of Nondestructive Evaluation 37:57, July 2018.
J. Maier, M. Kachelrieß et al. Robustness of DSE. Med. Phys. 46(1):238-249, January 2019.

Results on Simulated Projection Data

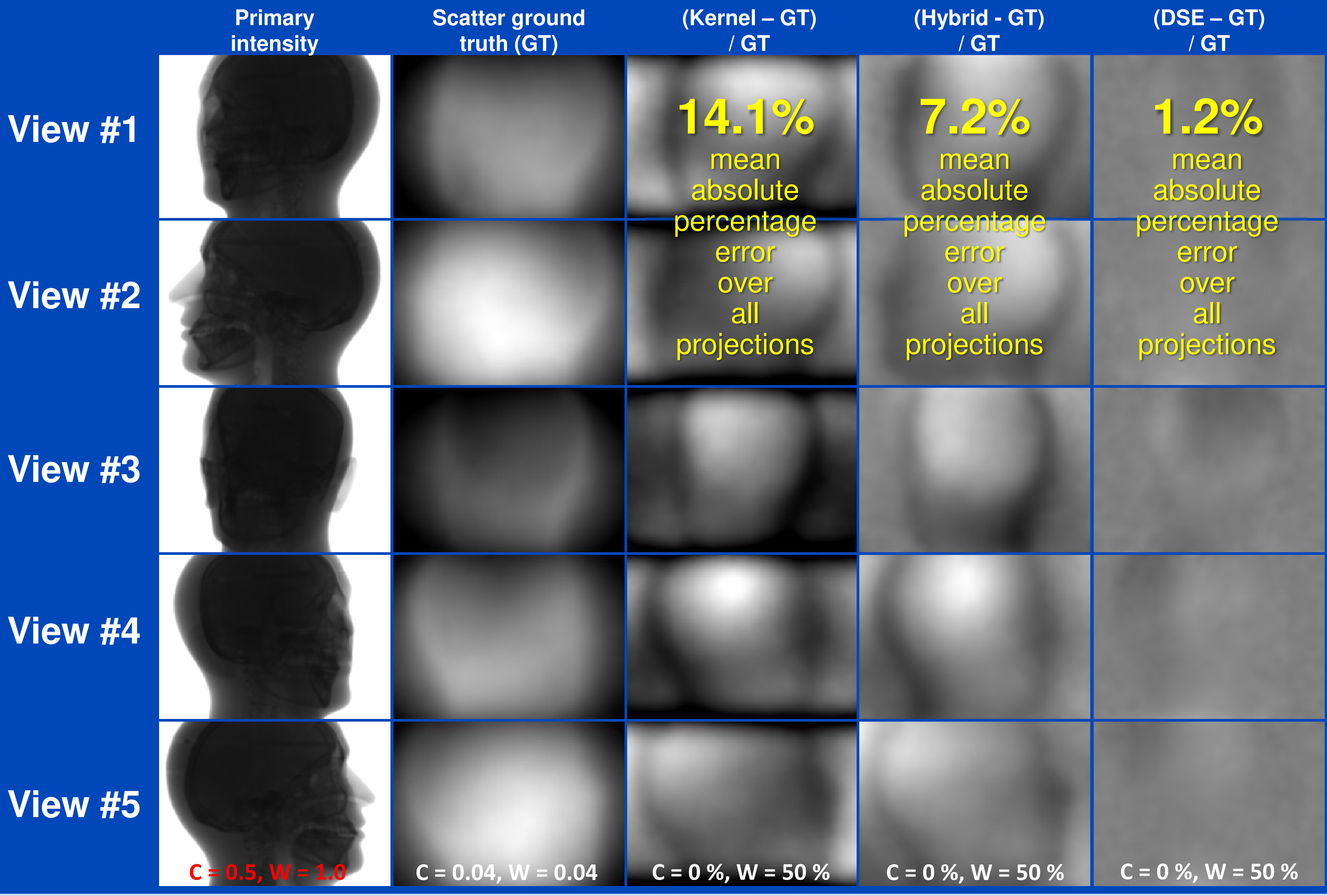

DSE trained to estimate scatter from **primary plus scatter**: High accuracy

Reconstructions of Simulated Data

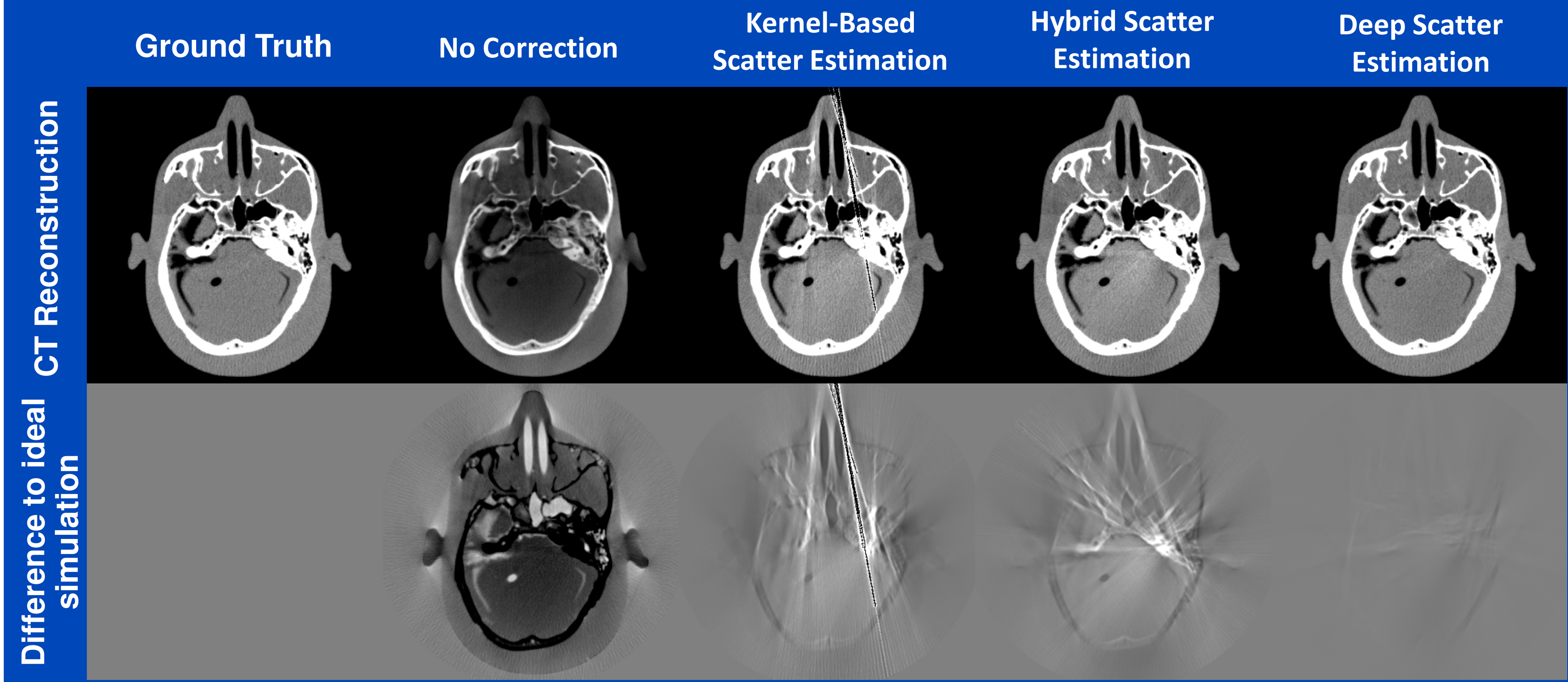

C = 0 HU, W = 1000 HU

J. Maier, M. Kachelrieß et al. Deep scatter estimation (DSE). Journal of Nondestructive Evaluation 37:57, July 2018.
J. Maier, M. Kachelrieß et al. Robustness of DSE. Med. Phys. 46(1):238-249, January 2019.

Testing of the DSE Network for Measured Data (120 kV)

DKFZ table-top CT

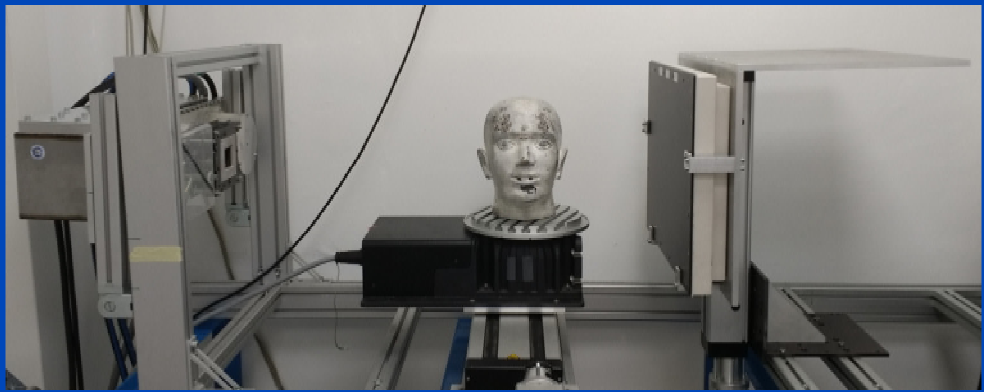

- Measurement of a head phantom at our in-house table-top CT.
- Slit scan measurement serves as ground truth.

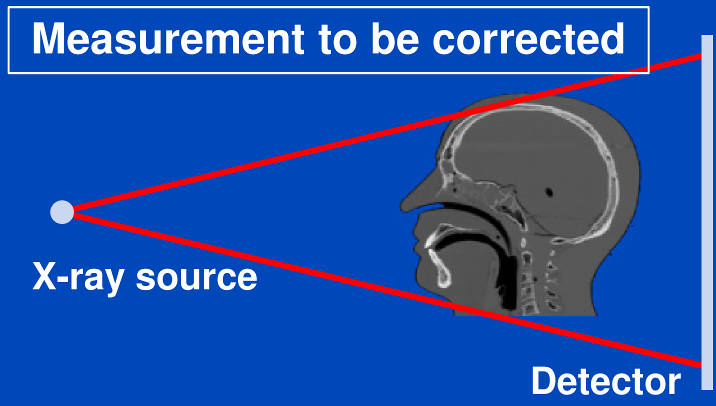

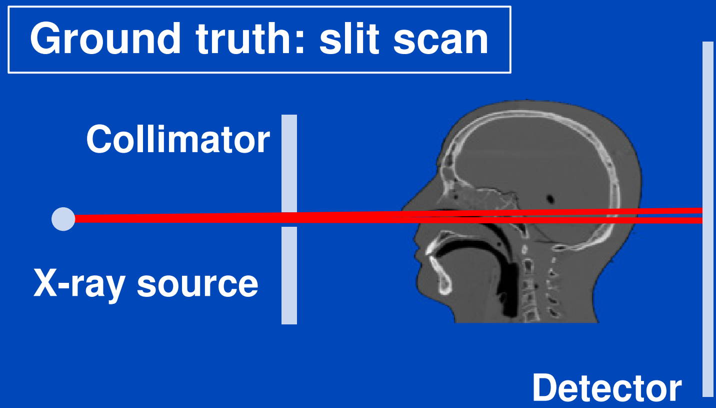

J. Maier, M. Kachelrieß et al. Deep scatter estimation (DSE). Journal of Nondestructive Evaluation 37:57, July 2018.
J. Maier, M. Kachelrieß et al. Robustness of DSE. Med. Phys. 46(1):238-249, January 2019.

Reconstructions of Measured Data

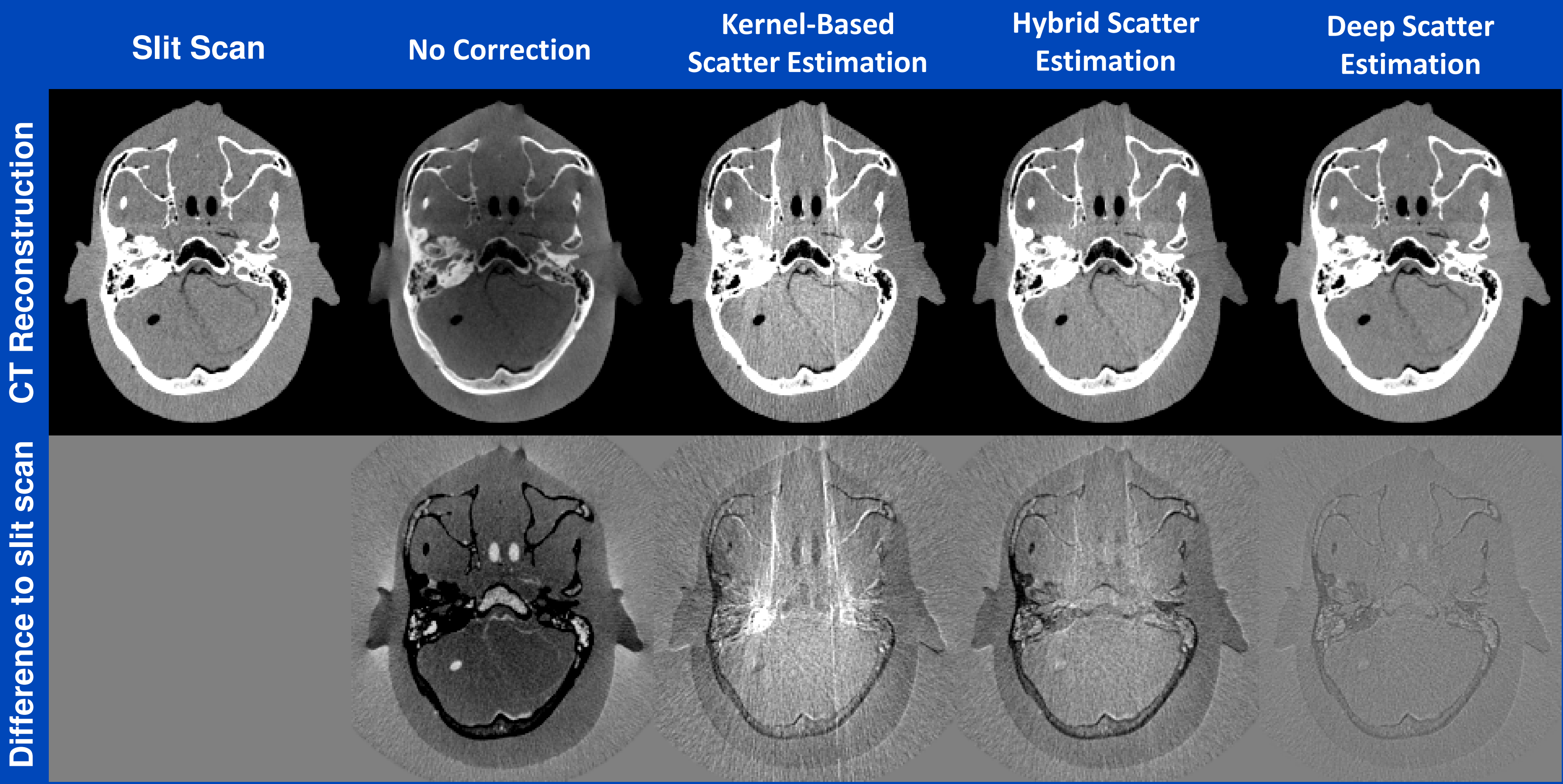

C = 0 HU, W = 1000 HU

J. Maier, M. Kachelrieß et al. Deep scatter estimation (DSE). Journal of Nondestructive Evaluation 37:57, July 2018.
J. Maier, M. Kachelrieß et al. Robustness of DSE. Med. Phys. 46(1):238-249, January 2019.

Standard reconstruction

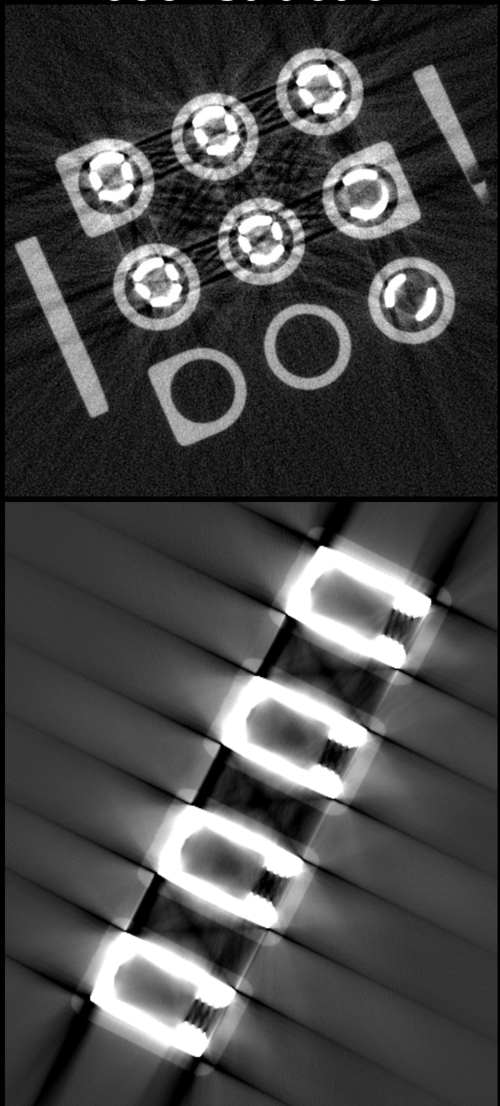

Simulation-based removal of
- beam hardening artifacts
- off-focal radiation artifacts
- focal spot blurring artifacts
- detector blurring artifacts
- **scatter artifacts**
- …

Presented at Wels 2016

Simulation-based artifact correction

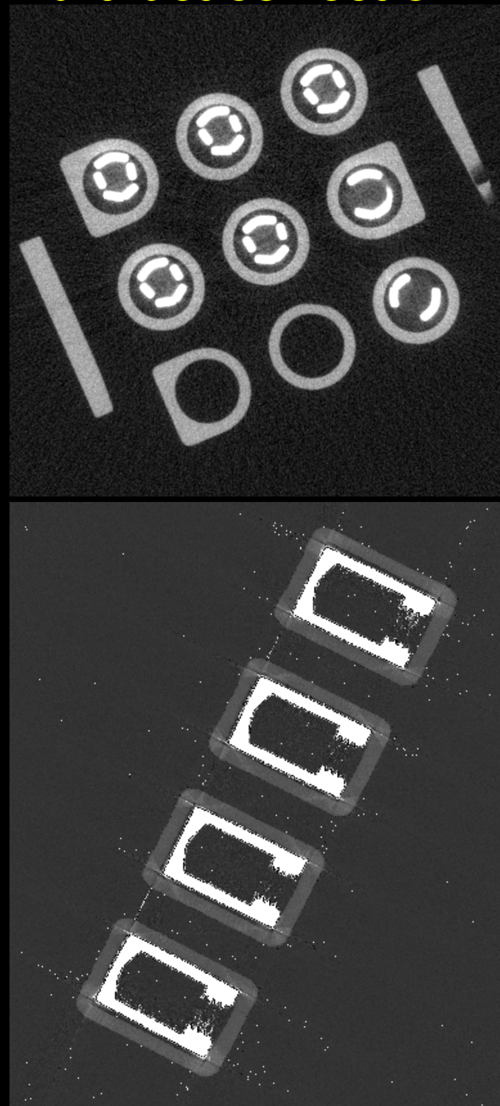

J. Maier, M. Kachelrieß et al. Simulation-based artifact correction (SBAC) for metrological computed tomography. Meas. Sci. Technol. 28(6):065011, May 2017.

Simulation Study: Training Data

- Simulation of 16416 projections using different objects and parameter settings to train the DSE network.
- Training on a GeForce GTX 1080 for 80 epochs using the Keras framework, an Adam optimizer and a mini-batch size of 16.

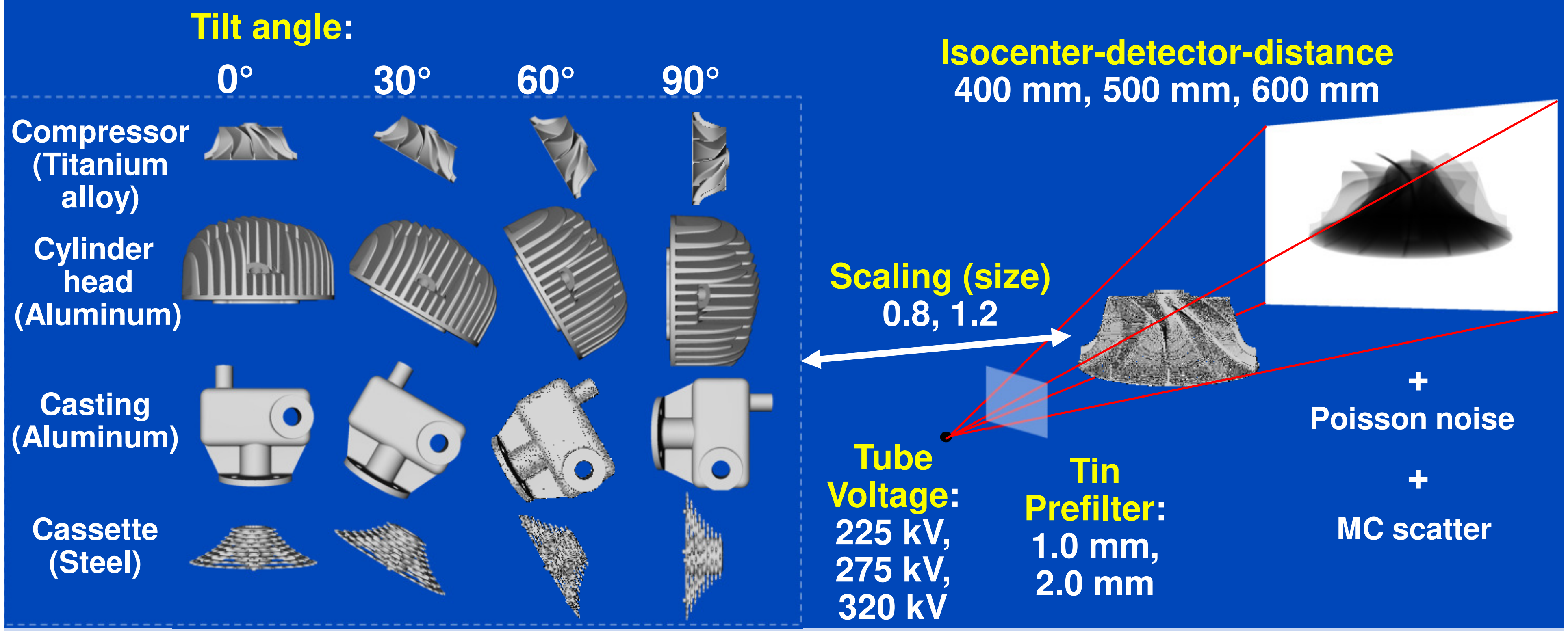

J. Maier, M. Kachelrieß et al. Deep scatter estimation (DSE). Journal of Nondestructive Evaluation 37:57, July 2018.
J. Maier, M. Kachelrieß et al. Robustness of DSE. Med. Phys. 46(1):238-249, January 2019.

dkfz.

Simulation Study: Testing Data

- Simulation of a tomography (720 projection / 360°) of five components using acquisition parameters that differ from the ones used to generate the training data set.

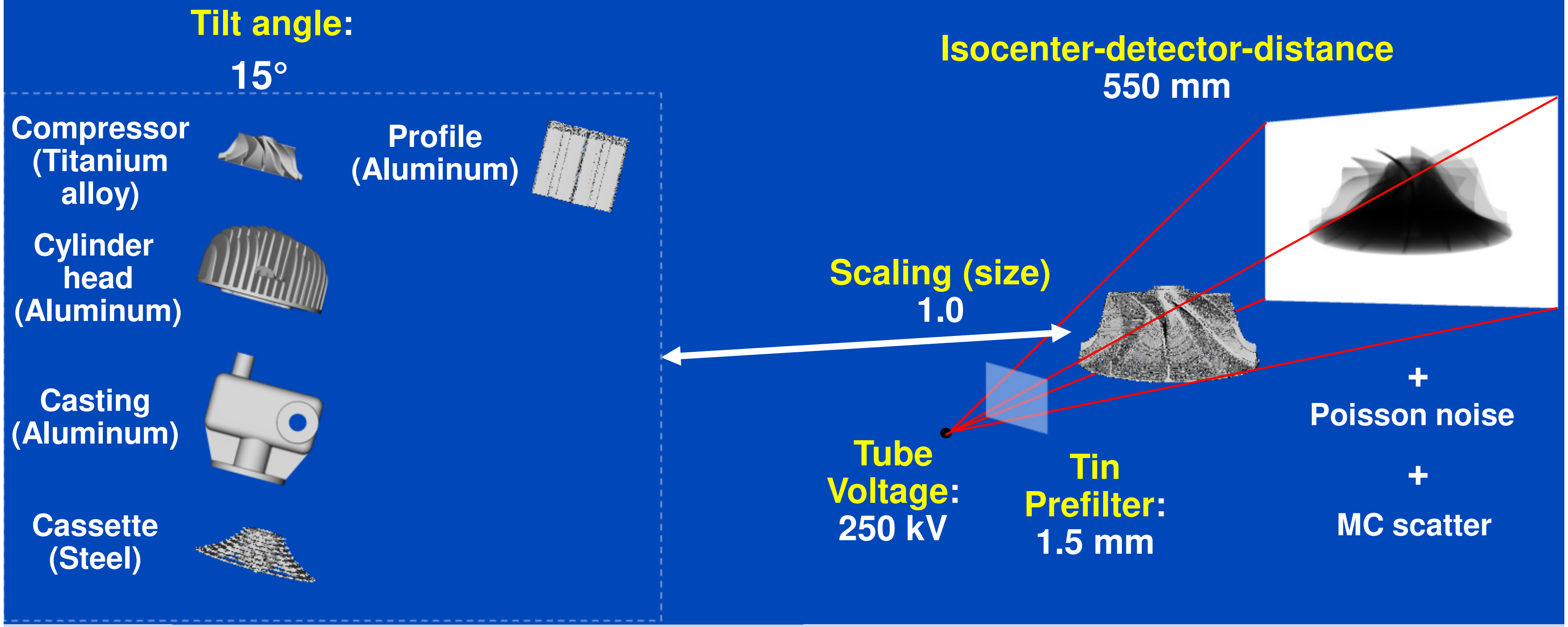

J. Maier, M. Kachelrieß et al. Deep scatter estimation (DSE). Journal of Nondestructive Evaluation 37:57, July 2018.
J. Maier, M. Kachelrieß et al. Robustness of DSE. Med. Phys. 46(1):238-249, January 2019.

Test Performance for Different Inputs

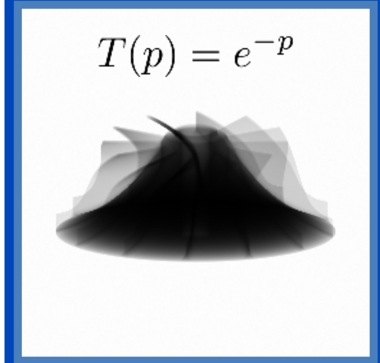

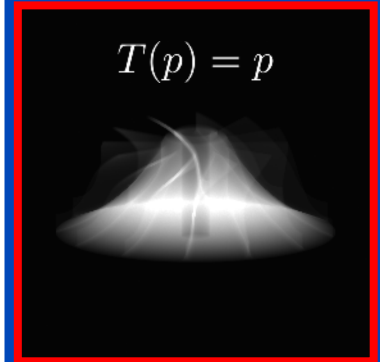

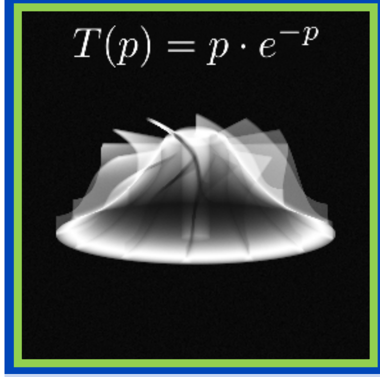

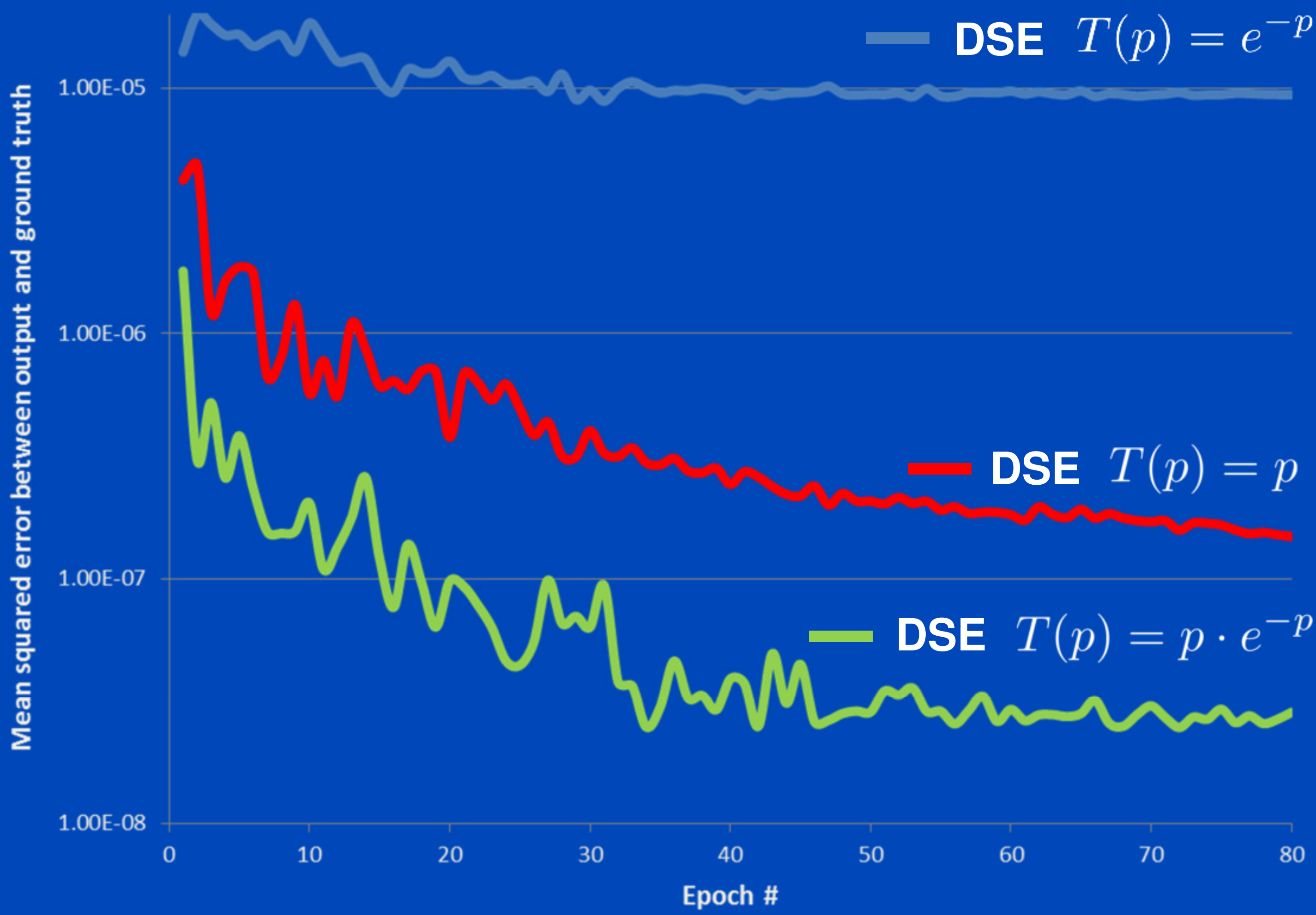

J. Maier, M. Kachelrieß et al. Deep scatter estimation (DSE). Journal of Nondestructive Evaluation 37:57, July 2018.
J. Maier, M. Kachelrieß et al. Robustness of DSE. Med. Phys. 46(1):238-249, January 2019.

dkfz.

Results

Scatter estimates for simulated testing data

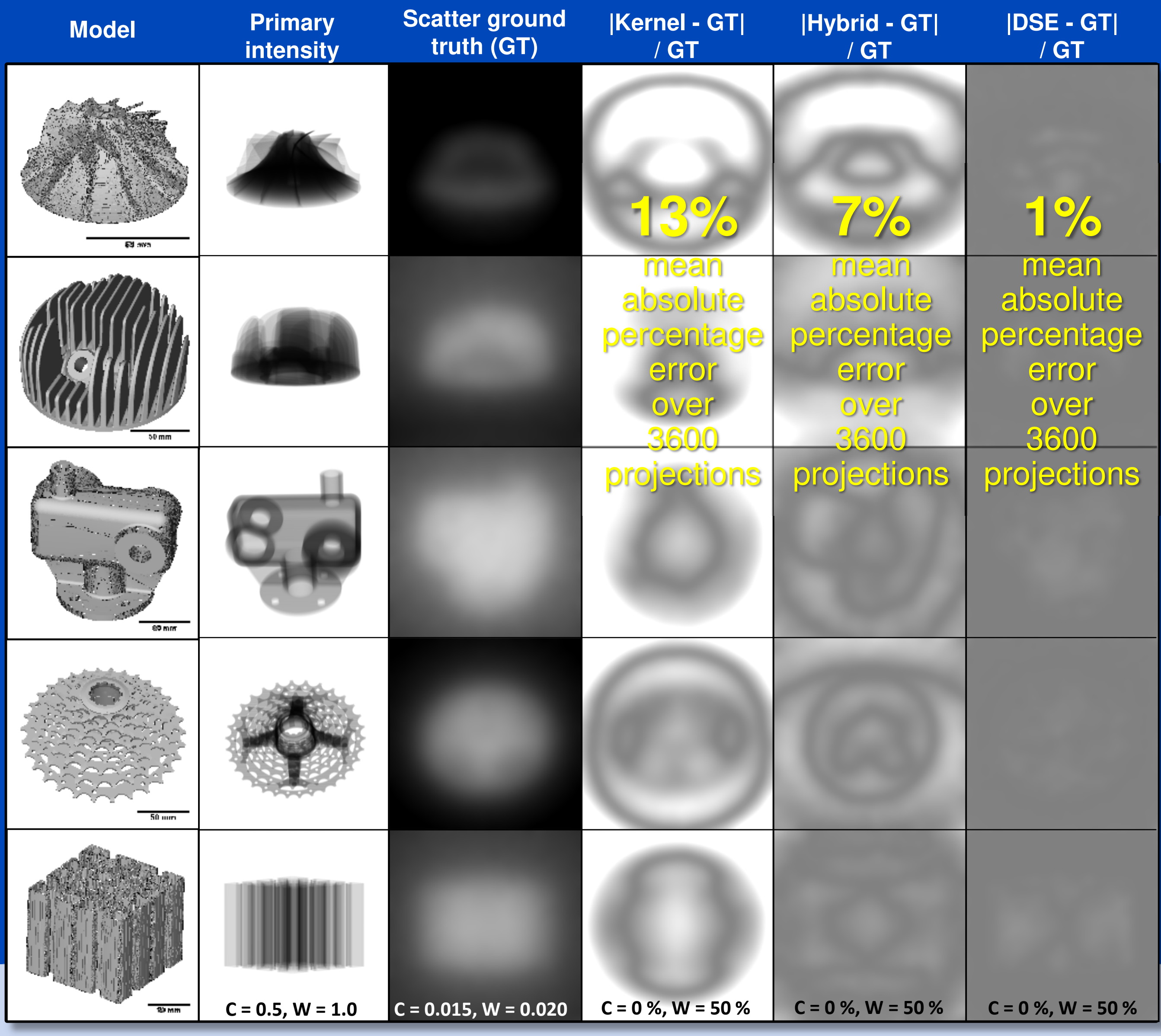

Results

CT reconstructions of scatter corrected testing data

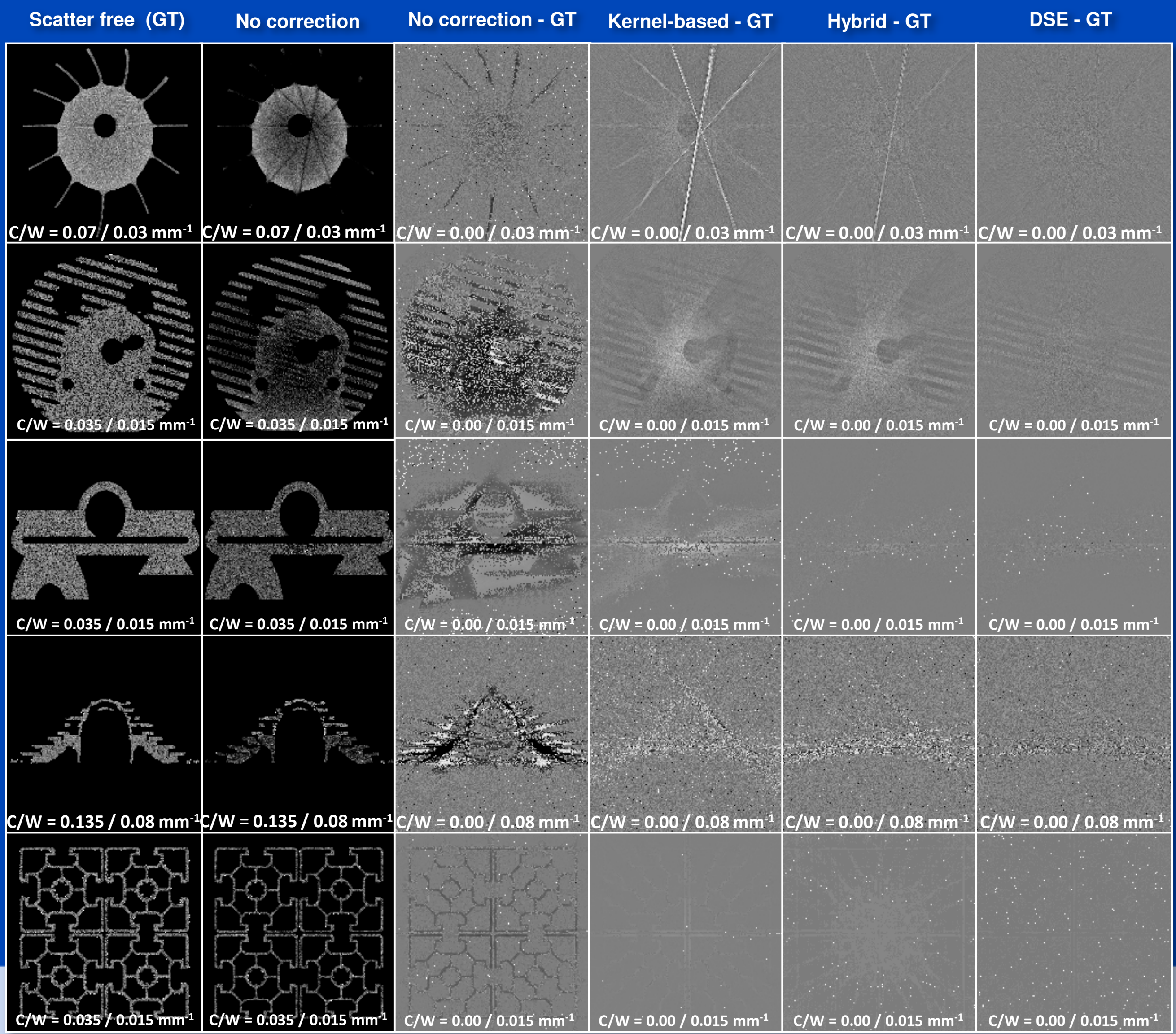

dkfz.

Application to Measured Data

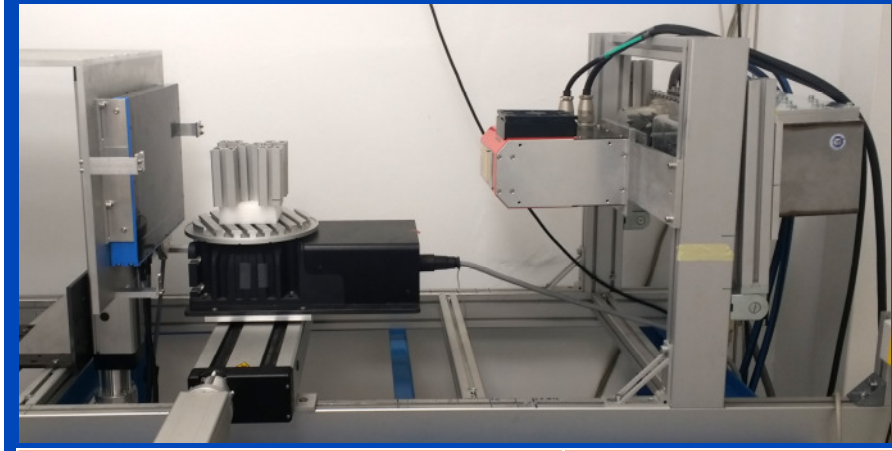

- Measurement at DKFZ table-top CT
- Tomography of aluminum profile (720 projections / 360°)
- 110 kV Hamamatsu micro-focus x-ray tube
- Varian flat detector

	Training	Testing
Components	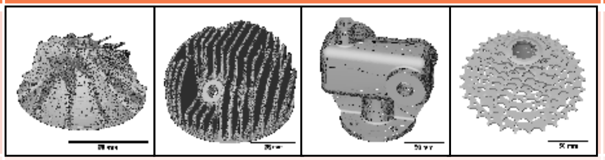	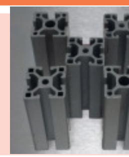
Detector elements	768×768	768×768
Source-detector distance	580 mm	580 mm
Source-isocenter distance	100 mm, 110 mm, 120 mm	110 mm
Tilt angle	0°, 30°, 60°, 90°	0°
Tube voltage	100 kV, 110 kV, 120 kV	110 kV
Copper prefilter	1.0 mm, 2.0 mm	2.0 mm
Scaling	1.0	-
Number of projections	8208	720

Results

Performance of DSE for measured data

Projection data

Component | MC scatter | |Kernel-based - MC| / MC | |Hybrid - MC| / MC | |DSE - GT| / MC

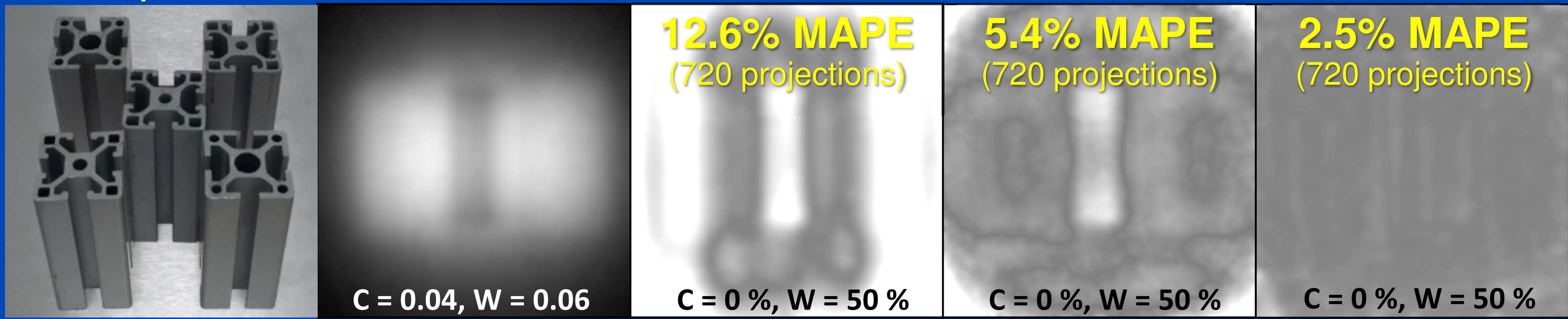

CT reconstructions

Monte Carlo (GT) | No correction | Kernel-based | Hybrid | DSE

CT reconstruction

Difference to Monte Carlo

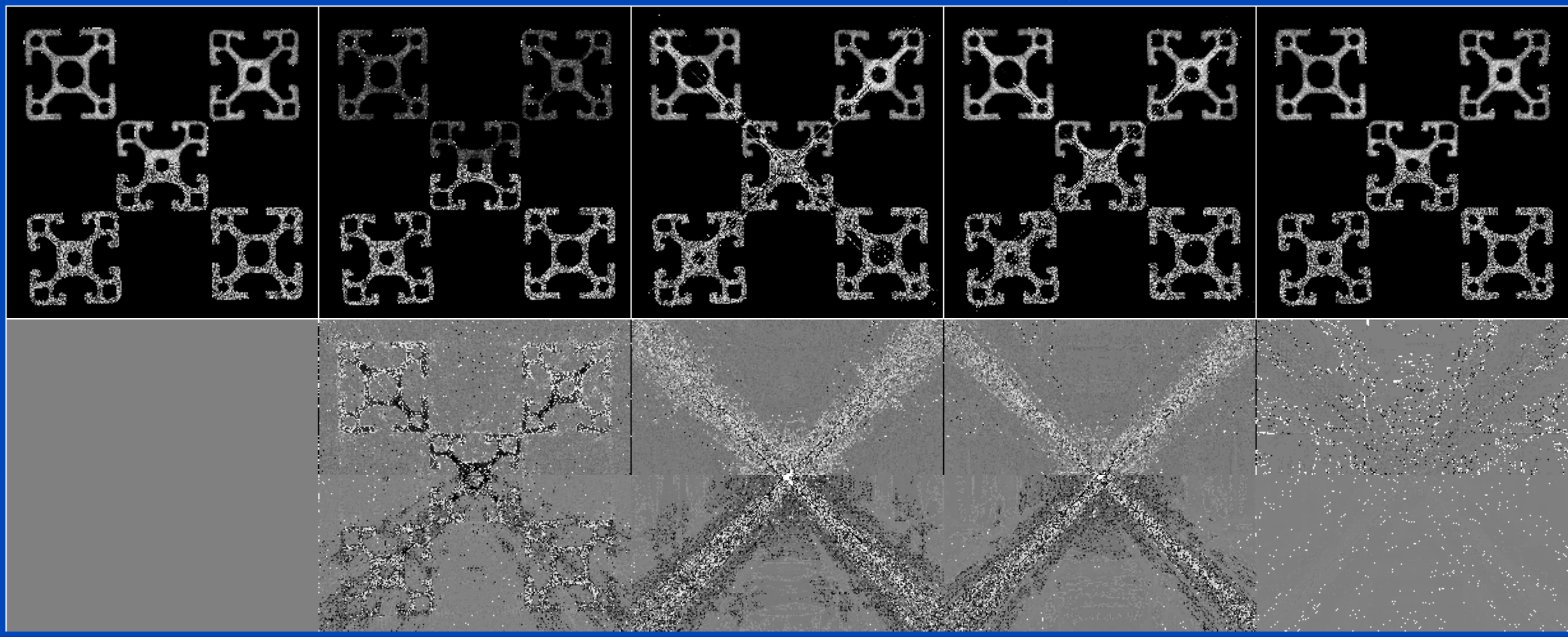

A simple detruncation was applied to the rawdata before reconstruction. Images were clipped to the FOM before display. C = -200 HU, W = 1000 HU.

Truncated DSE

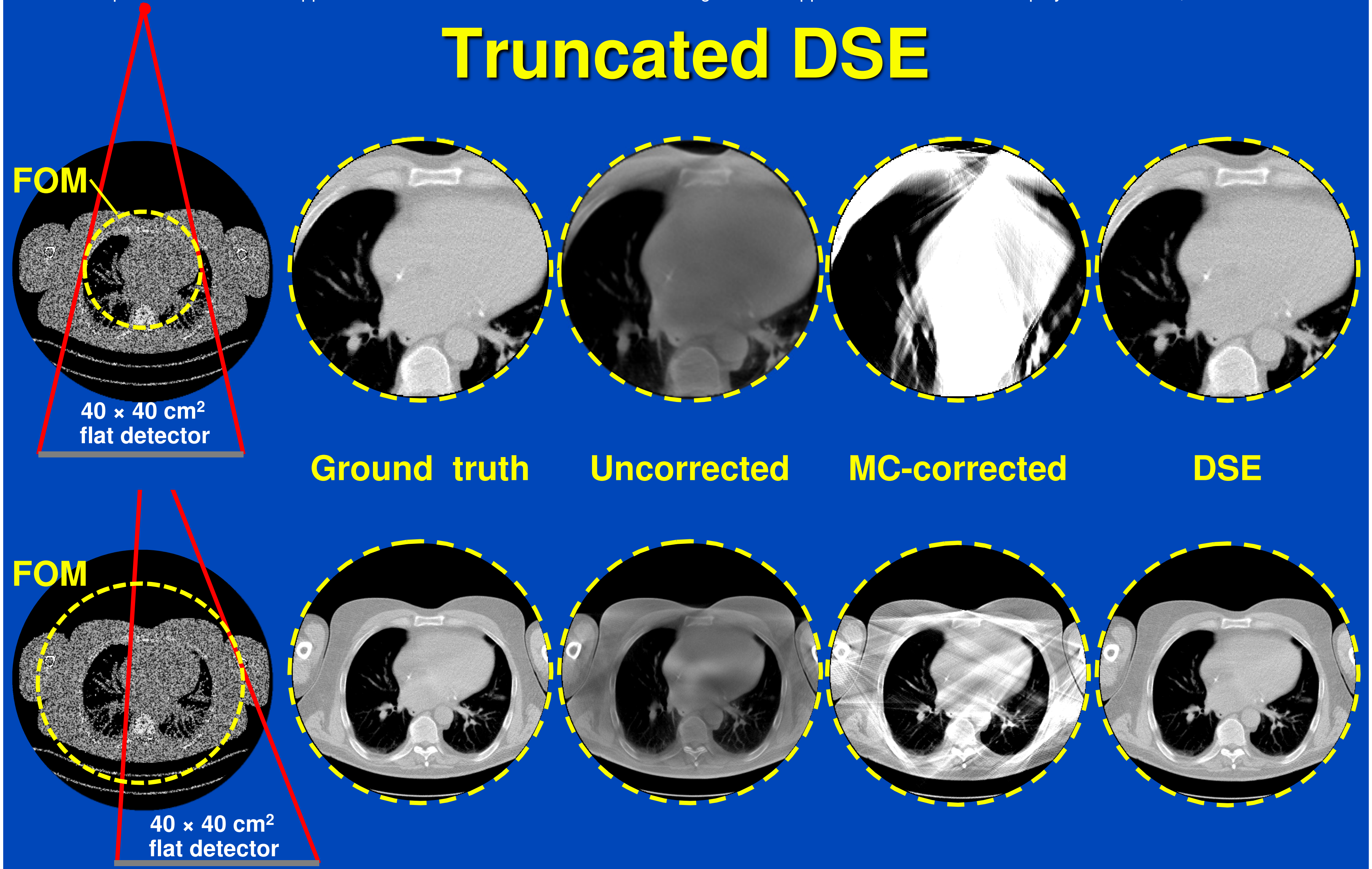

To learn why MC fails at truncated data and what significant efforts are necessary to cope with that situation see [Kachelrieß et al. Effect of detruncation on the accuracy of MC-based scatter estimation in truncated CBCT. Med. Phys. 45(8):3574-3590, August 2018].

Does DSE Generalize to Different Anatomical Regions?

- Simulation parameters:
  - 7 head and 14 thorax/abdomen clinical CT data sets
  - Apply affine transforms to obtain 28 volumes for each region
  - Regions: head, thorax and abdomen
  - Tube Voltage: 120 kV, 140 kV.
  - Prior volumes: 28 head phantoms
  - Simulate 45 projections over 360° for each volume and voltage
  - Number of z-Positions: 1 for head, 4 for thorax and abdomen
  - Data augmentation for head: vertical & horizontal flipping
  - Total number of projections: 2 × 28 × 45 × 2 × 2 = 10080

J. Maier, M. Kachelrieß et al. Deep scatter estimation (DSE). Journal of Nondestructive Evaluation 37:57, July 2018.
J. Maier, M. Kachelrieß et al. Robustness of DSE. Med. Phys. 46(1):238-249, January 2019.

Neural Network & Training

- DSE was implemented using the U-net architecture shown below
- The training was performed on an NVIDIA Quadro P6000 for 80 epochs using an Adam optimizer and a batch size of 16.

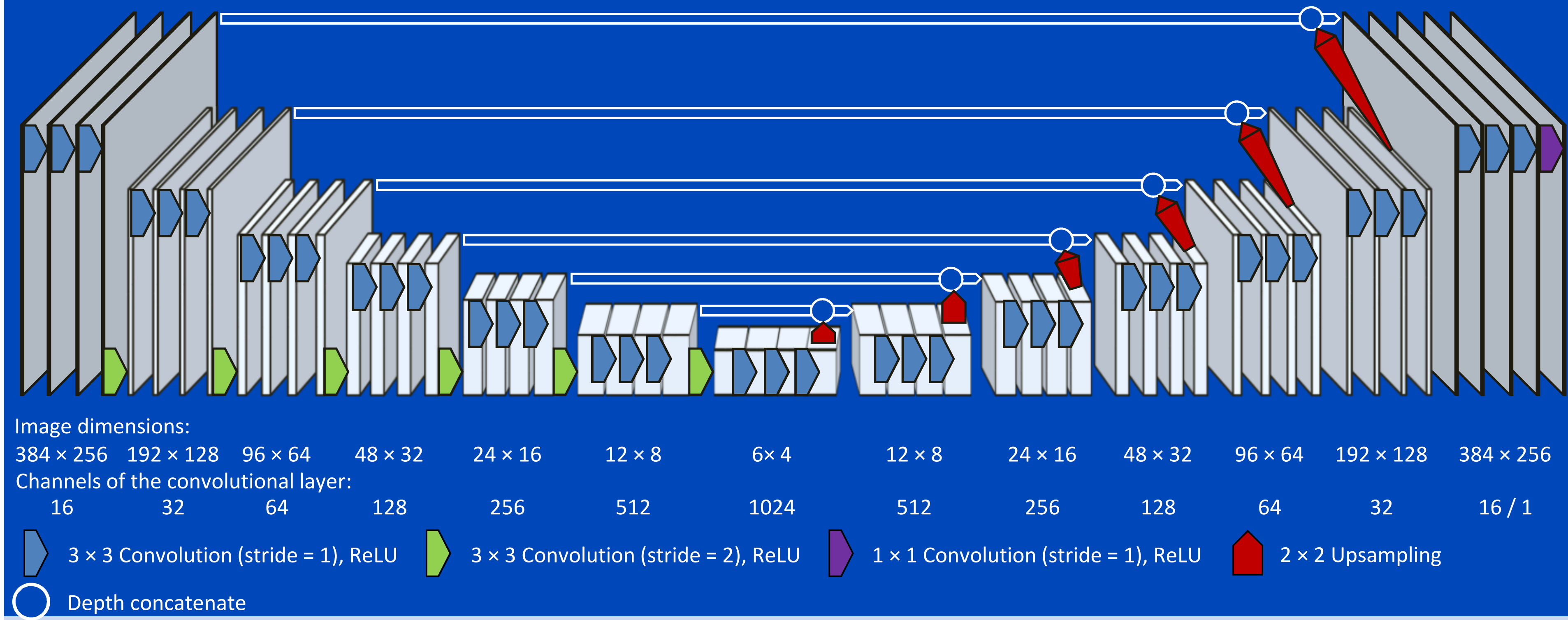

J. Maier, M. Kachelrieß et al. Deep scatter estimation (DSE). Journal of Nondestructive Evaluation 37:57, July 2018.
J. Maier, M. Kachelrieß et al. Robustness of DSE. Med. Phys. 46(1):238-249, January 2019.

dkfz.

Results

KSE	Head	Thorax	Abdomen
Head	14.5	26.8	32.5
Thorax	16.2	18.5	19.4
Abdomen	16.8	22.1	17.8
All data	14.9	20.5	19.3

DSE	Head	Thorax	Abdomen
Head	1.2	21.1	32.7
Thorax	8.8	1.5	9.1
Abdomen	11.9	10.9	1.3
All data	1.8	1.4	1.4

Values shown are the mean absolute percentage errors (MAPEs) of the testing data.
Note that thorax and head suffer from truncation due to the small size of the 40×30 cm flat detector.

J. Maier, M. Kachelrieß et al. Deep scatter estimation (DSE). Journal of Nondestructive Evaluation 37:57, July 2018.
J. Maier, M. Kachelrieß et al. Robustness of DSE. Med. Phys. 46(1):238-249, January 2019.

Results

	Testing Head	Thorax	Abdomen
Training			
KSE			
Head	14.5	26.8	32.5
Thorax	16.2	18.5	19.4
Abdomen	16.8	22.1	17.8
All data	14.9	20.5	19.3
HSE (Truncated prior, 22 cm FOM)			
-	6.2	293.2	237.6
HSE (Truncated prior, shifted detector, 40 cm FOM)			
-	-	22.9	26.5
DSE, $M_{\text{ep}} : e^{-p_{\text{sim}}} \longrightarrow S_{\text{MC}}$			
Head	3.9	17.6	23.5
Thorax	12.2	2.5	11.6
Abdomen	27.1	13.2	2.3
All data	4.7	2.5	2.4
DSE, $M_{\text{p}} : p_{\text{sim}} \longrightarrow S_{\text{MC}}$			
Head	1.3	14.9	15.2
Thorax	6.7	1.6	7.7
Abdomen	15.7	12.1	1.5
All data	1.7	1.6	1.6
DSE, $M_{\text{pep}} : p_{\text{sim}} \cdot e^{-p_{\text{sim}}} \longrightarrow S_{\text{MC}}$			
Head	1.2	21.1	32.7
Thorax	8.8	1.5	9.1
Abdomen	11.9	10.9	1.3
All data	1.8	1.4	1.4

Mean absolute percentage error of the kernel-based scatter estimation (KSE), the hybrid scatter estimation (HSE) and the deep scatter estimation (DSE) with respect to the ground truth scatter distribution (MC simulation). Training data were generated simulating head, thorax and abdomen data at 120 kV, 140 kV. The training was performed for head, thorax and abdomen data separately as well as using all data together (left column). DSE was trained for three different mappings ($M_{\text{ep}} : e^{-p_{\text{sim}}} \rightarrow S_{\text{MC}}$, $M_{\text{p}} : p_{\text{sim}} \rightarrow S_{\text{MC}}$, $M_{\text{pep}} : p \cdot e^{-p_{\text{sim}}} \rightarrow S_{\text{MC}}$). Note that there are no training data for the HSE as it is optimized on a coarse MC simulation of the testing data.

Values shown are the mean absolute percentage errors (MAPEs) of the testing data.
Note that thorax and head suffer from truncation due to the small size of the 40×30 cm flat detector.

dkfz.

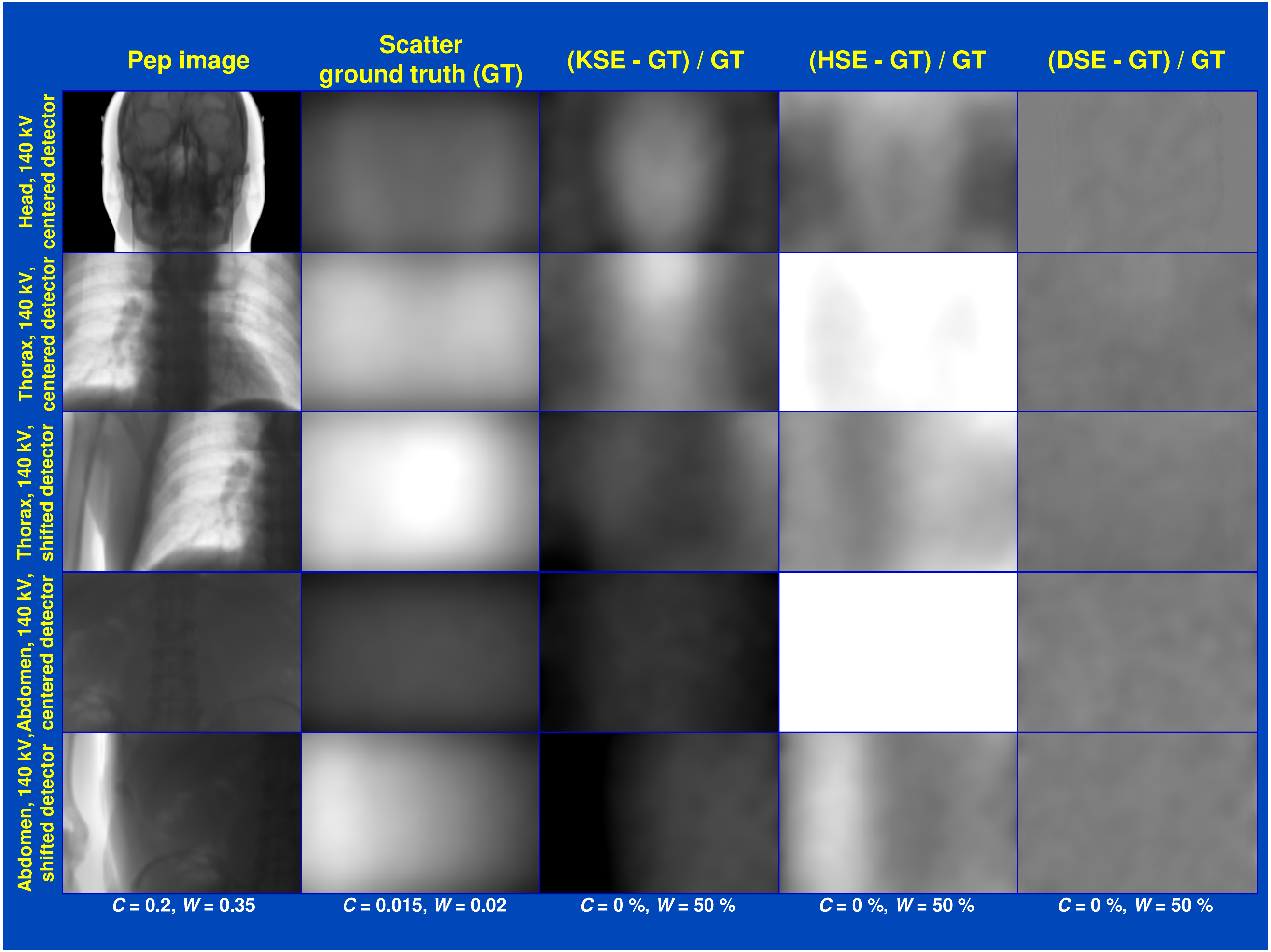

Pep image
Scatter ground truth (GT)
(KSE - GT) / GT
(HSE - GT) / GT
(DSE - GT) / GT
Head, 140 kV centered detector
Thorax, 140 kV, centered detector
Thorax, 140 kV, shifted detector
Abdomen, 140 kV, centered detector
Abdomen, 140 kV, shifted detector
C = 0.2, W = 0.35
C = 0.015, W = 0.02
C = 0 %, W = 50 %
C = 0 %, W = 50 %
C = 0 %, W = 50 %

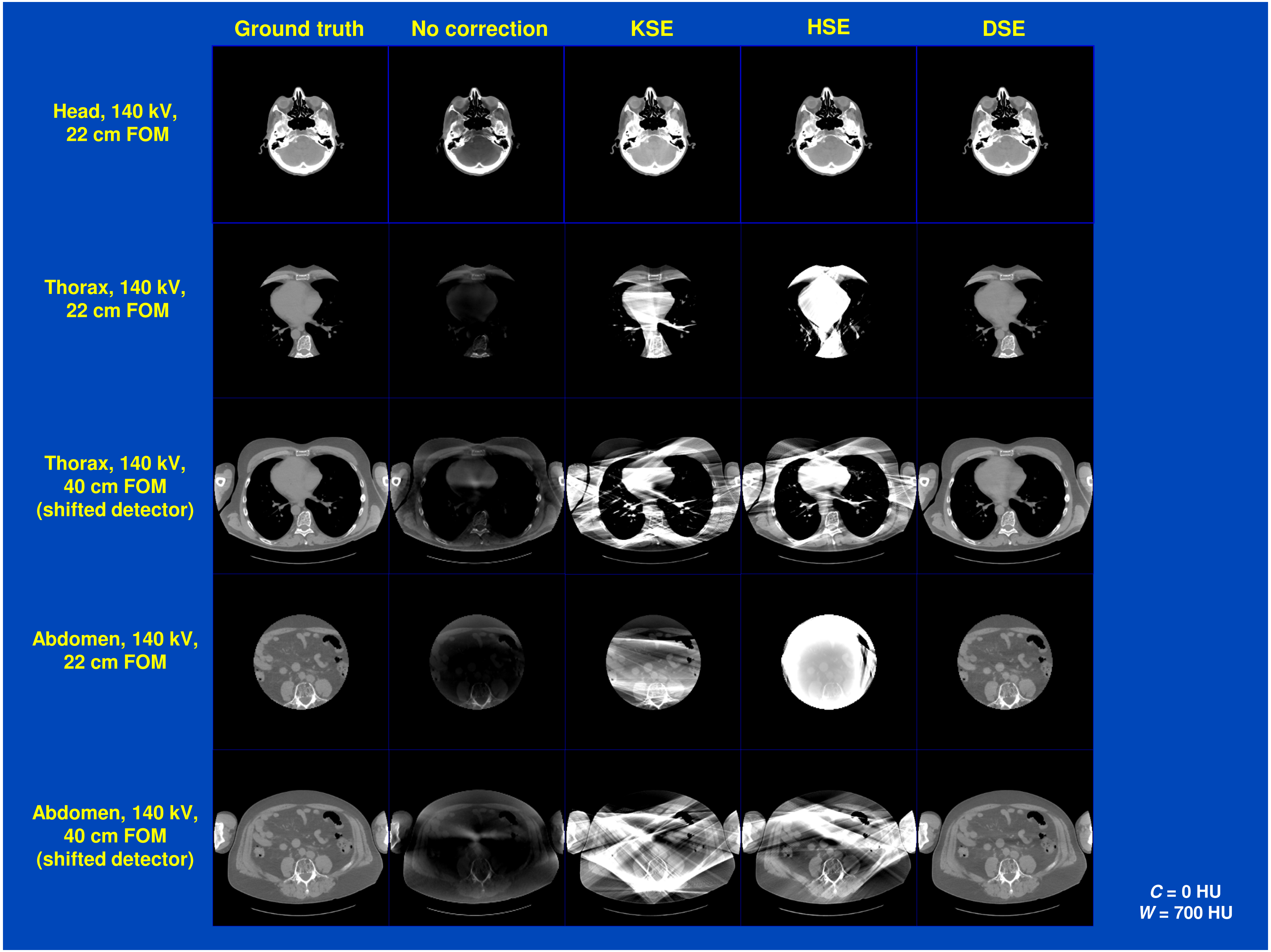
Ground truth
No correction
KSE
HSE
DSE
Head, 140 kV, 22 cm FOM
Thorax, 140 kV, 22 cm FOM
Thorax, 140 kV, 40 cm FOM (shifted detector)
Abdomen, 140 kV, 22 cm FOM
Abdomen, 140 kV, 40 cm FOM (shifted detector)
C = 0 HU
W = 700 HU

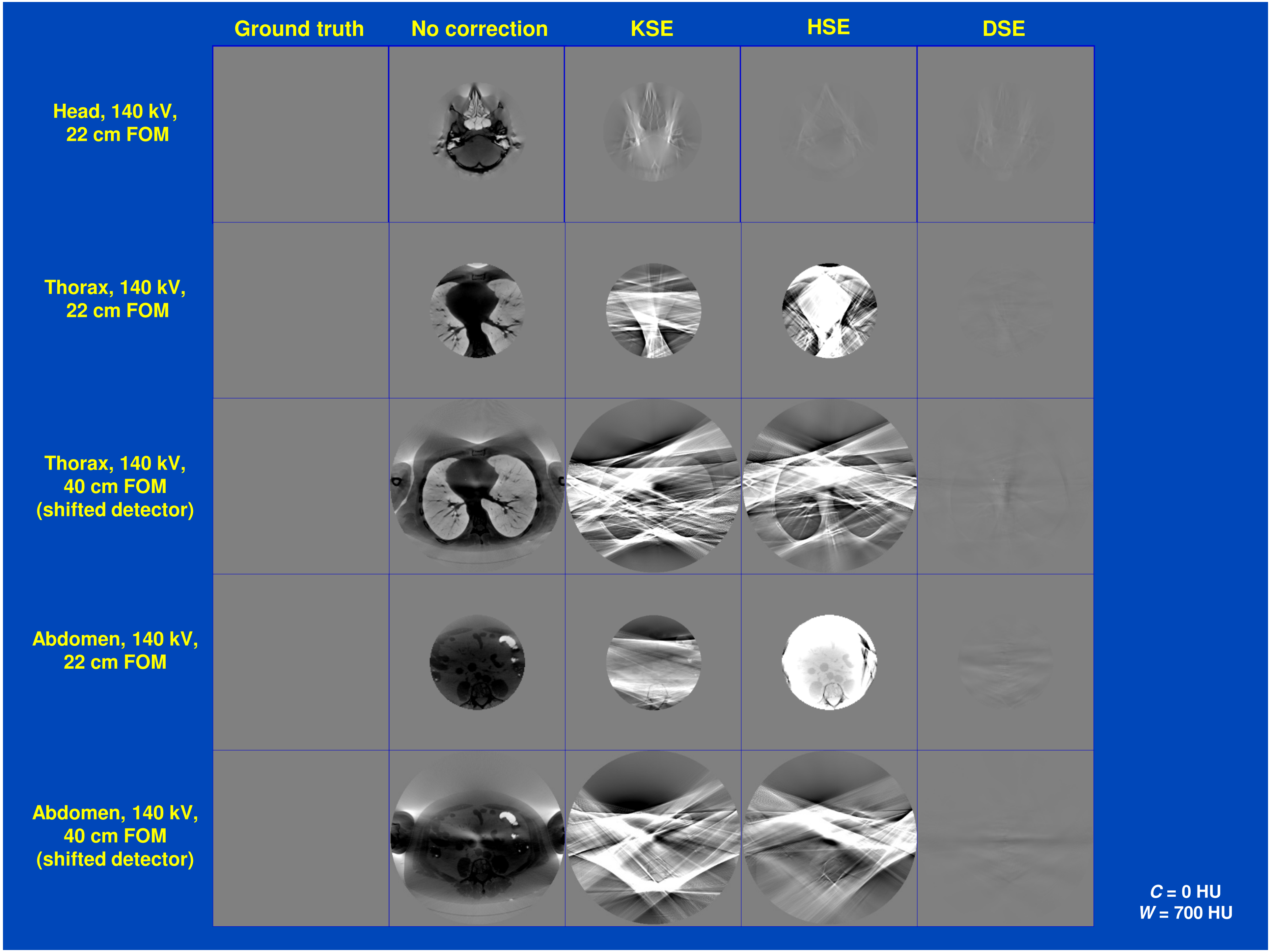
Ground truth
No correction
KSE
HSE
DSE
Head, 140 kV, 22 cm FOM
Thorax, 140 kV, 22 cm FOM
Thorax, 140 kV, 40 cm FOM (shifted detector)
Abdomen, 140 kV, 22 cm FOM
Abdomen, 140 kV, 40 cm FOM (shifted detector)
C = 0 HU
W = 700 HU

Conclusions on DSE

- DSE needs about 20 ms per projection. It is a fast and accurate alternative to Monte Carlo (MC) simulations.
- DSE outperforms kernel-based approaches in terms of accuracy and speed.
- Interesting observations
  - DSE can estimate scatter from a single (!) x-ray image.
  - DSE can accurately estimate scatter from a primary+scatter image.
  - DSE cannot accurately estimate scatter from a primary only image.
  - DSE may thus outperform MC even though DSE is trained with MC.
- DSE is not restricted to reproducing MC scatter estimates.
- DSE can rather be trained with any other scatter estimate, including those based on measurements.

Estimation of Dose Distributions

- Useful to study dose reduction techniques
  - Tube current modulation
  - Prefiltration and shaped filtration
  - Tube voltage settings
  - ...
- Useful to estimate patient dose
  - Risk assessment requires segmentation of the organs (difficult)
  - Often semiantropomorphic patient models take over
  - The infamous k-factors that convert DLP into D_{eff} are derived this way, e.g. k_{chest} = 0.014 mSv/mGy/cm
  - ...
- Could be useful for patient-specific CT scan protocol optimization
- However: Dose estimation does not work in real time!

J. Maier, E. Eulig, S. Dorn, S. Sawall, and M. Kachelrieß. Real-time patient-specific CT dose estimation using a deep convolutional neural network. Proc. IEEE MIC 2018.

Deep Dose Estimation (DDE)

- **Train a UNet to predict patient dose given a CT image and a photo effect dose image**
- **Training data**
  - **15 CT patient data sets segmented into air, fat, soft tissue, and bone**
  - **Simulate projection data by forward projection (120 kV, 720 projections, circle scans at 20 different z-positions to equally cover pelvis, abdomen, thorax and head).**
  - **Simulate scans without bowtie, with botwie, with bowtie and TCM**
  - **In total 15×20×3 = 900 data sets are reconstructed**
  - **Use Monte Carlo software RayConStruct-MC to calculate the patient dose distribution, thereby accounting for Rayleigh, Compton and photo effect.**
  - **Calculate photo effect dose distribution by direct backprojection and energy deposition in each voxel**
- **Training**
  - **U-Net sees the CT volumes and the corresponding first order (photoeffect) dose volumes and is trained to predict the patient dose distribution.**
  - **Since bone is underrepresented in all of the data sets, bone voxels received a twenty-fold weight in our MSE-based pixel-wise loss function**

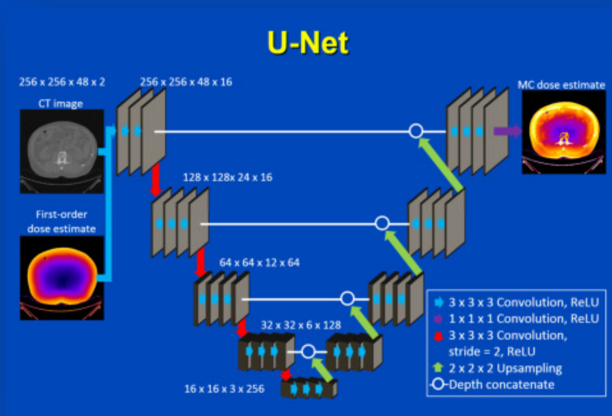

J. Maier, E. Eulig, S. Dorn, S. Sawall, and M. Kachelrieß. Real-time patient-specific CT dose estimation using a deep convolutional neural network. Proc. IEEE MIC 2018.

U-Net

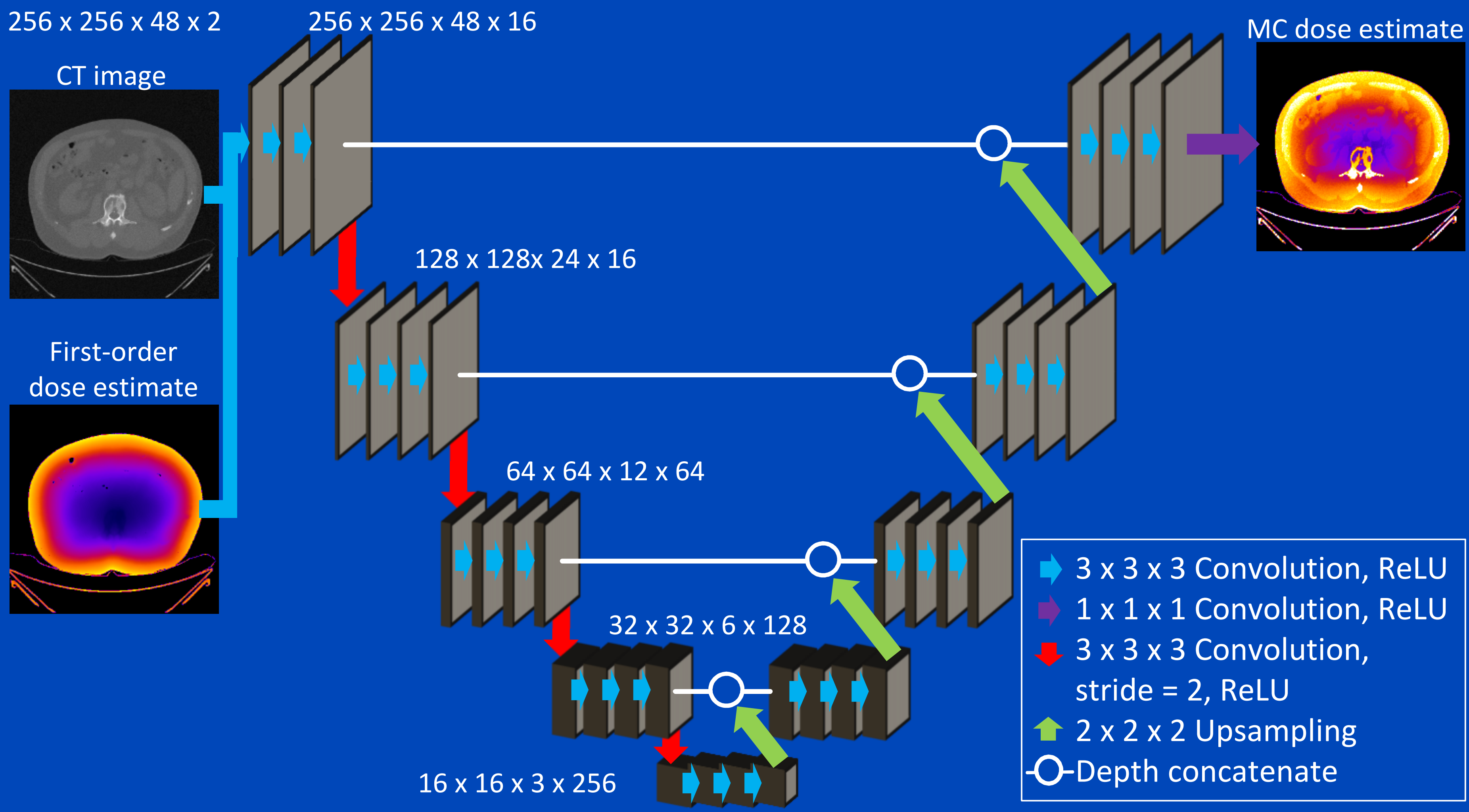

J. Maier, E. Eulig, S. Dorn, S. Sawall, and M. Kachelrieß. Real-time patient-specific CT dose estimation using a deep convolutional neural network. Proc. IEEE MIC 2018.

Deep Dose Estimation (DDE)

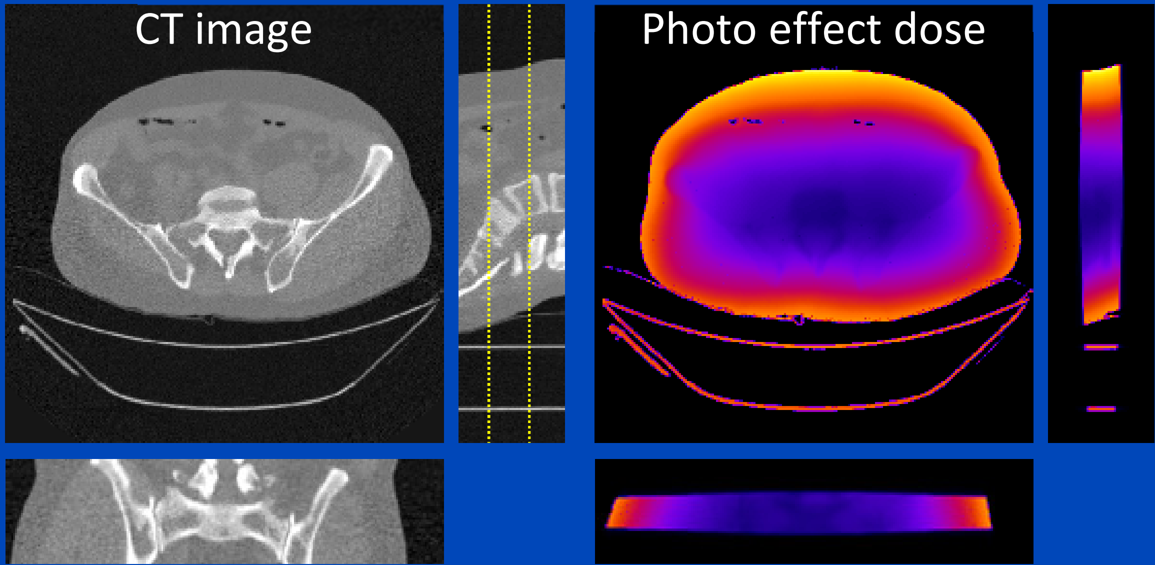

	MC	DDE
48 slices	1 h	0.25 s
whole body	20 h	5 s

MC uses 16 CPU kernels
DDE uses one Nvidia Quadro P600 GPU

DDE training took 30 h for 200 epochs,
720 samples, 48 slices per sample

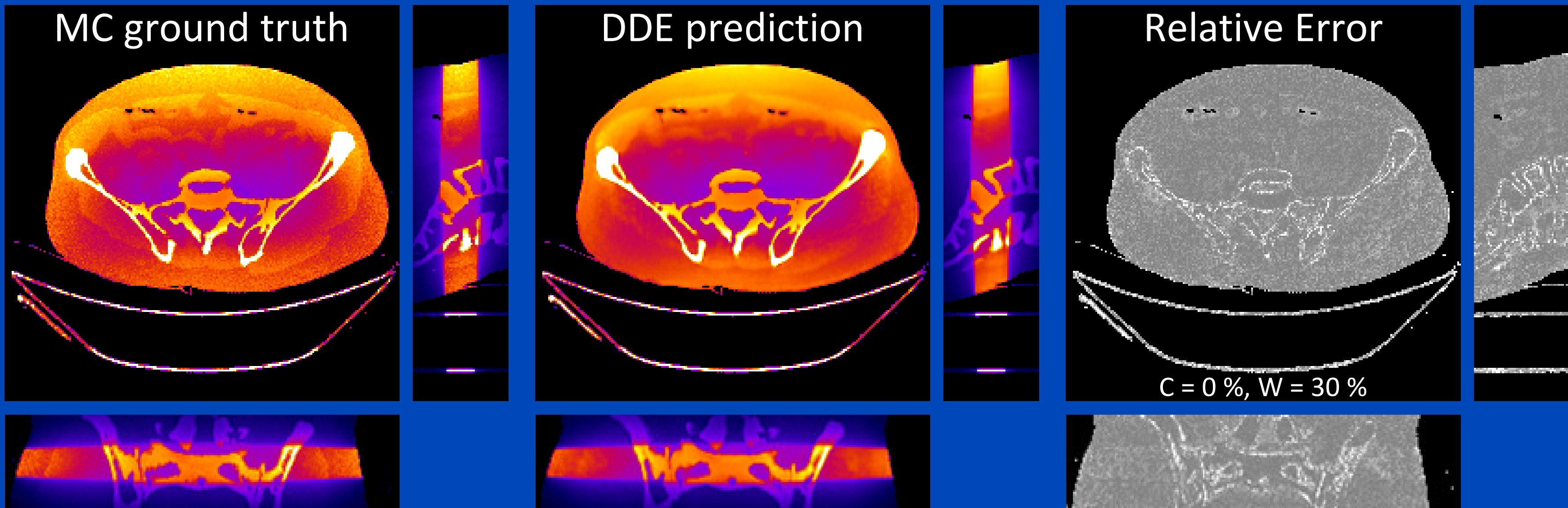

J. Maier, E. Eulig, S. Dorn, S. Sawall, and M. Kachelrieß. Real-time patient-specific CT dose estimation using a deep convolutional neural network. Proc. IEEE MIC 2018.

Conclusions on DDE

- As shown, DDE works well with 360° circle scans.
- What is not shown in this presentation is that DDE can be trained to provide accurate dose predictions
  - for sequence scans
  - for partial scans (less than 360°)
  - for spiral scans
  - for different tube voltages
  - for scans with and without bowtie filtration
  - for scans with tube current modulation
- In practice it may therefore be not necessary to perform separate training runs for these cases.
- Thus, accurate real-time patient dose estimation may become feasible with DDE.

J. Maier, E. Eulig, S. Dorn, S. Sawall, and M. Kachelrieß. Real-time patient-specific CT dose estimation using a deep convolutional neural network. Proc. IEEE MIC 2018.

Part 4:

Image Reconstruction

Often "Just" Image Restoration

- Speeding up iterative reconstruction by training a CNN to convert an FBP image into an iterative image
  - Canon‘s AiCE algorithm
  - GE‘s True Fidelity algorithm
  - plus a few more algorithms proposed in the literature
- Noise reduction by training, e.g. a mapping from low dose to high dose images
  - many examples in the literature, some in this presentation
- Artifact reduction in image domain
  - many examples in the literature, one shown in this presentation
- …

Sometimes “Real” Image Reconstruction

- Networks employing data consistency layers
- Networks including backprojection layers
- Learning of backprojectors
- End-to-end training from sinogram to image
- Unrolled iterative reconstruction with learned priors
- …

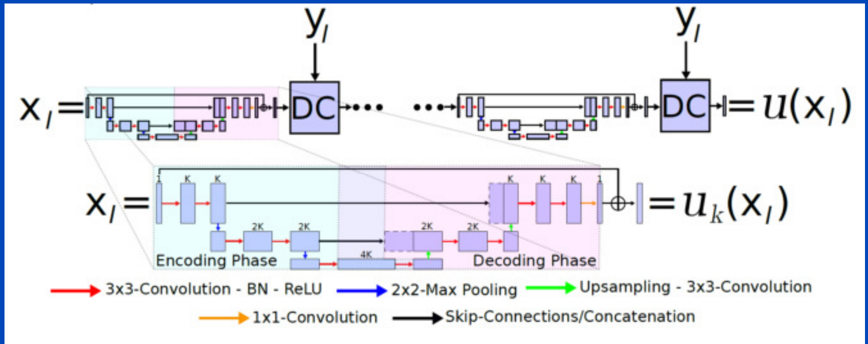

Sparse CT Recon with Data Consistency Layers (DCLs)

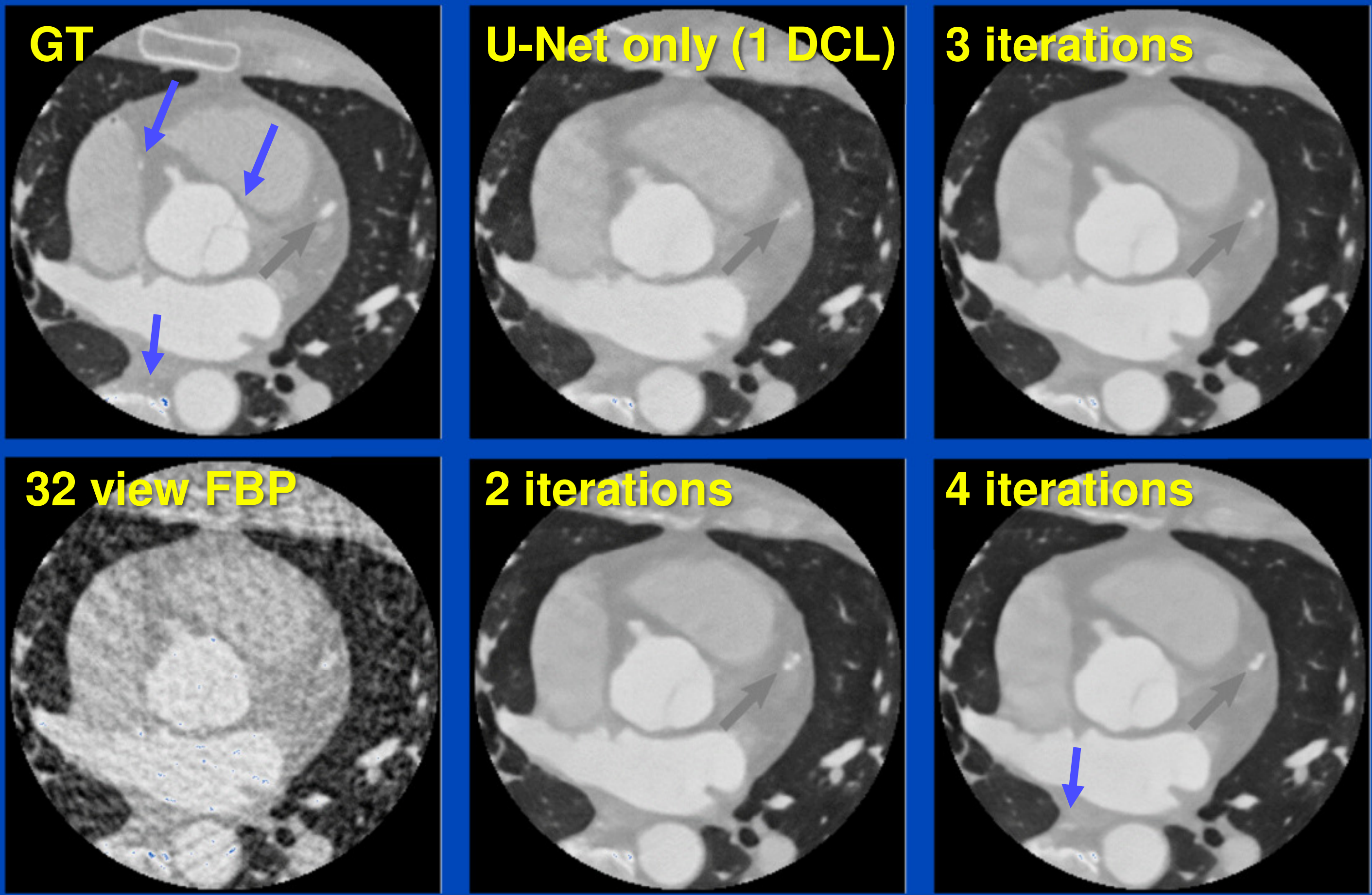

A. Kofler, M. Haltmeier, C. Kolbitsch, M. Kachelrieß, and M. Dewey. A U-Nets Cascade for Sparse View Computed Tomography, MICCAI 2018

dkfz.

Variational Network-Based Image Reconstruction

$$C(\boldsymbol{f}) = \|\boldsymbol{R}\cdot\boldsymbol{f} - \boldsymbol{p}\|_{\boldsymbol{W}}^2 + R(\boldsymbol{f})$$

$$\boldsymbol{\nabla} C(\boldsymbol{f}) = \boldsymbol{R}^{\mathrm{T}}\cdot\boldsymbol{W}\cdot(\boldsymbol{R}\cdot\boldsymbol{f} - \boldsymbol{p}) + \boldsymbol{\nabla} R(\boldsymbol{f})$$

$$\boldsymbol{f}^{(t+1)} = \boldsymbol{f}^{(t)} - \lambda\boldsymbol{\nabla} C(\boldsymbol{f}^{(t)})$$

Highly simplified example. Varnets work for a much wider class of cost functions whose NN-based minimization is motivated by the primal dual approach.

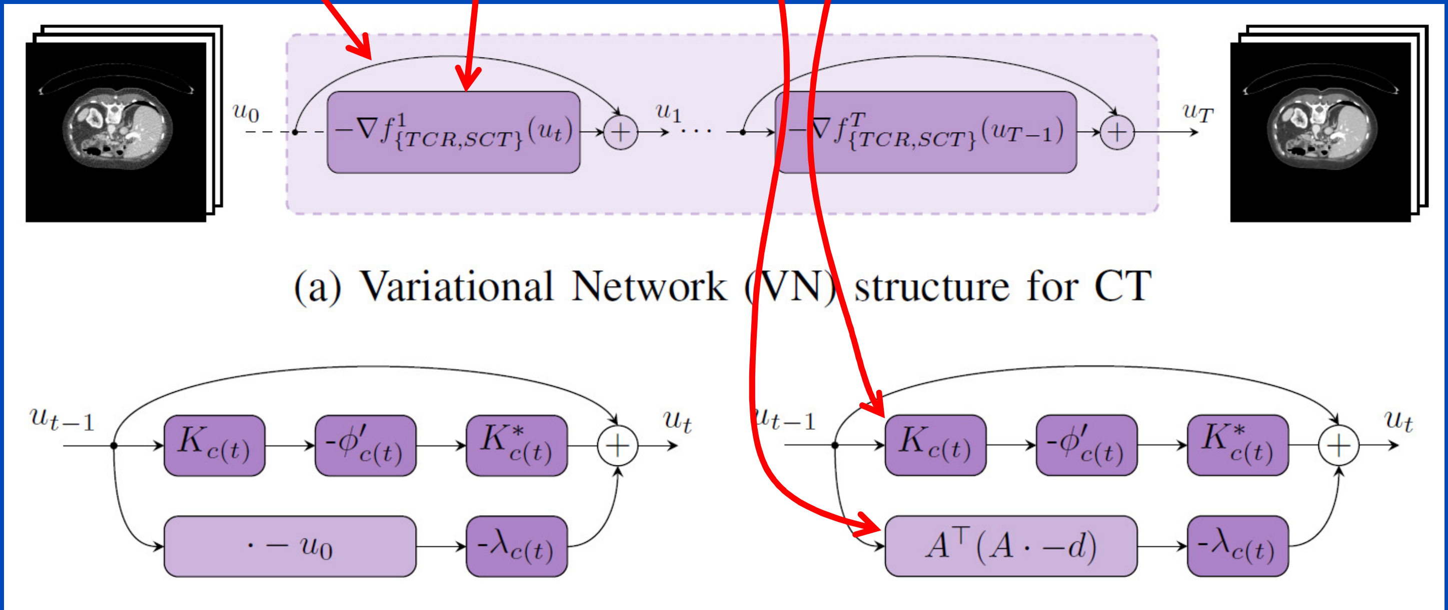

(a) Variational Network (VN) structure for CT

(b) VU for CT denoising

(c) VU for CT reconstruction

E. Kobler, R. Otazo et al. Variational network learning for low-dose CT. Proc. 5th CT-Meeting:430-434, 2018.

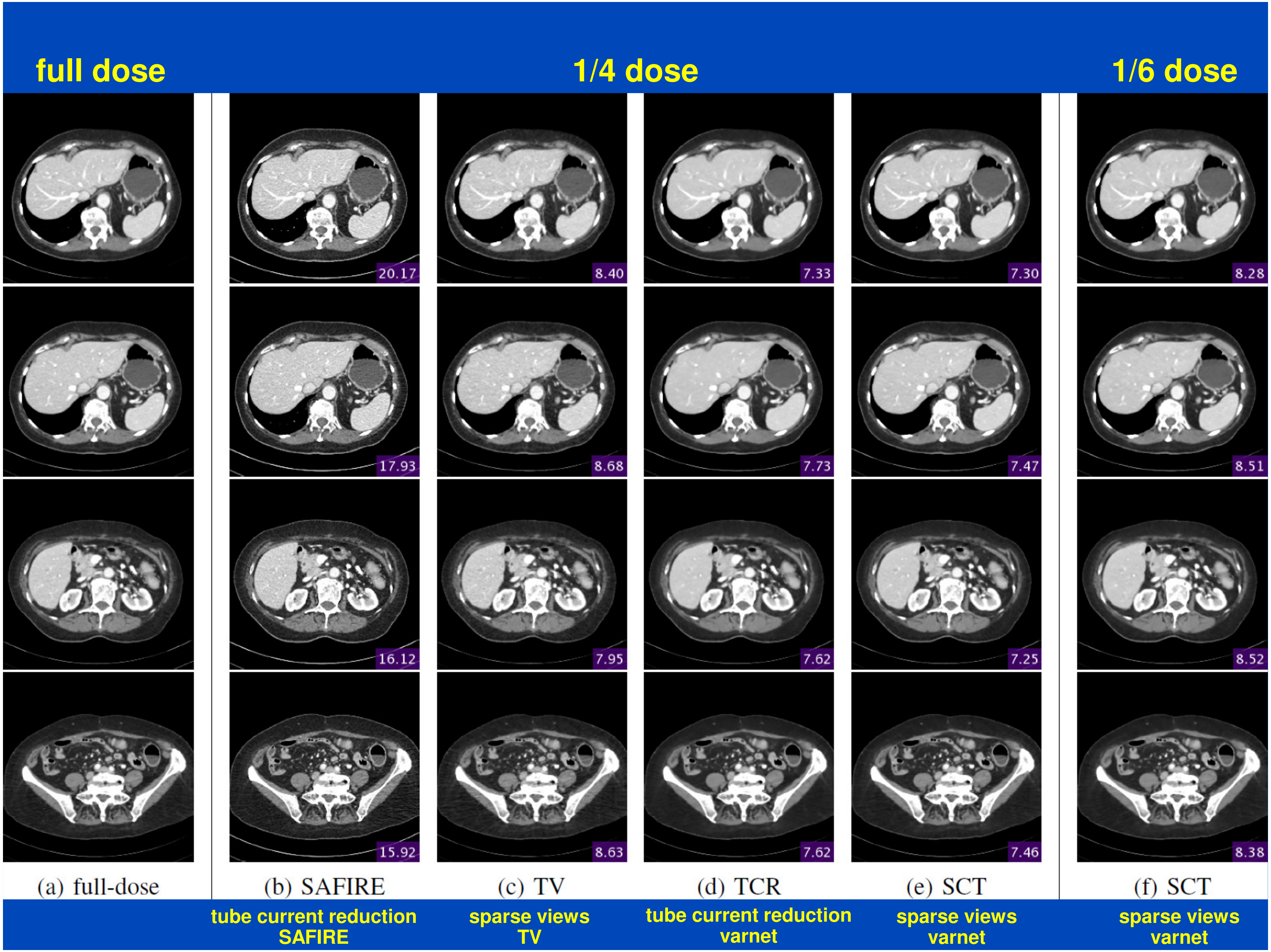
full dose
1/4 dose
1/6 dose
20.17
8.40
7.33
7.30
8.28
17.93
8.68
7.73
7.47
8.51
16.12
7.95
7.62
7.25
8.52
15.92
8.63
7.62
7.46
8.38
(a) full-dose
(b) SAFIRE
(c) TV
(d) TCR
(e) SCT
(f) SCT
tube current reduction
SAFIRE
sparse views
TV
tube current reduction
varnet
sparse views
varnet
sparse views
varnet

Conclusions on Deep CT

- Machine learning will play a significant role in CT optimization.
- High potential for
  - Artifact correction
  - Noise and dose reduction
  - Real-time dose assessment (also for RT)
  - ...
- Care has to be taken
  - Underdetermined acquisition, e.g. sparse view or limited angle CT, require the net to make up information!
  - Nice looking images do not necessarily represent the ground truth.
  - Data consistency layers may ensure that the information that is made up is consistent with the measured data.
  - ...

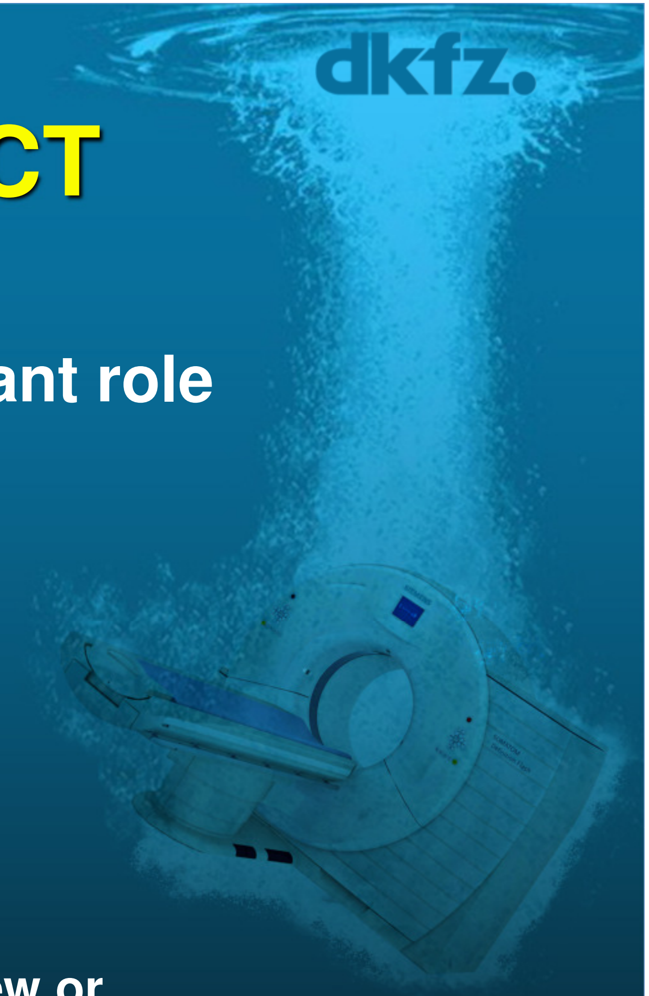

Which DSA is Real and Which is Fake?

Find out tomorrow 11:10, room Studio 2019!

Thank You!

The 6th International Conference on

Image Formation in X-Ray Computed Tomography

Conference Chair: **Marc Kachelrieß**, German Cancer Research Center (DKFZ), Heidelberg, Germany

This presentation will soon be available at www.dkfz.de/ct.
Job opportunities through DKFZ's international Fellowship programs (marc.kachelriess@dkfz.de).
Parts of the reconstruction software were provided by RayConStruct® GmbH, Nürnberg, Germany.